NASA Technical Memorandum 100883

Flowfield Measurements in the NASA Lewis Research Center 9- by 15-Foot Low-Speed Wind Tunnel

Christopher E. Hughes
Lewis Research Center
Cleveland, Ohio

March 1989

NASA

FLOWFIELD MEASUREMENTS IN THE NASA LEWIS RESEARCH CENTER

9- BY 15-FOOT LOW-SPEED WIND TUNNEL

Christopher E. Hughes
National Aeronautics and Space Administration
Lewis Research Center
Cleveland, Ohio 44135

E-4116

SUMMARY

An experimental investigation was conducted in the NASA Lewis 9- by 15-Foot Low-Speed Wind Tunnel to determine the flow characteristics in the test section during wind tunnel operation. In the flowfield investigation, a 20-probe pitot-static flow survey rake, spanning the test section horizontally, was used to obtain cross-sectional total and static pressure surveys at four axial locations in the test section, including near the entrance, the model test plane, and the exit. At each axial location, the cross-sectional flowfield surveys were made by repositioning the pitot-static flow survey rake vertically. In addition, a calibration of the new wind tunnel rake instrumentation, used to determine the wind tunnel operating conditions, was performed. A correlation was determined between the pressures measured by the wind tunnel upstream and downstream rakes and the pressures measured in the test section model test plane at the model centerline location. Boundary layer surveys were also made at three axial locations in the test section: near the entrance, the model test plane, and the exit. The test section flowfield investigation was conducted at tunnel Mach numbers 0.20, 0.15, 0.10, and 0.05.

The test section profile results from the investigation indicate that fairly uniform total pressure profiles (outside the test section boundary layer) and fairly uniform static pressure and Mach number profiles (away from the test section walls and downstream of the test section entrance) exist throughout the wind tunnel test section. The static pressure and Mach number results near the test section walls were influenced by the flow around the test section wall slots and by the large contraction ratio in the tunnel inlet section near the test section entrance. The largest variations in the total pressure, static pressure, and Mach number profiles occurred at a tunnel Mach number of 0.20 and diminished at lower tunnel Mach numbers.

The results of the wind tunnel rake instrumentation calibration indicate that differences exist between the pressures measured by wind tunnel rakes and the pressures measured in the model test plane at the model centerline location at all tunnel Mach numbers, but these differences diminish at lower tunnel Mach numbers. Therefore, pressure measurements obtained from either of the wind tunnel rakes to define the wind tunnel operating conditions must be corrected to determine accurate freestream conditions at the model centerline at all tunnel conditions.

The test section boundary layer survey results indicate that the boundary layer thickness varies throughout the test section, from approximately 2.8 to 3.5 in. near the test section entrance, to approximately 5.3 in. near the model test plane, and from approximately 7.3 to 13.5 in. near the test section exit.

INTRODUCTION

In support of the NASA Lewis Research Center Advanced Turboprop Project propeller research program, an investigation was conducted in the NASA Lewis 9- by 15-Foot Low-Speed Wind Tunnel (LSWT) to determine the test section flow characteristics. The wind tunnel flow characteristics have been previously documented (ref. 1). However, with the addition of acoustic insulation in the test section and the replacement of portions of the wind tunnel pressure instrumentation which provides the wind tunnel operating conditions, another investigation was necessary to determine the test section flowfield properties during wind tunnel operation.

In propeller testing, the aerodynamic performance of the propeller is expressed in terms of efficiency. The propeller performance depends on several performance parameters, including the propeller power and the freestream velocity. At a constant propeller rotational speed, a 1.0-percent change in the freestream velocity near the propeller takeoff design point changes the power absorbed by the propeller approximately 1.3 percent and changes the propeller efficiency approximately 0.5 percent. Therefore, an accurate velocity distribution at the propeller-model plane of rotation in the test section must be known to correctly calculate the propeller performance.

The test section flowfield investigation consisted of several parts. The first part was the determination of the pressure and Mach number profiles at four axial locations in the test section. The axial survey locations were chosen to obtain pressure data near the test section entrance, the model test plane (that is, the plane of the test section where the model is located during testing, including the propeller-model plane of rotation), and the test section exit. The second part of the investigation was the calibration of the new wind tunnel rake instrumentation used to determine the wind tunnel flow conditions. A relationship was found between the total and static pressures measured by the upstream and downstream wind tunnel rakes and the total and static pressures measured at the model centerline location in the model test plane. Finally, the test section boundary layer profile was determined at three axial locations in the test section: near the test section entrance, the model test plane, and the test section exit. Flowfield measurements were made at wind tunnel Mach numbers 0.20, 0.15, 0.10, and 0.05.

This report presents the results of the investigation conducted to determine the flow characteristics in the test section of the NASA Lewis 9- by 15-Foot Low-Speed Wind Tunnel. The results shown include pressure, Mach number, and boundary layer profiles at the four axial survey locations, including the test section entrance, the model test plane, and the test section exit. In addition, calibration results are presented that correlate the pressures measured at the model test plane with the pressures measured by the wind tunnel rake instrumentation used to define the wind tunnel operating conditions.

SYMBOLS

M Mach number

P pressure, psi

Q total pressure minus static pressure, psi

Subscripts:

cl model test plane centerline condition

ref reference condition

s static condition

t total condition

0 freestream condition

1 upstream wind tunnel rake condition

2 downstream wind tunnel rake condition

APPARATUS AND PROCEDURE

Apparatus

The 9- by 15-Foot Low-Speed Wind Tunnel (LSWT) is illustrated in figure 1. The overall wind tunnel circuit is shown in figure 1(a). As shown, the test section is located in the return leg of the 8- by 6-Foot Supersonic Wind Tunnel (SWT). In figure 1(b), a diagram of the test section is shown. The test section measures approximately 28.6 ft, from the end of the tunnel inlet section to the beginning of the tunnel diffuser section.

The photographs in figure 2 show the instrumentation hardware used in the investigation. Figure 2(a) is a view of the test section looking downstream from the entrance. The north wall of the test section is on the left. Acoustic treatment in the test section is provided by perforated boxes covering all the test section surfaces. Several of the forward boundary layer survey rakes are shown on the left. Slots in the test section north wall are shown running from the left side to the center of the photograph. The upstream wind tunnel rake is shown in the upper left corner. The pitot-static flow survey rake, installed horizontally in the test section, is on the right. The vertical tube, perpendicular to the flow survey rake, is the secondary support tube. The downstream wind tunnel rake is directly above the flow survey rake, next to the secondary support tube, at the right. The model test plane boundary layer survey rake is next to the downstream wind tunnel rake. Figure 2(b) provides a view of the test section instrumentation looking upstream from the test section exit. The large airfoil-shaped hardware around the test section exit is the aft boundary layer survey rakes.

Figure 3 shows the location of the wind tunnel rake instrumentation and the locations of the forward, model test plane, and aft boundary layer survey rakes used in the investigation. The forward boundary layer rake locations, near the test section entrance at test section station 28, are shown in figure 3(a). As shown, two forward boundary layer rakes were used on the tunnel ceiling and sidewalls, and one rake on the tunnel floor. The test section station number is the distance (in inches) from the beginning of the test

section. Test section station 0 corresponds to tunnel station 27.7 (fig. 1(b)) where the tunnel station number is the distance (in feet) from the beginning of the tunnel inlet section. The axial locations of the boundary layer rakes in the test section were determined by the location of the total pressure probe on top of the rake. The boundary layer survey rakes located near the same axial location in the test section were given the same test section station number. Figure 3(b) shows locations for the aft boundary layer survey rakes near the test section exit, at test section station 336. Each tunnel surface was instrumented with two aft boundary layer rakes. The test section locations of the model test plane boundary layer rake and the two wind tunnel rakes are shown in figure 3(c). The model test plane boundary layer rake was located at test section station 210. The upstream tunnel rake was located at test section station 8, and the downstream tunnel rake was located at test section station 210. The downstream tunnel rake and the model test plane boundary layer rake were positioned to obtain pressure measurements near the Advanced Turboprop Project propeller-model plane of rotation.

The pitot-static flow survey rake used in the investigation is shown in figure 4. Figure 4(a) provides a schematic overview of the flow survey rake, as seen from upstream of the rake and looking downstream. The flow survey rake consisted of 20 pitot-static pressure survey probes mounted on a main support tube that spanned the test section horizontally, and was mounted to the tunnel structure at both ends of the main support tube. The survey probes on either end of the rake were located approximately 0.5 ft from the test section walls. Near the middle of the flow survey rake, a vertical secondary support tube, mounted to the test section floor and ceiling, was used to stiffen the flow survey rake and prevent the rake from vibrating during testing. The spacing of the survey probes on the flow survey rake allowed better data resolution in the propeller-model plane of rotation and near the test section walls. (The location of the model centerline in the model test plane is 2 ft to the left of the test section centerline, looking downstream). Figure 4(b) is a photograph of a portion of the flow survey rake showing the left side, or north wall, mounting location and survey probes 1 through 8. The clustering of survey probes in the test section boundary layer and in the location of the model test plane can be seen. Figure 4(c) shows details of a typical pitot-static pressure survey probe used in the flow survey rake. Each survey probe consisted of a single total pressure measurement (obtained at the hemispherical-shaped end of the probe) and a single static pressure measurement (provided by eight equally spaced holes at the same axial location around the outside of the probe). The survey probe design allowed a large tolerance of flow angularity. The axial location of the flow survey rake in the test section was determined by the location of the static pressure measurment on the model centerline survey probe (probe 8).

The upstream wind tunnel rake at test section station 8 is shown in figure 5(a). The downstream wind tunnel rake, at test section station 210, is similar in design to the upstream wind tunnel rake. Both tunnel rakes are now part of the permanent wind tunnel instrumentation. The pitot-static pressure probe design used in the wind tunnel rakes is similar to the pressure survey probe design used in the flow survey rake. The axial location of the wind tunnel rake instrumentation in the test section, like the location of the flow survey rake, was determined by the location of the static pressure measurement on the rake. Figure 5(b) provides details of the wind tunnel rakes. The pitot-static pressure probe is mounted at the bottom of the rake. The wind

tunnel rakes extend approximately 12.25 in. into the flowfield from the test section ceiling, which is far enough into the test section to avoid the test section boundary layer. Four total temperature thermocouples were mounted on the rake above the pressure probe, far enough away to avoid influencing the flowfield around the pressure probe.

Figure 6 provides details typical of the forward boundary layer survey rakes. Figure 6(a) is a closeup view of one forward boundary layer survey rake located near the test section entrance at test section station 28. The seven forward boundary layer rakes were similar to the boundary layer rake shown, having seven total pressure probes and being typically 5.75 in. tall. On each forward boundary layer rake, the farthest probe from the tunnel surface (the seventh probe) was not used. A schematic of the total pressure probe locations on the forward boundary layer survey rakes is shown in figure 6(b), and typical dimensions for each of the forward boundary layer rakes are given in table I(a). Figure 7(a) shows the model test plane boundary layer survey rake located at test section station 210. The rake was approximately 12.5 in. tall and consisted of 24 total pressure probes 0.5 in. apart. A schematic of the total pressure probe locations on the model test plane boundary layer survey rake is shown in figure 7(b), and dimensions of the model test plane boundary layer rake are given in table I(b). Figure 8(a) shows a typical aft boundary layer survey rake located near the test section exit at test section station 336. A schematic of the total pressure probe locations on the aft boundary layer rakes is shown in figure 8(b), and typical dimensions for each of the aft boundary layer rakes are given in table I(c). The eight aft boundary layer rakes were typically 24.5 in. tall and consisted of 16 total pressure probes; however, the first and the last probes on each of the rakes were not used.

Instrumentation

During the investigation, two separate Electronically Scanned Pressure (ESP) measurement systems were used to obtain pressure data. The ESP system consists of a module with individual pressure ports. Each port consists of a dedicated differential pressure transducer, with one side of the transducer connected to a constant reference pressure. A single pressure measurement is obtained from each pressure port. In the investigation, one of the ESP systems used modules of 32 pressure ports, with each pressure port transducer having a full-scale measurement range of 30 psi (accurate to within ±0.10 percent of full scale). The other ESP system used modules of 16 pressure ports, with each pressure port transducer having a full-scale measuring range of 2 psi (accurate to within ±0.10 percent of full scale).

The accuracy required in obtaining pressure data determined which ESP system was used during the investigation. The total and static pressures from the pitot-static flow survey rake were measured by using the 2-psi ESP system in order to obtain more accurate pressure measurements at lower tunnel Mach numbers. This system was also used to measure the total and static pressures from the wind tunnel rake instrumentation at test section stations 8 and 210 (fig. 3). The 30-psi ESP system was used to measure total pressures during the test section boundary layer surveys, where the accuracy of the pressure measurements was not as important.

Other pertinent instrumentation in the flowfield investigation was used to obtain the wind tunnel total temperature. Total temperatures from the wind tunnel rakes were measured with Chromel-Alumel thermocouples (fig. 5).

Procedure

The investigation consisted primarily of three parts: (1) determination of the wind tunnel test section flow characteristics in a cross-sectional plane at four axial locations in the test section; (2) calibration of the new wind tunnel rake instrumentation by correlating the total pressure and static pressure measured at each wind tunnel rake with the total pressure and static pressure measured at the model centerline location in the test section model test plane; and (3) determination of the test section boundary layer at three axial locations in the test section. During the investigation, the upstream wind tunnel rake at test section station 8 was used to obtain the wind tunnel operating conditions (total and static pressure and total temperature). These tunnel operating conditions are referred to as the "reference conditions." From the reference conditions, the wind tunnel flow velocity was determined. The flowfield investigation was conducted at reference Mach numbers 0.20, 0.15, 0.10, and 0.05.

Figure 9 shows the locations where axial flowfield surveys were made in the test section. Total and static pressure measurements were taken at four axial survey locations in the test section, corresponding to test section stations 12, 134, 215, and 294 (and axial survey locations 1, 2, 3, and 4, respectively). At each axial survey location, pressure measurements were made at three vertical survey locations, except at test section station 215 (axial survey location 3) where 10 vertical locations were investigated. In table II, the vertical survey test matrix used at each axial survey location is given. The flowfield survey locations were selected to provide information on the flow characteristics within the test section, particularly near the test section model test plane. At test section station 215, more detailed survey information was obtained near the Advanced Turboprop Project propeller-model plane of rotation.

Total and static pressure flowfield survey measurements were made in the test section with the 20-probe pitot-static flow survey rake (fig. 4). Pressure measurements were taken at all four reference Mach numbers for each vertical survey location at each axial survey location. At each reference Mach number, five data points were recorded at 30-sec intervals to allow for transients in the flow. The 20 total and static pressure measurements obtained with the flow survey rake were recorded simultaneously for each data point. The flow survey rake was repositioned to a new vertical survey location after pressure measurements were made at the four reference Mach numbers. At the completion of the vertical survey test matrix (depending on the axial survey location, table II), the flow survey rake was moved to a new axial survey location in the test section.

The pitot-static flow survey rake was alsc used to calibrate the new wind tunnel rake instrumentation, at test section stations 8 and 210 (fig. 3), that provides the wind tunnel flow conditions. For the wind tunnel rake instrumentation calibration, the flow survey rake was positioned at test section station 215 (axial survey location 3, fig. 9), at the center of the test section (vertical survey location 7, table I). Total and static pressure measurements

were made at each reference Mach number at the model centerline location in the test section model test plane (corresponding to survey probe 8 (fig. 4) on the flow survey rake). The model centerline pressure measurements were later correlated with the total and static pressure measurements taken simultaneously at each of the wind tunnel rake locations.

The boundary layer profile surveys taken at test section stations 28, 210, and 336 (near the test section entrance, the model test plane, and the test section exit, respectively (fig. 3)) were done in conjunction with the pitot-static flowfield surveys at each reference Mach number. In order to minimize any effect of the flow survey rake on the boundary layer survey results, a boundary layer survey was done with the flow survey rake positioned at the farthest point away from the boundary layer survey location.

RESULTS AND DISCUSSION

To provide a qualitative summary of the test section flowfield survey, results are presented as total pressure, static pressure, and Mach number ratio contours. Both the cross-sectional and axial contours present results obtained only within the area investigated with the flow survey rake, not the entire test section cross-sectional or axial planes. The differences between the pressure ratio contour levels represent the accuracy of the results, or ±0.030 percent. The differences between Mach number ratio contour levels also represent the accuracy of the pressure results, since the Mach number is calculated from the total and the static pressure. The accuracy of the Mach number results, however, decreases at lower reference Mach numbers since the error of the pressure measurement introduced into the Mach number calculation becomes more significant. More detailed representations of the test section flowfield survey results are presented in appendixes A through F.

Test Section Cross-Sectional Profiles

Test section cross-sectional flowfield survey results at each axial survey location are presented in figures 10 to 12 for reference Mach numbers 0.20, 0.15, and 0.10. The figures present total and static pressure ratio and Mach number ratio contours for vertical survey locations 3, 7, and 11 (table I) at axial survey locations 1, 2, and 4 (fig. 9), and vertical survey locations 2 through 11 at axial survey location 3 (fig. 9). The flow survey results at reference Mach number 0.05 are not shown since the pressure and Mach number variations in the test section could not be seen in the results. Table III(a) provides a summary of the cross-sectional total and static pressure and Mach number variations in the test section at reference Mach number 0.20.

Total pressure cross-sectional flowfield survey results at axial survey locations 2, 3, and 4 are shown in figure 10. The results at axial survey location 1 are not presented since the total pressure variations were not large enough to be seen in the contour results at any reference Mach number. The results at the other axial survey locations show a near uniform total pressure distribution across the test section at all reference Mach numbers, with the largest total pressure differences occurring within the test section boundary layer. The largest total pressure difference observed outside the boundary

layer was at axial survey location 4 at reference Mach number 0.20 (table III(a) and fig. 10(g)). The thicker wall boundary layer at the axial survey locations farther downstream is evident in the results. The irregular shape of the boundary layer, especially toward the upper portion of the test section, can possibly be attributed to flow around the test section wall slots (figs. 10(a), (d), and (e)). The total pressure variations were not as large at lower tunnel Mach numbers (figs. 10(c), (f), and (i)).

Figure 11 presents the static pressure cross-sectional flowfield survey results at axial survey locations 1 through 4. The results show a large static pressure variation in the test section at axial survey location 1 near the test section entrance (figs. 11(a) to (c)), due to the large contraction ratio of the inlet section. Smaller static pressure variations are shown downstream of axial survey location 1 and away from the test section walls (figs. 11(d), (g), and (j)). Near the test section walls, the static pressure profiles appear to be affected by the flow around the test section wall slots, since large variations can be seen there, especially at reference Mach number 0.20 (figs. 11(d), (g), and (j)). Part of the static pressure variation observed near the center of the test section may possibly be due to a flow survey rake hardware problem, since the pressure difference persists at nearly the same level for all axial survey locations at each reference Mach number. However, the error introduced into the static pressure results is on the order of the accuracy of the results, or ±0.030 percent. Away from the test section walls, the largest difference in static pressure measured was at axial survey location 1 at reference Mach number 0.20 (table III(a) and fig. 11(a)). Downstream of axial survey location 1, farther away from the influence of the inlet section contraction ratio, the largest difference in static pressure was measured at axial survey location 4, near the test section exit, at a reference Mach number of 0.20 (table III(a) and fig. 11(j)). The variations in static pressure were smaller at lower tunnel Mach number (figs. 11(c), (f), (i), and (l)).

Mach number cross-sectional flowfield survey results at axial survey locations 1 through 4 are shown in figure 12. The results indicate the same trends as the total and static pressure survey results. Large Mach number variations, caused by flow distortions induced by the large inlet section contraction ratio, were found at axial survey location 1 (figs. 12(a) to (c)). Smaller Mach number differences were found in the test section downstream of axial survey location 1 and away from the test section walls (figs. 12(d), (g), and (j)). The largest difference in Mach number was found at axial survey location 1 at reference Mach number 0.20 (table III(a) and fig. 12(a)). Downstream from axial survey location 1, the largest Mach number difference was found at axial survey location 3 (table III(a) and fig. 12(d)). The thicker boundary layer downstream can be seen in the figure, with large variations in Mach number near the upper portion of the test section (figs. 12(d), (g), and (j)) which are probably due to the flow around the test section wall slots. The Mach number variations were smaller at lower reference Mach numbers, especially at the upper portions of the test section (figs. 11(c), (f), (i), and (l)).

Test Section Axial Profiles

Test section axial flowfield survey results are presented in figures 13 to 15. Total and static pressure ratio and Mach number ratio contours are

presented for axial survey locations 1 through 4 at vertical survey locations 3, 7 and 11 (table I) at reference Mach numbers 0.20, 0.15, and 0.10. The flowfield survey results are not shown at reference Mach number 0.05, since the pressure and Mach number variations in the test section could not be seen in the contour results. Table III(b) provides a summary of the variations in the axial total and static pressure, and Mach number in the test section at reference Mach number 0.20.

Total pressure axial flowfield survey results are presented in figure 13. The total pressure uniformity in the test section outside the test section boundary layer is shown in the figure. The largest downstream variation in total pressure outside the boundary layer was at vertical survey location 11 at reference Mach number 0.20 (table III(b) and fig. 13(g)). The axial growth in the test section boundary layer can also be seen in the figure, with a significantly larger boundary layer toward the upper portion of the test section (figs. 13(g) to (i)). The total pressure variations were smaller at lower Mach number (figs. 13(c), (f), and (i)).

Figure 14 presents the static pressure axial flowfield survey results. A large variation in the static pressure near the test section entrance at axial survey location 1, due to the large inlet section contraction ratio, can be seen at all vertical survey locations. A smaller variation in the static pressure across the test section downstream of the test section entrance can also be seen at all vertical survey locations. The largest variation in static pressure from axial survey locations 1 to 4 was found at vertical survey location 7 at reference Mach number 0.20 (table III(b) and fig. 14(d)). Downstream from the test section entrance (and away from the influence of the inlet section), the largest static pressure variation, from axial survey locations 2 to 4, was found at vertical survey location 3 at reference Mach number 0.20 (table III(b) and fig. 14(a)). The possible error introduced into the static pressure results by the hardware problem with the flow survey rake can be seen in the figure near the center of the test section at all vertical survey locations. This is especially true farther downstream, where the static pressure contours are farther apart, and the static pressure variations are smaller. The flow around the test section wall slots, and its effect on the static pressure, can be seen as a change in the direction of the contours near the test section walls, especially at reference Mach number 0.20 (figs. 14(a), (d), and (g)). The axial variations in the static pressure were smaller at lower tunnel Mach number (figs. 14(c), (f), and (i)).

The Mach number axial flowfield survey results are presented in figure 15. The large Mach number variations at axial survey location 1 near the test section entrance, which diminish downstream, can be seen at all the vertical survey locations. The largest variation in the Mach number in the test section from axial survey locations 1 to 4 was found at vertical survey location 7 at reference Mach number 0.20 (table III(b) and fig. 15(d)). The largest variation in the Mach number downstream from the test section entrance, from axial survey locations 2 to 4, was found at vertical survey location 3 at reference Mach number 0.20 (table III(b) and fig. 15(a)). The thicker boundary layer downstream in the test section, especially near the upper portion of the test section, can also be seen (figs. 15(g) to (i)). The Mach number variations were smaller at lower reference Mach numbers (figs. 15(c), (f), and (i)).

Wind Tunnel Instrumentation Calibration

Figures 16 and 17 present the wind tunnel rake instrumentation total and static pressure calibration results. The results are presented in terms of the ratio of the model centerline pressure to wind tunnel rake pressure as a function of the normalized tunnel rake Q (total minus static pressure). The results provide a correlation between the total pressure and static pressure measured at the wind tunnel rake locations (figs. 3 and 9) and the total pressure and static pressure measured at the model centerline location in the model test plane (axial survey location 3, test section station 215), near the propeller-model plane of rotation (fig. 9). The total and static pressure calibration results were curvefit, and equations were derived for use in calculating the flow conditions at the model centerline during testing. These wind tunnel rake pressure calibration equations, applicable at all tunnel flow conditions, are given in appendix G. Table IV provides a summary of the total pressure, static pressure, and Mach number differences between the wind tunnel rake locations and the model centerline location at a reference Mach number of 0.20.

The results of the total pressure calibration of the wind tunnel rake instrumentation are presented in figure 16. The correlation between the total pressure measured at the upstream tunnel rake (test section station 8) and at the model centerline is shown in figure 16(a). Figure 16(b) shows the correlation between the total pressure measured at the downstream tunnel rake (test section station 210) and at the model centerline. At all reference Mach numbers, the model centerline total pressure was lower than the total pressure at either wind tunnel rake location. However, the total pressure differences between the upstream tunnel rake and the model centerline were smaller than the differences between the downstream tunnel rake and the model centerline. The largest total pressure differences were found at reference Mach number 0.20 (table IV).

The results of the static pressure calibration of the wind tunnel rake instrumentation are presented in figure 17. The correlation between the static pressure measured at the upstream tunnel rake and at the model centerline location are shown in figure 17(a). At all reference Mach numbers, the static pressure was lower at the model centerline than at the upstream tunnel rake. In figure 17(b), the correlation between static pressure measured at the downstream tunnel rake and at the model centerline location is presented. Here, the model centerline static pressure was higher than the downstream tunnel rake static pressure at all reference Mach numbers. The largest differences in static pressure occurred at reference Mach number 0.20 (table IV).

The differences in total pressure and static pressure between the model centerline location and the wind tunnel rake locations in terms of Mach number are given in table IV. At an upstream tunnel rake Mach number of 0.20, the Mach number at the model centerline is approximately 2.65 percent higher, or Mach number 0.2053; at a downstream tunnel rake Mach number of 0.20, the model centerline Mach number is approximately 0.90 percent lower, or Mach 0.1982.

Test Section Boundary Layer Profiles

The test section boundary layer survey results are presented in figures 18 to 20 for reference Mach numbers 0.20, 0.15, 0.10, and 0.05. The results are presented in terms of the distance from the tunnel surface and the ratio of the

rake probe total pressure to reference total pressure. At each reference Mach number, the approximate thickness of the tunnel boundary layer at any particular boundary layer survey location was determined from the profile results where the total pressure measured was 99.9 percent of the reference total pressure (which was the upstream wind tunnel rake total pressure during the investigation). Table V provides a summary of the boundary layer thickness results at reference Mach number 0.20 for all the test section boundary layer survey locations.

The forward boundary layer profiles at test section station 28, near the test section entrance (fig. 3(a)), are shown in figure 18. The results show that the boundary layer is fairly uniform across the test section entrance, varying from 2.7 to 3.5 in. (table V). In figure 19, the boundary layer profiles at test section station 210, near the model test plane (fig. 3(c)), are shown. The boundary layer thickness, approximately 5.3 in., is larger at this location than at test section station 28. The aft boundary layer profiles at test section station 336, near the test section exit (fig. 3(b)), are shown in figure 20. At this location, there is a large variation in the boundary layer thickness across the test section (table V). The thickest part of the boundary layer occurs near the upper portion of the test section (fig. 20(a)) at rake locations 10 and 15 (fig. 3(b)), varying between 13.3 and 13.8 in. This boundary layer thickness was nearly double the 7.3-in.-thick boundary layer on the tunnel floor at rake locations 12 and 13 (fig. 3(b).

CONCLUDING REMARKS

The total pressure, static pressure, and Mach number profiles obtained from an investigation of the flow characteristics in the test section of the 9- by 15-Foot Low-Speed Wind Tunnel indicate that the test section has very uniform total pressure distributions and fairly uniform static pressure and Mach number distributions at most axial locations in the test section at all tunnel Mach numbers. The largest variations in total and static pressure and Mach number occur near the test section walls and are probably caused by flow around the test section wall slots. In addition, larger variations in static pressure and Mach number occur nearer the test section entrance than at other axial locations downstream in the test section (away from the test section walls) at all tunnel Mach numbers. These larger variations are due to the influence of the large contraction ratio in the tunnel inlet section. The test section boundary layer thickness increases downstream with larger variations near the test section walls, especially at the upper portions of the test section and near the test section exit. These boundary layer variations are most likely due to the flow around the test section wall slots.

Near the model test plane in the test section, in this case the Advanced Turboprop Project propeller-model plane of rotation, the total and static pressure and Mach number distributions and the test section boundary layer are well behaved. The freestream conditions at the model centerline location can be calculated during testing by using the derived pressure calibration equations and the pressure measurements obtained from either of the two wind tunnel rakes located in the test section.

SUMMARY OF RESULTS

An investigation was conducted in the NASA Lewis 9- by 15-Foot Low-Speed Wind Tunnel to determine the flow characteristics in the test section during wind tunnel operation. The investigation was done to determine (1) the total pressure, static pressure, and Mach number profiles at four axial survey locations in the test section, including locations near the entrance, the model test plane, and the exit; (2) the correlation between the pressures measured by the new wind tunnel rake instrumentation which are used to define the tunnel operating conditions, and the pressures measured at the model centerline location; and (3) the boundary layer profiles near the test section entrance, the model test plane, and near the test section exit. The investigation was conducted at tunnel Mach numbers 0.20, 0.15, 0.10, and 0.05.

The total and static pressure flowfield surveys were done with a 20-probe pitot-static flow survey rake that was installed horizontally in the test section. At each of the axial survey locations in the test section, the flow survey rake was positioned to several vertical survey locations to obtain cross-sectional total and static pressure and Mach number profiles at each tunnel Mach number. The test section boundary layer surveys were done with multiprobe total pressure rakes at locations near the test section entrance, on the tunnel ceiling near the model test plane, and near the test section exit.

The results of the flowfield investigation were

(1) The cross-sectional and axial total pressure survey results obtained in the test section show very uniform profiles outside the test section boundary layer at all tunnel Mach numbers. The largest variations in total pressure were measured at tunnel Mach number 0.20. The largest cross-sectional total pressure variation was found near the test section exit (axial survey location 4, test section station 294), and was approximately 0.023 percent of the tunnel total pressure. The largest axial total pressure variation was found 2.5 ft above the center of the test section (vertical survey location 11), and was approximately 0.009 percent of the tunnel total pressure. The variations in total pressure in the test section diminished at lower tunnel Mach numbers.

(2) The cross-sectional and axial static pressure survey results obtained in the test section show fairly uniform profiles downstream of the test section entrance and away from the test section walls at all tunnel Mach numbers. Static pressure results near the test section entrance were affected by the large inlet section contraction ratio, while the static pressure results near the walls were affected by the flow around the test section wall slots. The largest variations in static pressure were found at tunnel Mach number 0.020. The largest cross-sectional static pressure variation was found near the test section entrance (axial survey location 1, test section station 12), and was approximately 0.126 percent of the tunnel static pressure. Downstream from the test section entrance, the largest cross-sectional static pressure variation was found near the test section exit and was approximately 0.030 percent. The largest axial static pressure variation was found at the center of the test section (vertical survey location 7), and was approximately 0.333 percent of the tunnel static pressure. Downstream from the entrance, the largest axial static pressure variation was found 2.5 ft below the center of the test section (vertical survey location 3) and was approximately 0.123 percent. The static pressure variations in the test section diminished at lower tunnel Mach numbers.

(3) The cross-sectional and axial Mach number survey results show fairly uniform profiles downstream of the test section entrance (where the results were affected by the tunnel inlet section) and away from the test section walls (where the results were affected by the wall boundary layer and the flow near the wall slots). The largest variations in the Mach number were found at tunnel Mach number 0.20. The largest cross-sectional Mach number variation was found near the test section entrance and was approximately 2.59 percent of the tunnel Mach number. Downstream from the test section entrance, the large cross-sectional Mach number variation was found in the model test plane (axial survey location 3, test section station 215), and was approximately 0.69 percent. The largest axial Mach number variation from the test section entrance was found at the center of the test section and was approximately 6.27 percent of the tunnel Mach number. Downstream from the entrance, the largest axial Mach number variation was found 2.5 ft below the center of the test section, and was approximately 2.26 percent. The Mach number variations in the test section diminished at lower tunnel Mach numbers.

(4) The wind tunnel rake total pressure calibration results indicate that the total pressure at the model centerline (at test section station 215) in the model test plane is lower than the total pressure at either the upstream or the downstream wind tunnel rake at all tunnel Mach numbers. At tunnel Mach number 0.20, the difference in total pressure between the model centerline and the upstream tunnel rake (test section station 8) was about 0.002 percent of the tunnel total pressure, and about 0.009 percent between the model centerline and the downstream tunnel rake (test section station 210). The wind tunnel rake static pressure calibration results indicate that the model centerline static pressure is lower than the static pressure at the upstream tunnel rake, but higher than the static pressure at the downstream tunnel rake, at all tunnel Mach numbers. At tunnel Mach number 0.20, the difference in static pressure between the model centerline and the upstream tunnel rake was about 0.153 percent of the tunnel static pressure, and about 0.041 percent between the model centerline and the downstream tunnel rake. In terms of Mach number, the model centerline Mach number is 2.65 percent higher (or Mach number 0.2053) than the upstream tunnel rake Mach number of 0.20, and the model centerline Mach number is 0.90 percent lower (or Mach number 0.1982) than the downstream tunnel rake Mach number of 0.20.

(5) The boundary layer profile results indicate that the boundary layer thickness is between approximately 2.7 and 3.5 in. near the test section entrance (test section station 28), and approximately 5.3 in. near the model test plane (test section station 210). Near the test section exit (test section station 336), the boundary layer thickness varies from approximately 7.3 in. on the test section floor to approximately 10.0 in. on the lower portion of the test section walls, 13.5 in. on the upper portion of the test section walls, and 9.3 in. on the test section ceiling.

APPENDIX A - TEST SECTION TOTAL PRESSURE CROSS-SECTIONAL PROFILES

Figures A-1 through A-4 provide quantitative information on the cross-sectional total pressure profiles in the test section for reference Mach numbers 0.20, 0.15, 0.10, and 0.05 at (1) axial survey locations 1, 2, and 4 (fig. 9) for vertical survey locations 3, 7, and 11 (table I), and (2) axial survey location 3 for vertical survey locations 2 through 11. The pressure ratio results are accurate to within ±0.004 psi (±0.030 percent). Some of the results within the test section boundary layer have been truncated for greater resolution of the results outside the boundary layer.

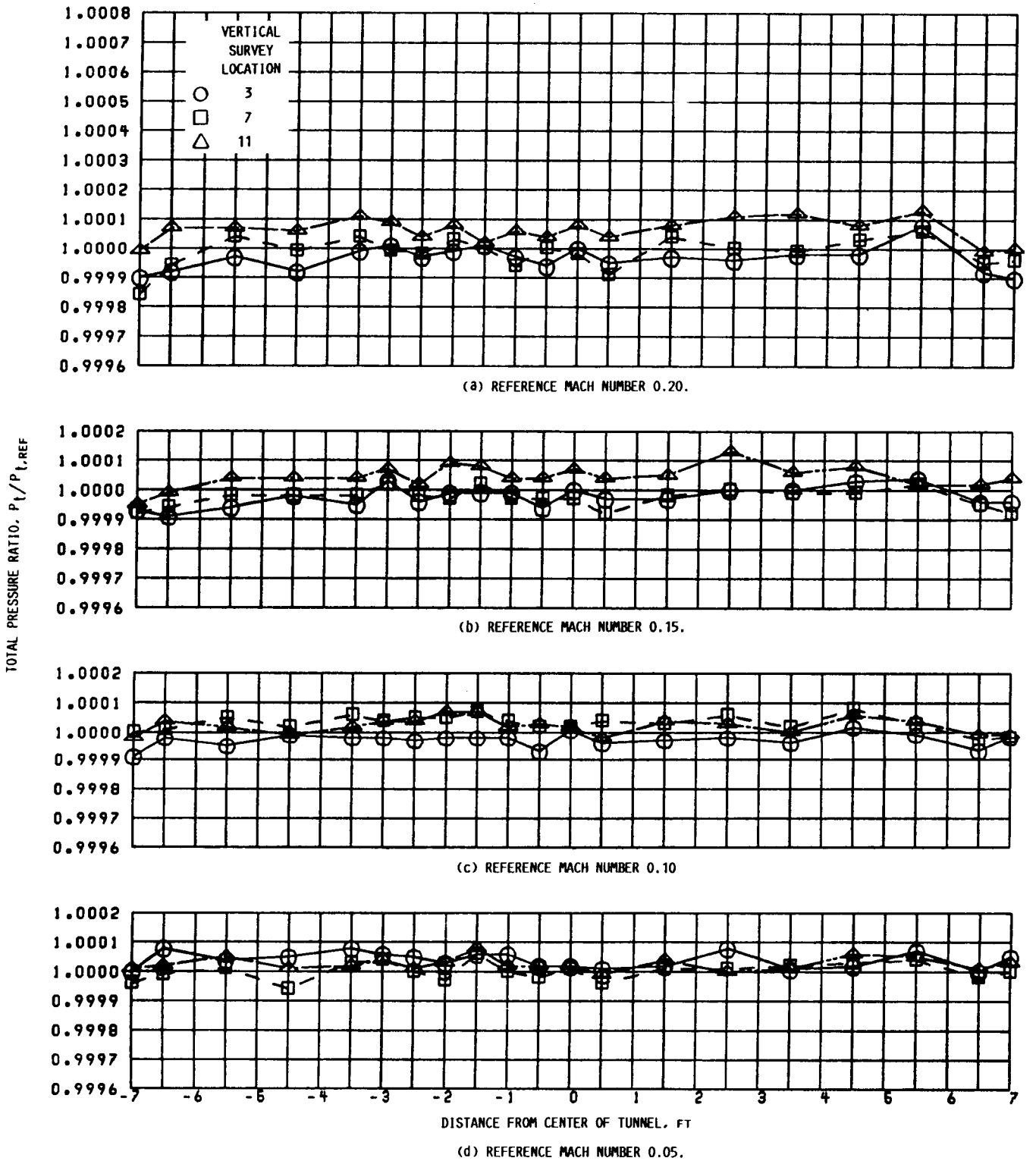

(a) REFERENCE MACH NUMBER 0.20.

(b) REFERENCE MACH NUMBER 0.15.

(c) REFERENCE MACH NUMBER 0.10

(d) REFERENCE MACH NUMBER 0.05.

FIGURE A-1. - TOTAL PRESSURE CROSS-SECTIONAL PROFILES AT AXIAL SURVEY LOCATION 1 (TEST SECTION STATION 12).

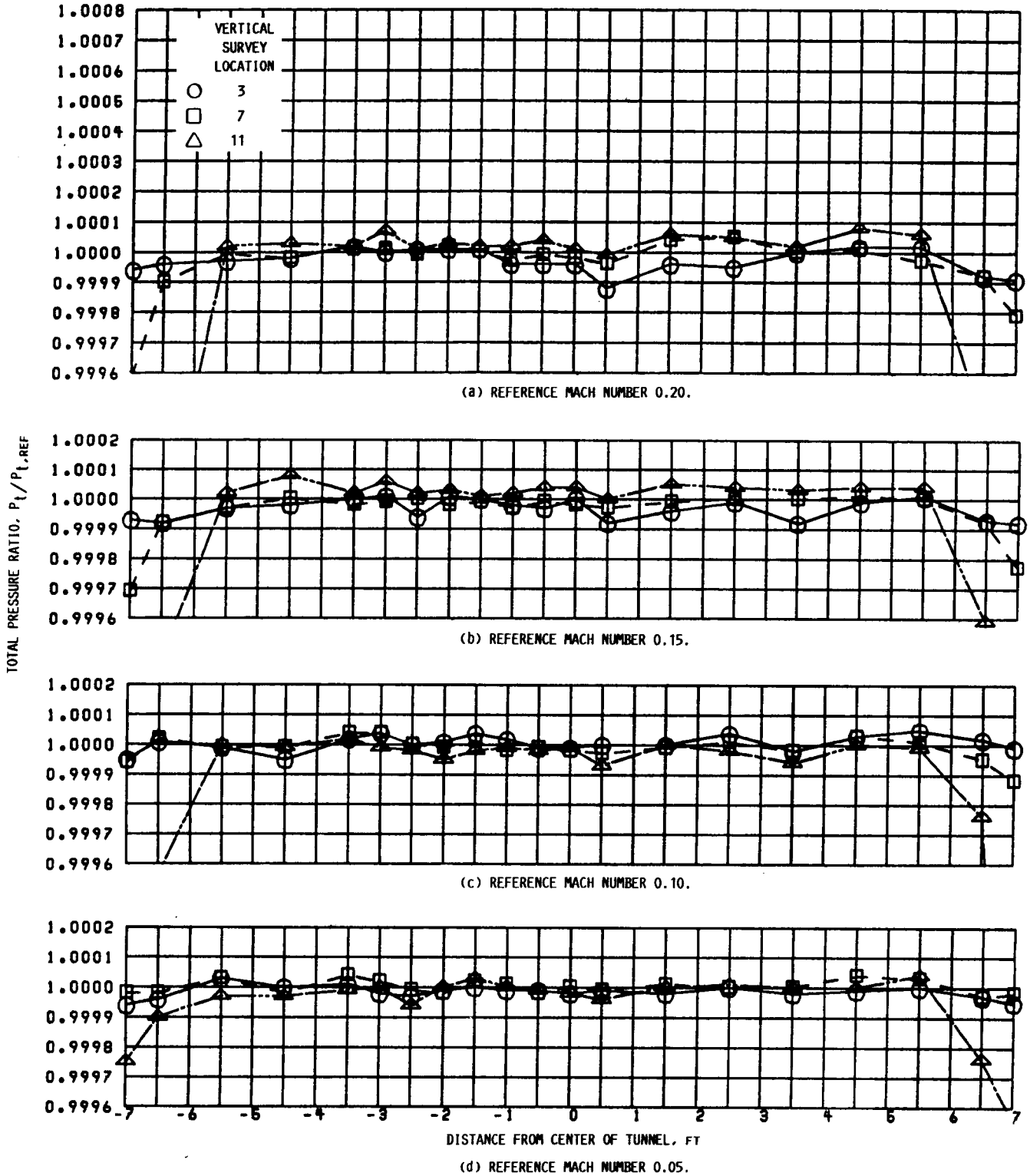

(a) REFERENCE MACH NUMBER 0.20.

(b) REFERENCE MACH NUMBER 0.15.

(c) REFERENCE MACH NUMBER 0.10.

(d) REFERENCE MACH NUMBER 0.05.

FIGURE A-2. - TOTAL PRESSURE CROSS-SECTIONAL PROFILES AT AXIAL SURVEY LOCATION 2 (TEST SECTION STATION 134).

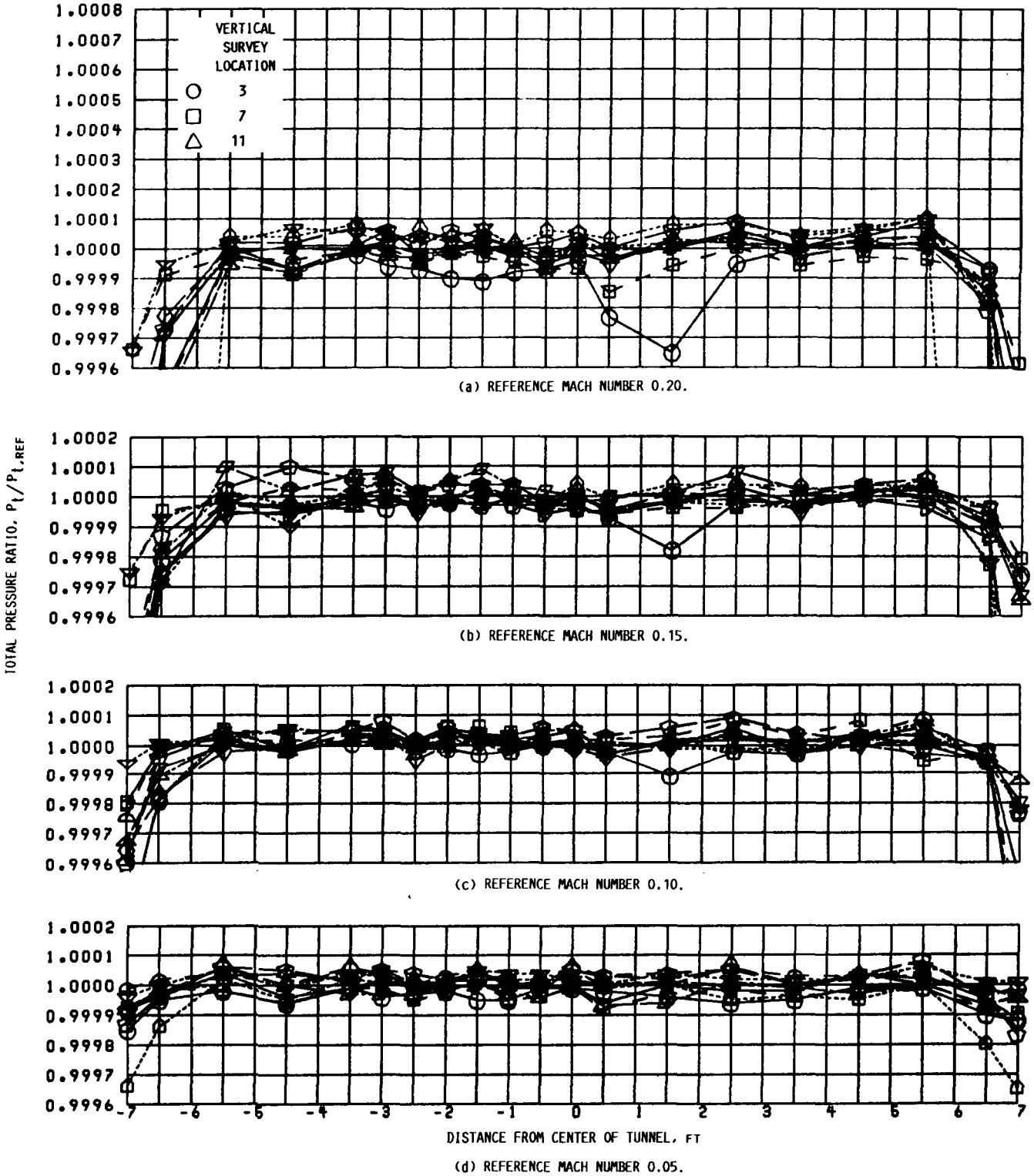

(a) REFERENCE MACH NUMBER 0.20.

(b) REFERENCE MACH NUMBER 0.15.

(c) REFERENCE MACH NUMBER 0.10.

(d) REFERENCE MACH NUMBER 0.05.

FIGURE A-3. - TOTAL PRESSURE CROSS-SECTIONAL PROFILES AT AXIAL SURVEY LOCATION 3 (TEST SECTION STATION 215).

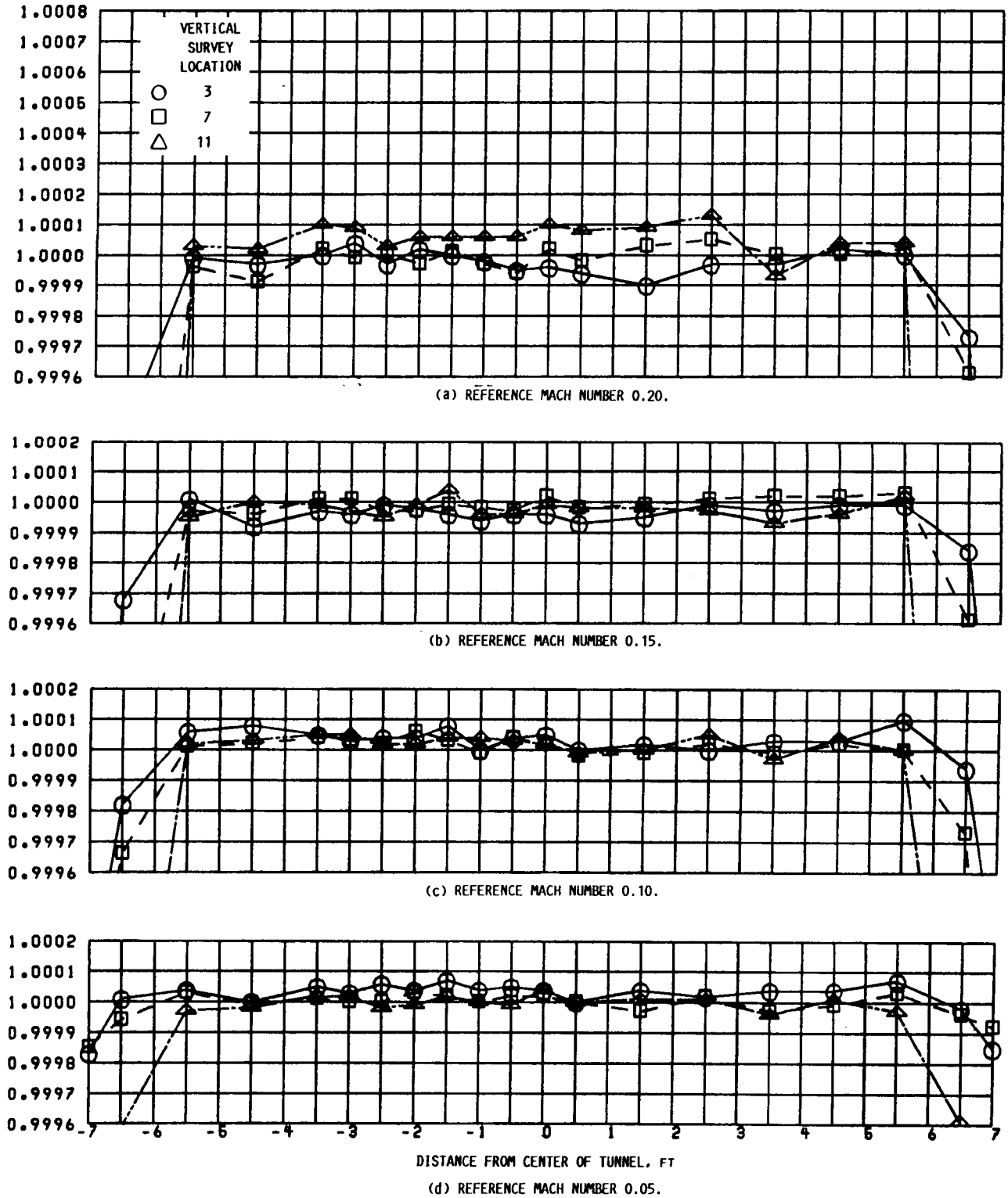

(a) REFERENCE MACH NUMBER 0.20.

(b) REFERENCE MACH NUMBER 0.15.

(c) REFERENCE MACH NUMBER 0.10.

(d) REFERENCE MACH NUMBER 0.05.

FIGURE A-4. - TOTAL PRESSURE CROSS-SECTIONAL PROFILES AT AXIAL SURVEY LOCATION 4 (TEST SECTION STATION 294).

APPENDIX B - TEST SECTION STATIC PRESSURE CROSS-SECTIONAL PROFILES

Figures B-1 through B-4 provide quantitative information on the cross-sectional static pressure profiles in the test section for reference Mach numbers 0.20, 0.15, 0.10, and 0.05 at (1) axial survey locations 1, 2, and 4 (fig. 9) for vertical survey locations 3, 7, and 11 (table I), and (2) axial survey location 3 at vertical survey locations 2 through 11. The pressure ratio results are accurate to within ±0.004 psi (±0.030 percent). Some of the results within the test section boundary layer have been truncated for greater resolution of the results outside the boundary layer. Results shown near the center of the test section, at distances from 0 to 2 ft, are questionable because of possible hardware problems encountered with the flow survey rake.

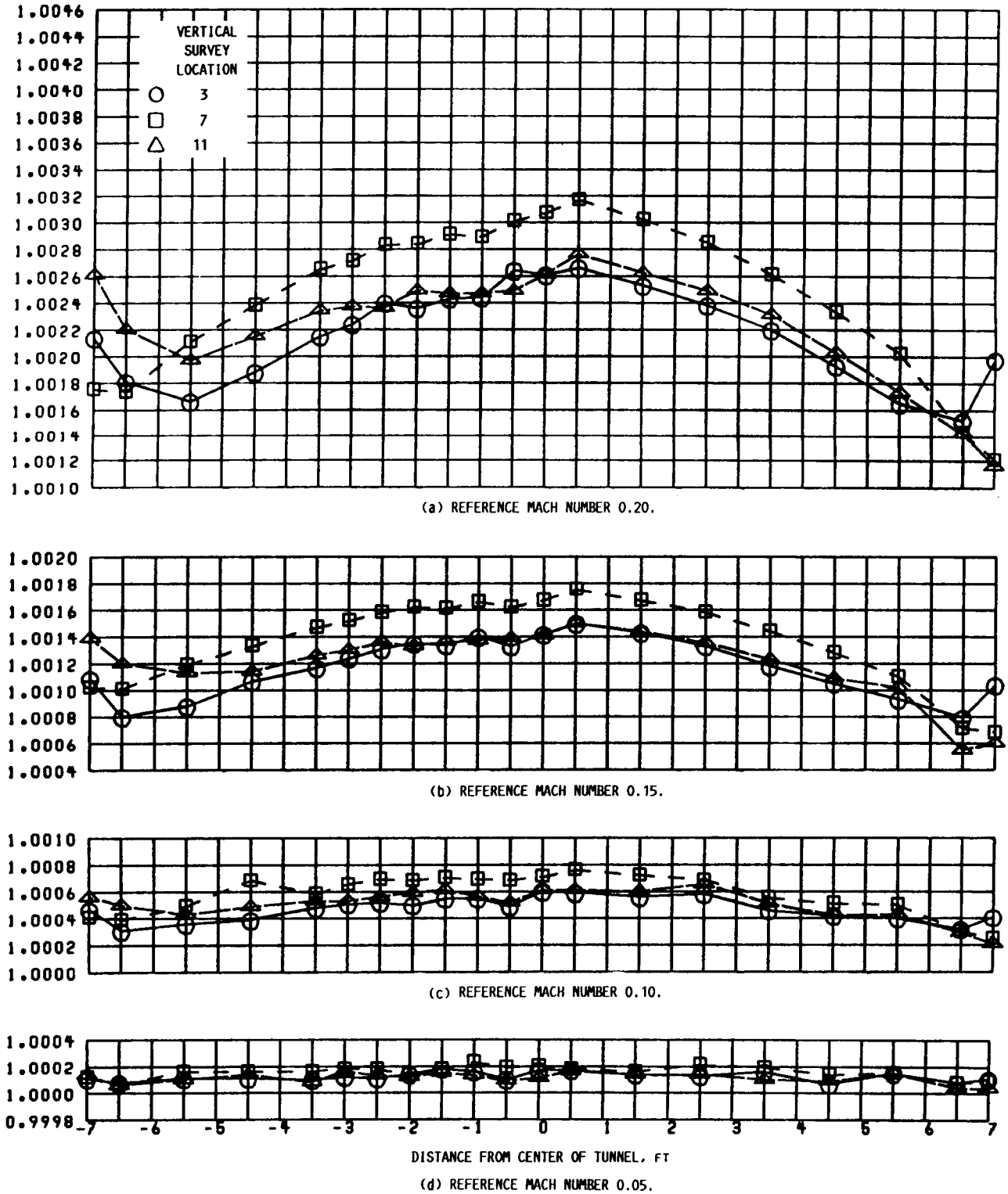

(a) REFERENCE MACH NUMBER 0.20.

(b) REFERENCE MACH NUMBER 0.15.

(c) REFERENCE MACH NUMBER 0.10.

(d) REFERENCE MACH NUMBER 0.05.

FIGURE B-1. - STATIC PRESSURE CROSS-SECTIONAL PROFILES AT AXIAL SURVEY LOCATION 1 (TEST SECTION STATION 12).

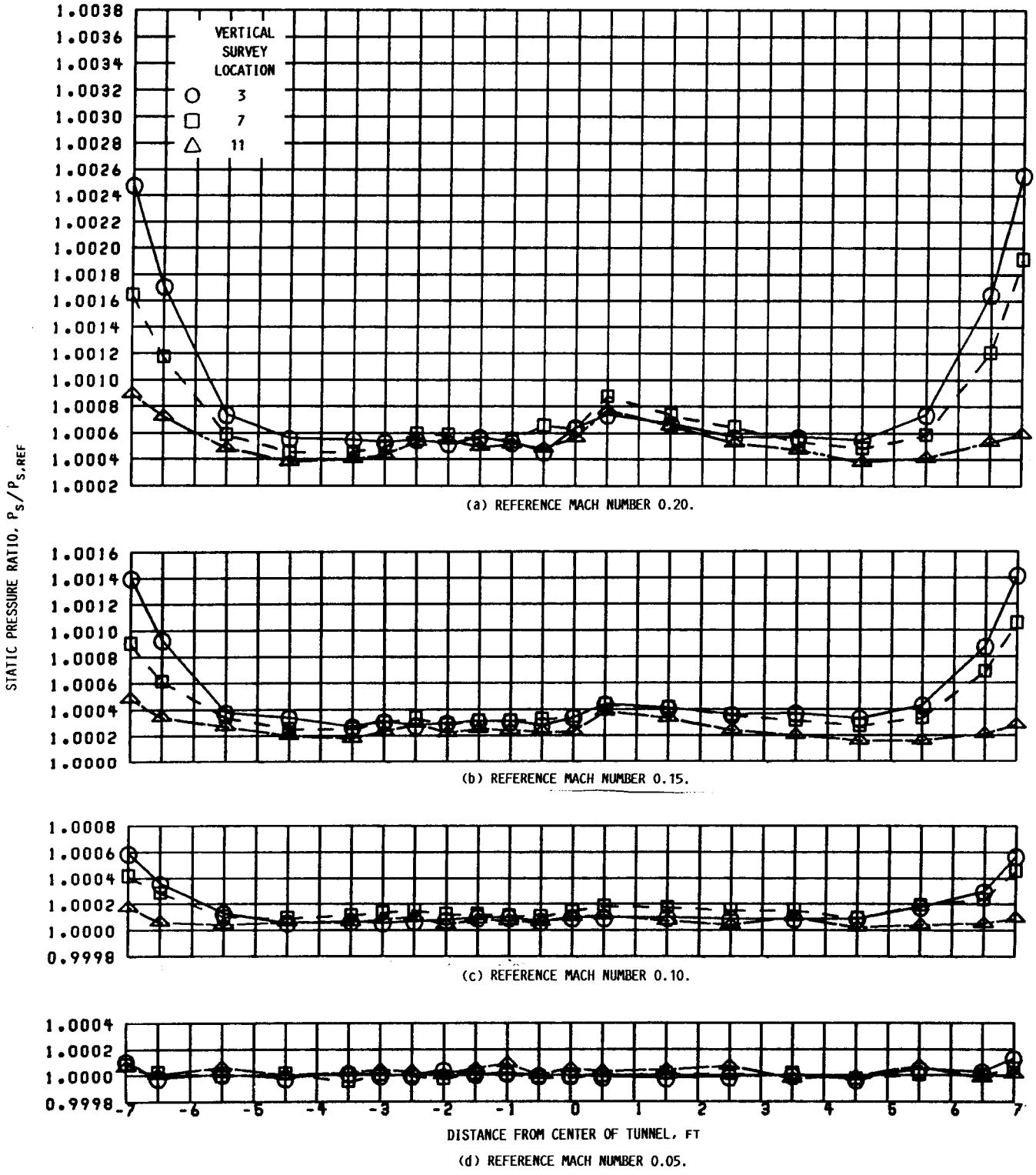

(a) REFERENCE MACH NUMBER 0.20.

(b) REFERENCE MACH NUMBER 0.15.

(c) REFERENCE MACH NUMBER 0.10.

(d) REFERENCE MACH NUMBER 0.05.

FIGURE B-2. - STATIC PRESSURE CROSS-SECTIONAL PROFILES AT AXIAL SURVEY LOCATION 2 (TEST SECTION STATION 134).

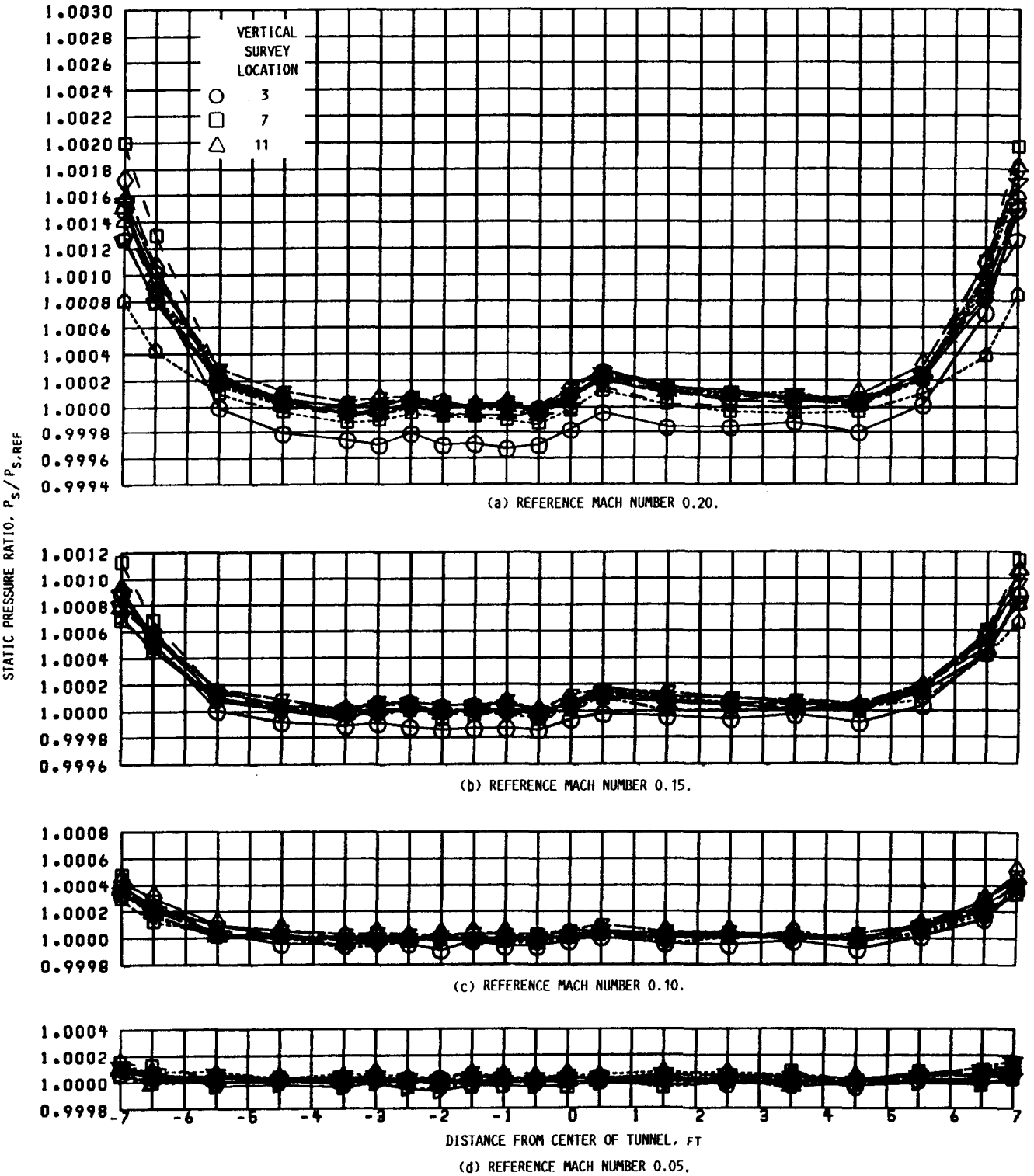

(a) REFERENCE MACH NUMBER 0.20.

(b) REFERENCE MACH NUMBER 0.15.

(c) REFERENCE MACH NUMBER 0.10.

(d) REFERENCE MACH NUMBER 0.05.

FIGURE B-3. - STATIC PRESSURE CROSS-SECTIONAL PROFILES AT AXIAL SURVEY LOCATION 3 (TEST SECTION STATION 215).

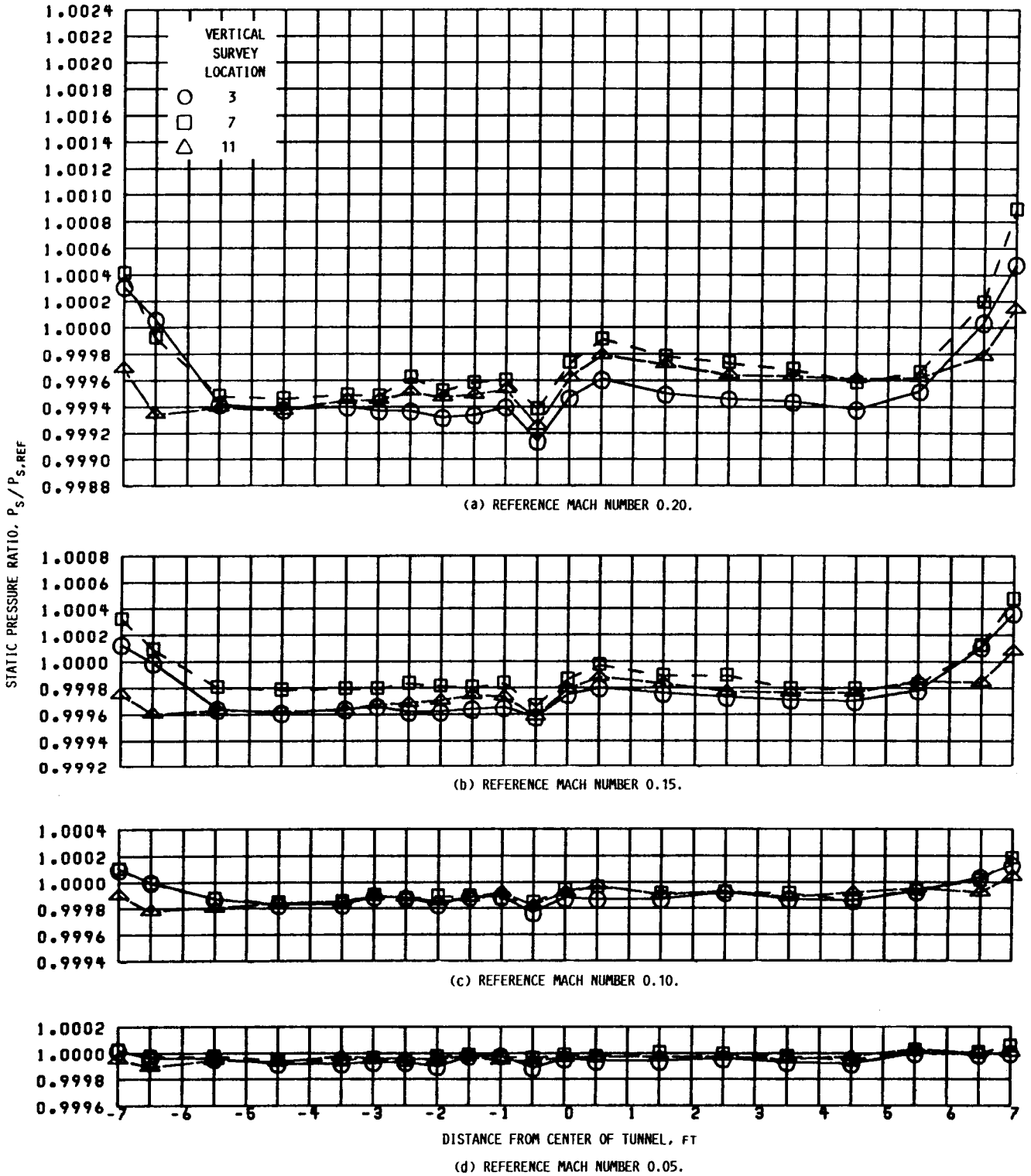

(a) REFERENCE MACH NUMBER 0.20.

(b) REFERENCE MACH NUMBER 0.15.

(c) REFERENCE MACH NUMBER 0.10.

(d) REFERENCE MACH NUMBER 0.05.

FIGURE B-4. - STATIC PRESSURE CROSS-SECTIONAL PROFILES AT AXIAL SURVEY LOCATION 4 (TEST SECTION STATION 294).

APPENDIX C - TEST SECTION MACH NUMBER CROSS-SECTIONAL PROFILES

Figures C-1 through C-4 provide quantitative information on the cross-sectional Mach number profiles in the test section for reference Mach numbers 0.20, 0.15, 0.10, and 0.05 at (1) axial survey locations 1, 2, and 4 (fig. 9) for vertical survey locations 3, 7, and 11 (table I), and (2) axial survey location 3 at vertical survey locations 2 through 11. The Mach number ratio results are accurate to within ±0.004 psi (±1.0 percent at reference Mach number 0.20, ±1.5 percent at reference Mach number 0.15, ±4.0 percent at reference Mach number 0.10, and ±16.0 percent at reference Mach number 0.05). Some of the results within the test section boundary layer have been truncated for greater resolution of the results outside the boundary layer. Results shown near the center of the test section, at distances from 0 to 2 ft, are questionable because of possible hardware problems encountered with the flow survey rake.

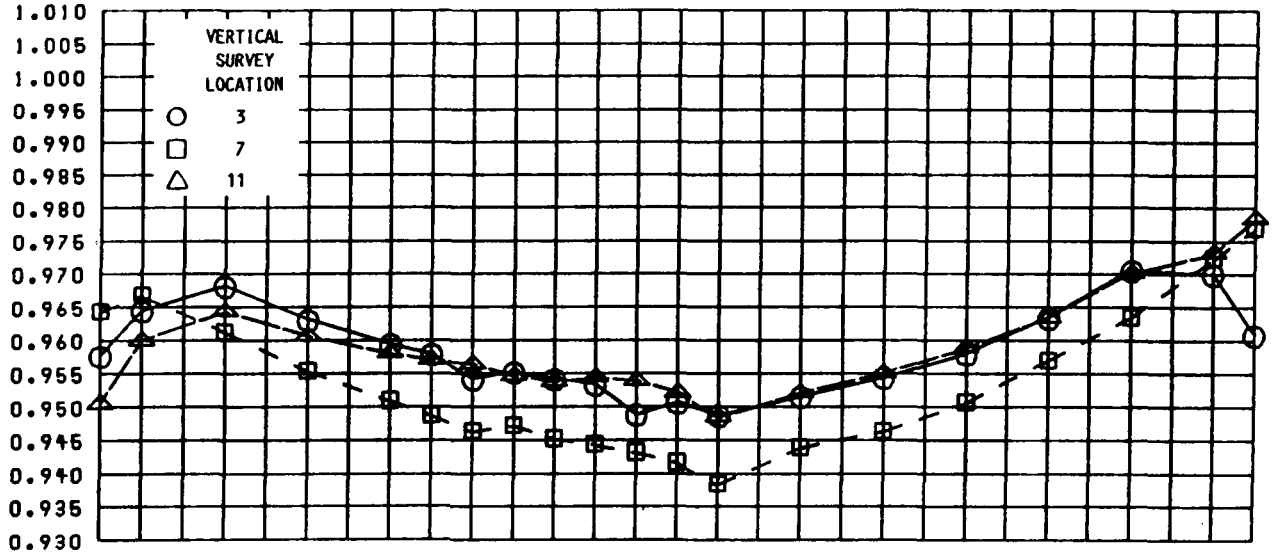

(a) REFERENCE MACH NUMBER 0.20.

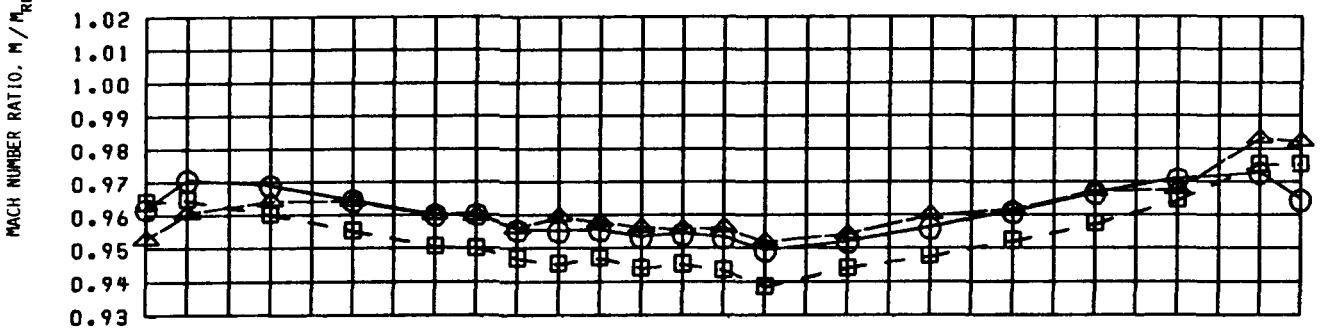

(b) REFERENCE MACH NUMBER 0.15.

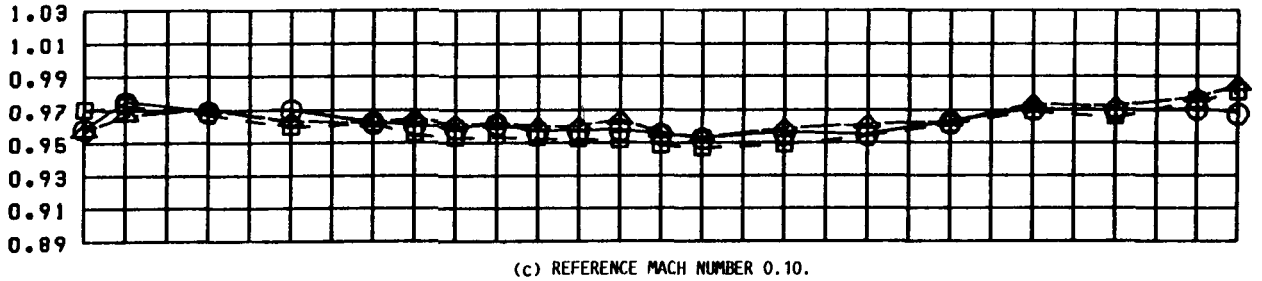

(c) REFERENCE MACH NUMBER 0.10.

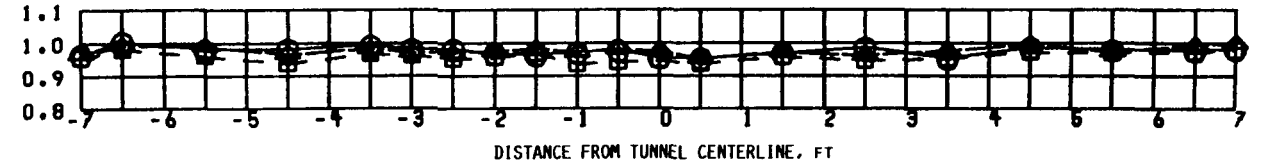

(d) REFERENCE MACH NUMBER 0.05.

FIGURE C-1. - MACH NUMBER PRESSURE CROSS-SECTIONAL PROFILES AT AXIAL SURVEY LOCATION 1 (TEST SECTION STATION 12).

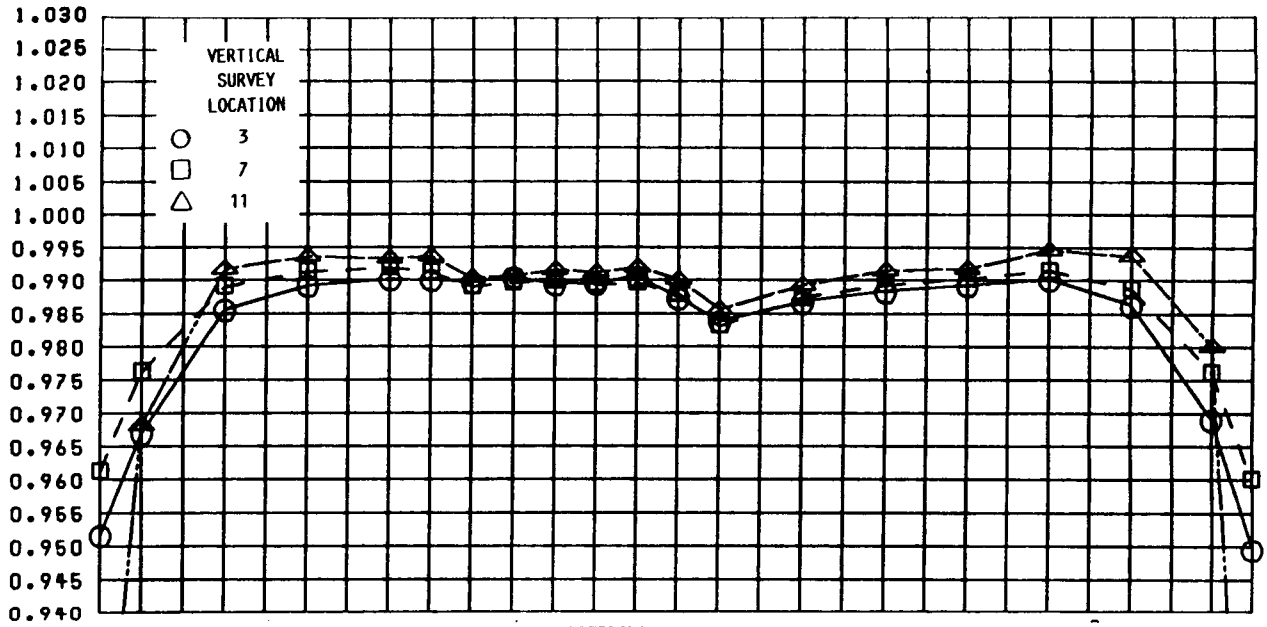

(a) REFERENCE MACH NUMBER 0.20.

MACH NUMBER RATIO, M/M_{REF}

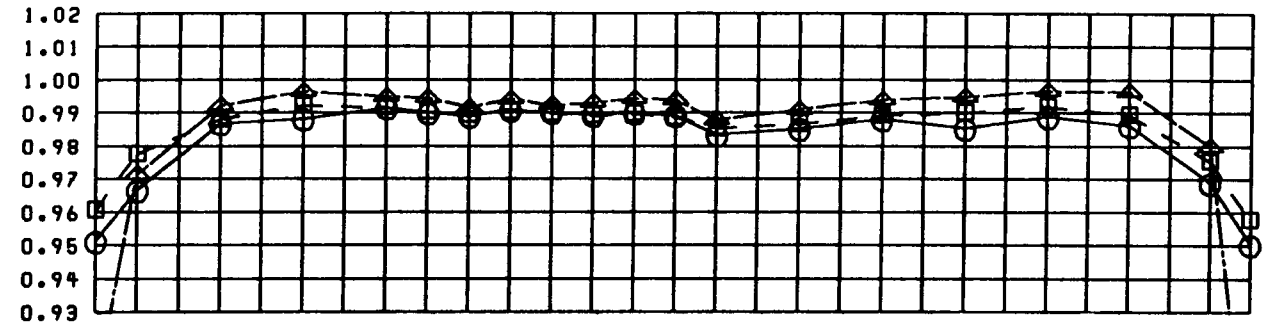

(b) REFERENCE MACH NUMBER 0.15.

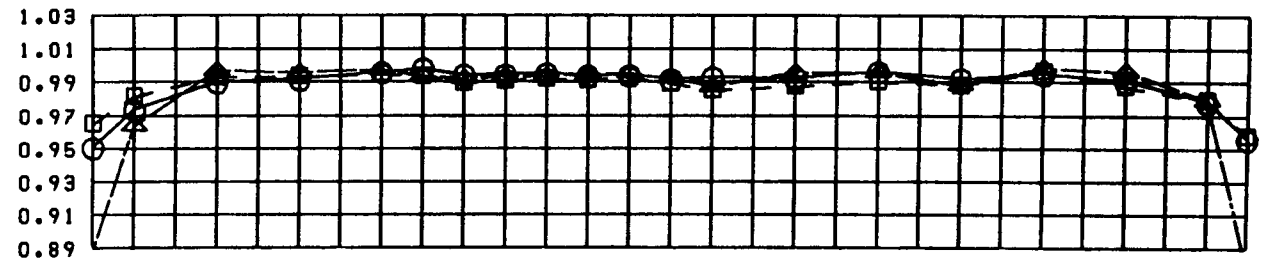

(c) REFERENCE MACH NUMBER 0.10.

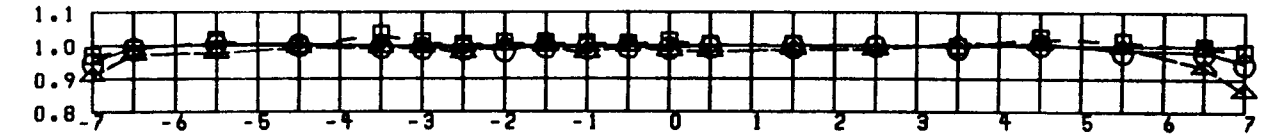

DISTANCE FROM TUNNEL CENTERLINE, FT

(d) REFERENCE MACH NUMBER 0.05.

FIGURE C-2. - MACH NUMBER PRESSURE CROSS-SECTIONAL PROFILES AT AXIAL SURVEY LOCATION 2 (TEST SECTION STATION 134).

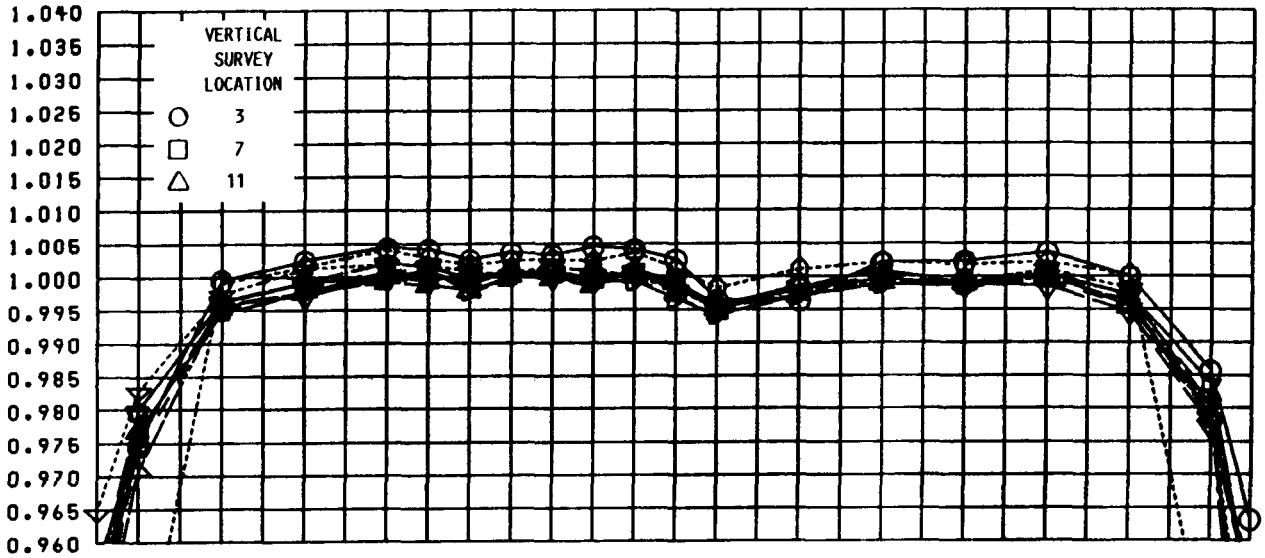

(a) REFERENCE MACH NUMBER 0.20.

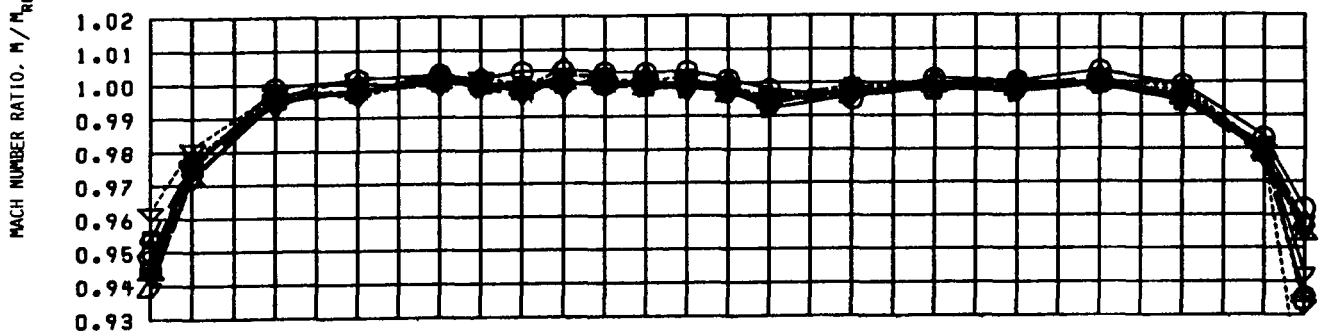

(b) REFERENCE MACH NUMBER 0.15.

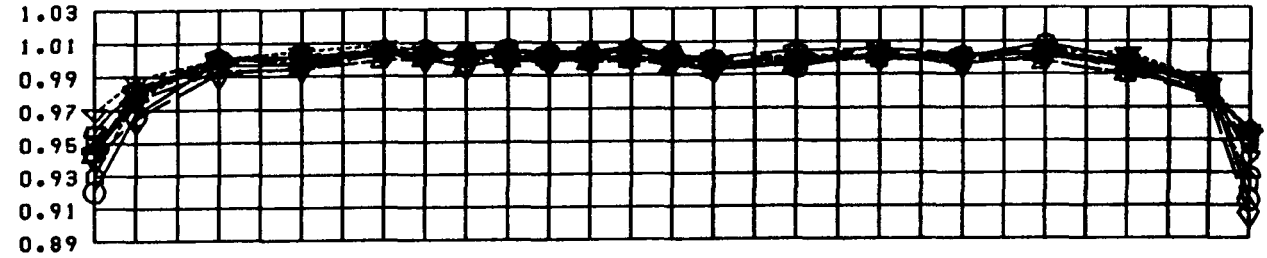

(c) REFERENCE MACH NUMBER 0.10.

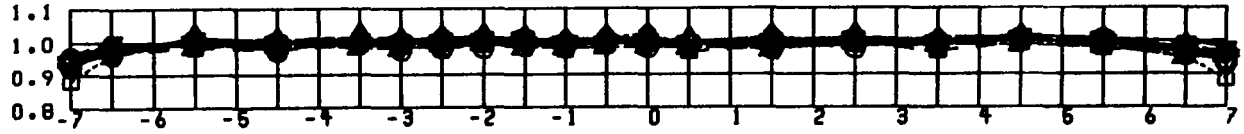

(d) REFERENCE MACH NUMBER 0.05.

FIGURE C-3. - MACH NUMBER PRESSURE CROSS-SECTIONAL PROFILES AT AXIAL SURVEY LOCATION 3 (TEST SECTION STATION 215).

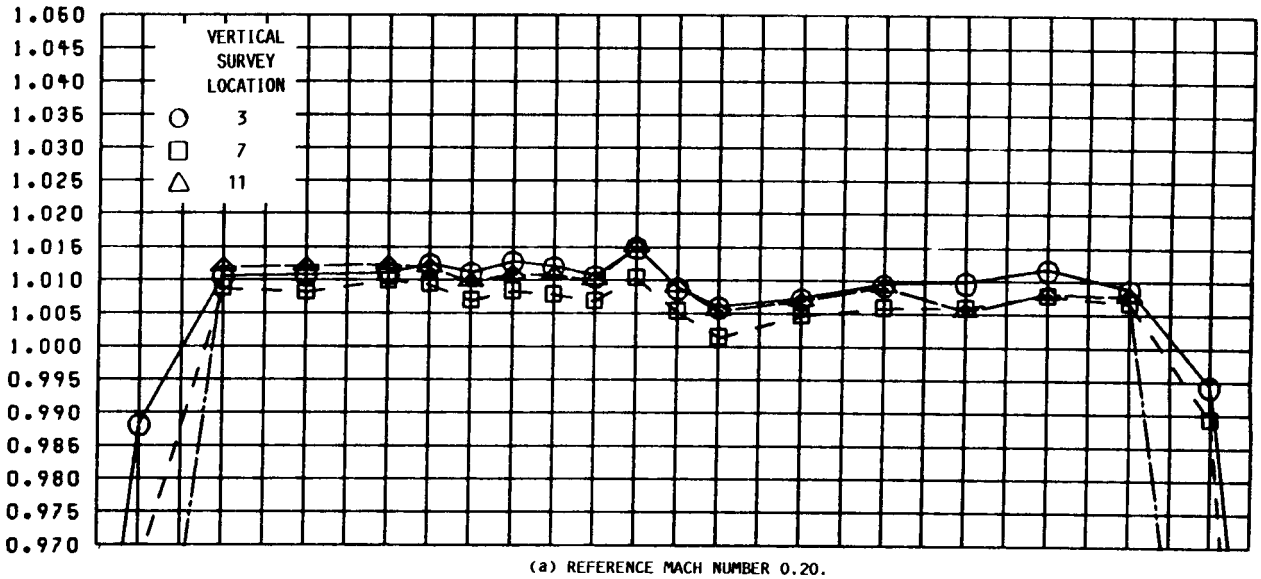

(a) REFERENCE MACH NUMBER 0.20.

MACH NUMBER RATIO, M/M_{REF}

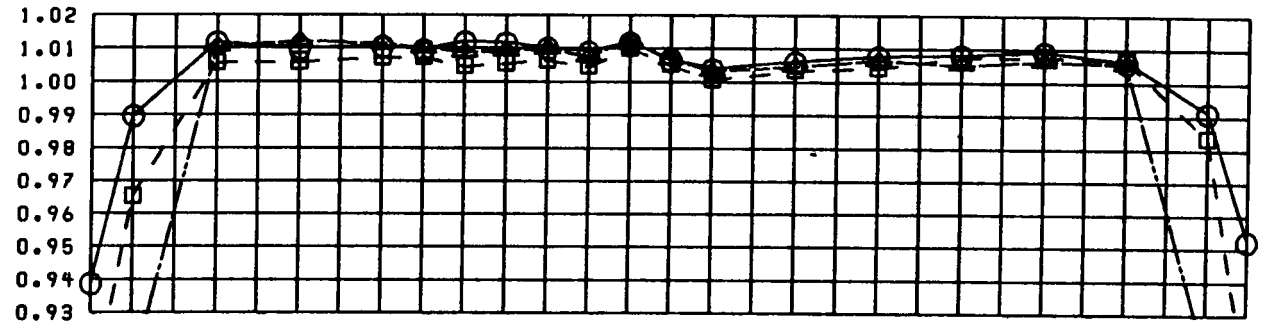

(b) REFERENCE MACH NUMBER 0.15.

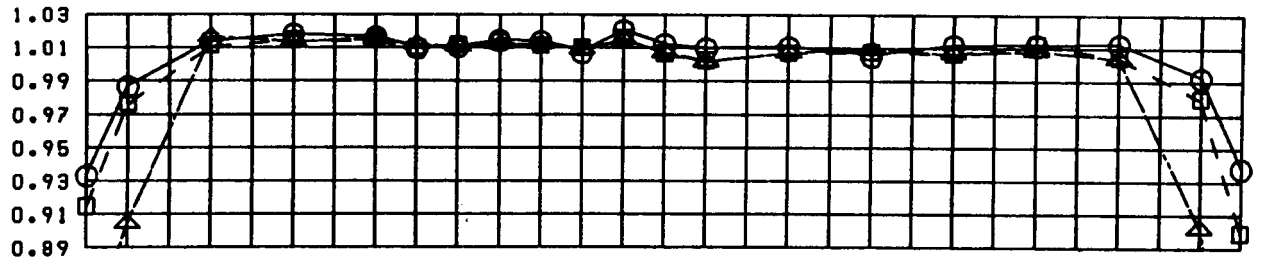

(c) REFERENCE MACH NUMBER 0.10.

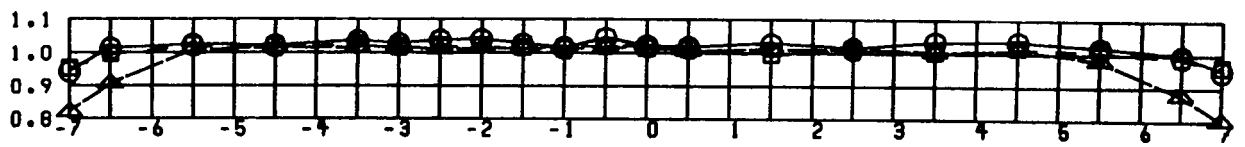

DISTANCE FROM TUNNEL CENTERLINE, FT

(d) REFERENCE MACH NUMBER 0.05.

FIGURE C-4. - MACH NUMBER PRESSURE CROSS-SECTIONAL PROFILES AT AXIAL SURVEY LOCATION 4 (TEST SECTION STATION 294).

APPENDIX D - TEST SECTION TOTAL PRESSURE AXIAL PROFILES

Figures D-1 through D-3 provide quantitative results on the axial total pressure profiles in the test section for reference Mach numbers 0.20, 0.15, 0.10, and 0.05 at vertical survey locations 3, 7, and 11 (table I) for axial survey locations 1 through 4 (fig. 9). The pressure ratio results are accurate to within ±0.004 psi (±0.030 percent). Some of the results within the test section boundary layer have been truncated for greater resolution of the results outside the boundary layer.

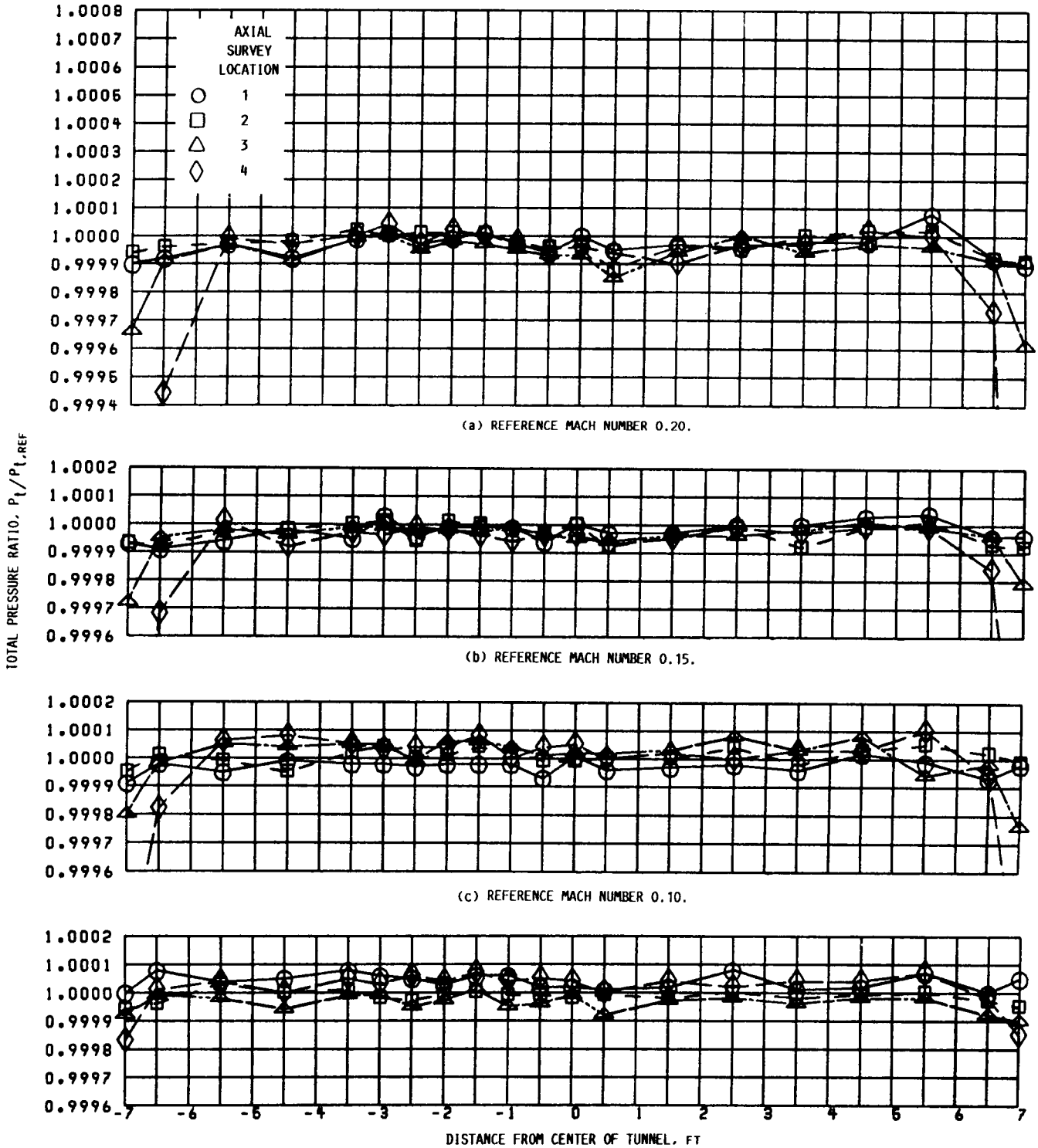

(a) REFERENCE MACH NUMBER 0.20.

(b) REFERENCE MACH NUMBER 0.15.

(c) REFERENCE MACH NUMBER 0.10.

(d) REFERENCE MACH NUMBER 0.05.

FIGURE D-1. - TOTAL PRESSURE AXIAL PROFILES AT VERTICAL SURVEY LOCATION 3 (2.5 FT) BELOW CENTER OF TUNNEL).

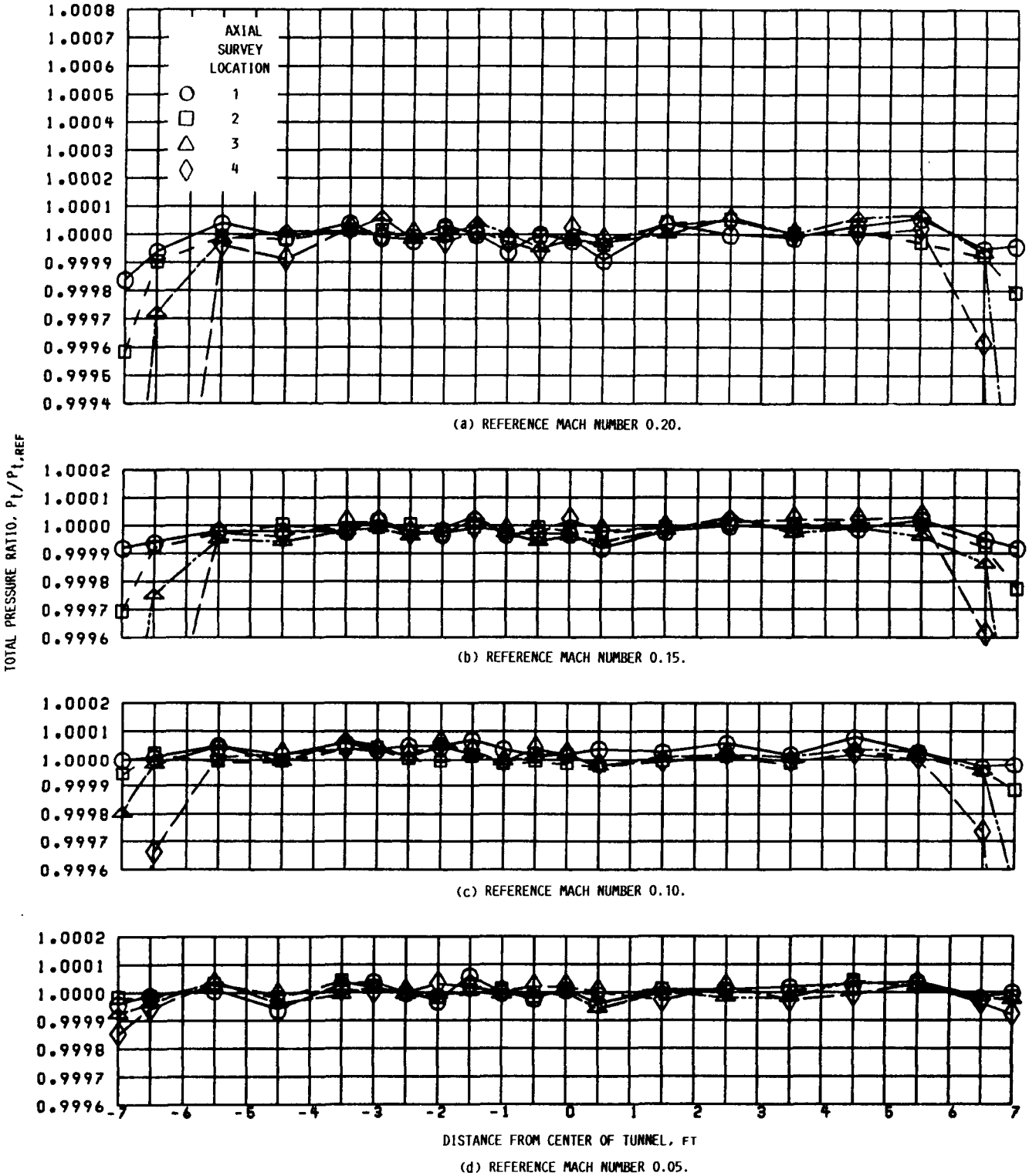

FIGURE D-2. - TOTAL PRESSURE AXIAL PROFILES AT VERTICAL SURVEY LOCATION 7 (AT CENTER OF TUNNEL).

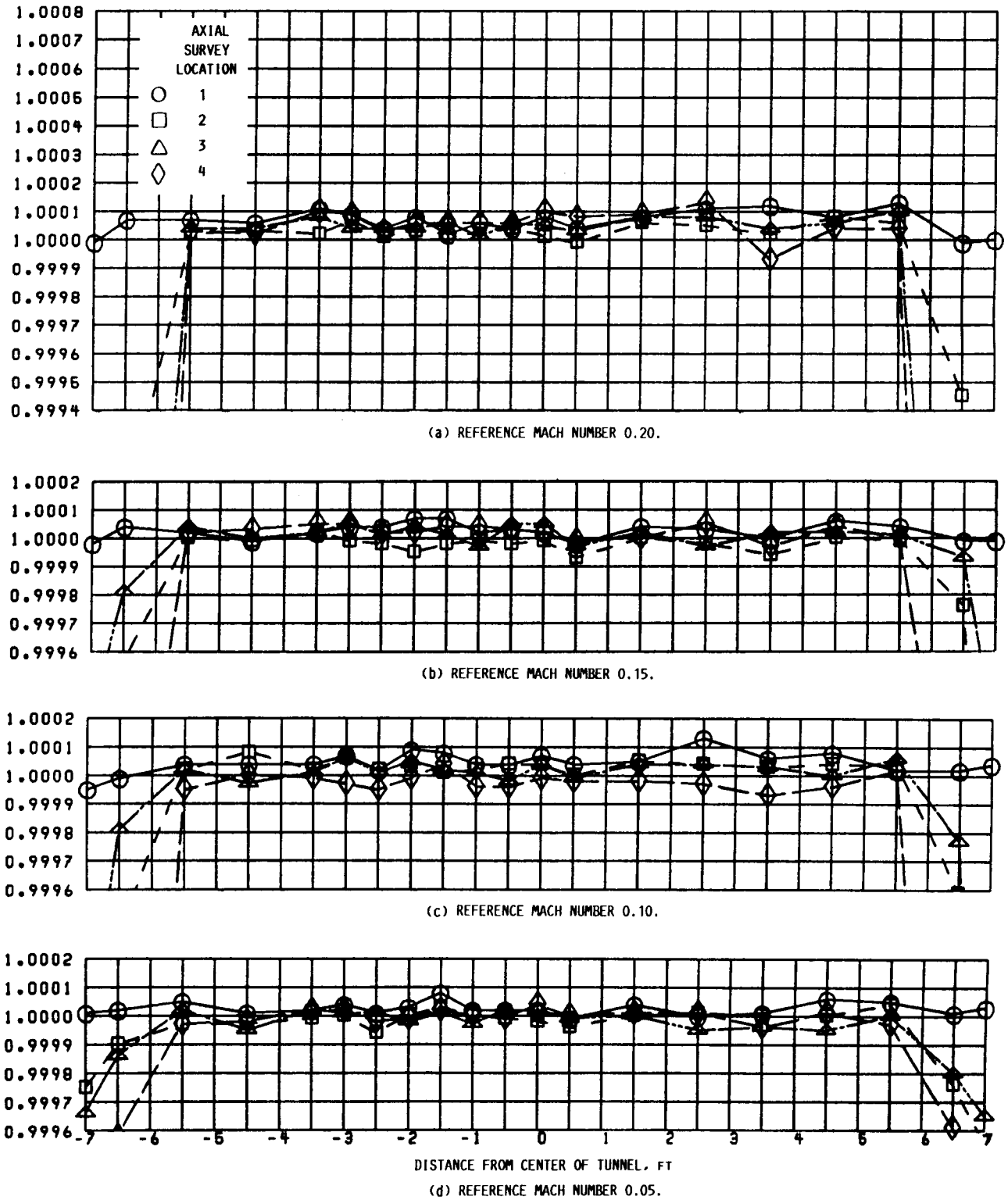

(a) REFERENCE MACH NUMBER 0.20.

(b) REFERENCE MACH NUMBER 0.15.

(c) REFERENCE MACH NUMBER 0.10.

(d) REFERENCE MACH NUMBER 0.05.

FIGURE D-3. - TOTAL PRESSURE AXIAL PROFILES AT VERTICAL SURVEY LOCATION 11 (2.5 FT ABOVE CENTER OF TUNNEL).

APPENDIX E - TEST SECTION STATIC PRESSURE AXIAL PROFILES

Figures E-1 through E-3 provide quantitative results on the axial static pressure profiles in the test section for reference Mach numbers 0.20, 0.15, 0.10, and 0.05 at vertical survey locations 3, 7, and 11 (table I) for axial survey locations 1 through 4 (fig. 9). The pressure ratio results are accurate to within ±0.004 psi (±0.030 percent). Some of the results within the test section boundary layer have been truncated for greater resolution of the results outside the boundary layer. Results shown near the center of the test section, at distances from 0 to 2 ft, are questionable because of possible hardware problems encountered with the flow survey rake.

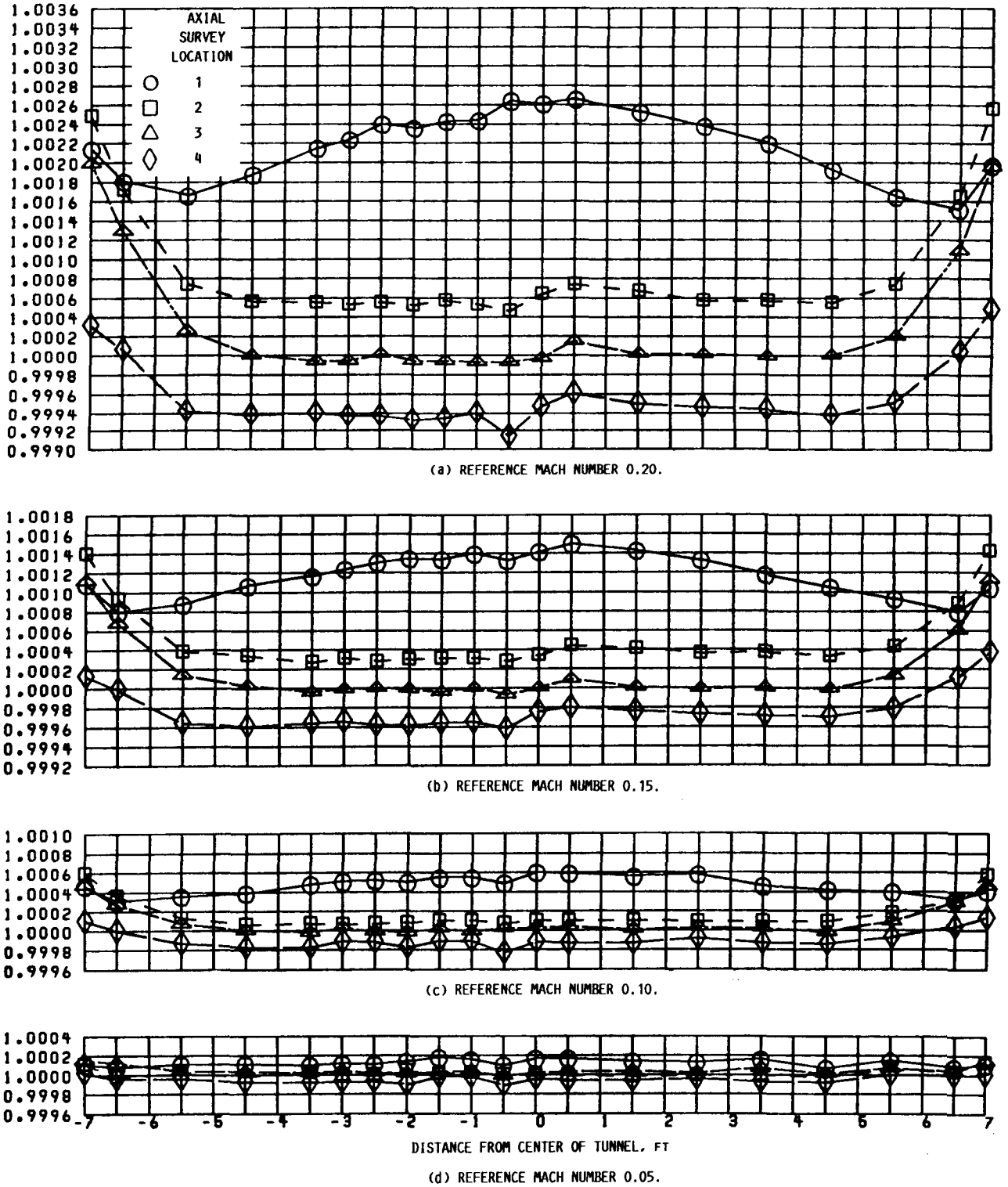

(a) REFERENCE MACH NUMBER 0.20.

(b) REFERENCE MACH NUMBER 0.15.

(c) REFERENCE MACH NUMBER 0.10.

(d) REFERENCE MACH NUMBER 0.05.

FIGURE E-1. - STATIC PRESSURE AXIAL PROFILES AT VERTICAL SURVEY LOCATION 3 (2.5 FT BELOW CENTER OF TUNNEL).

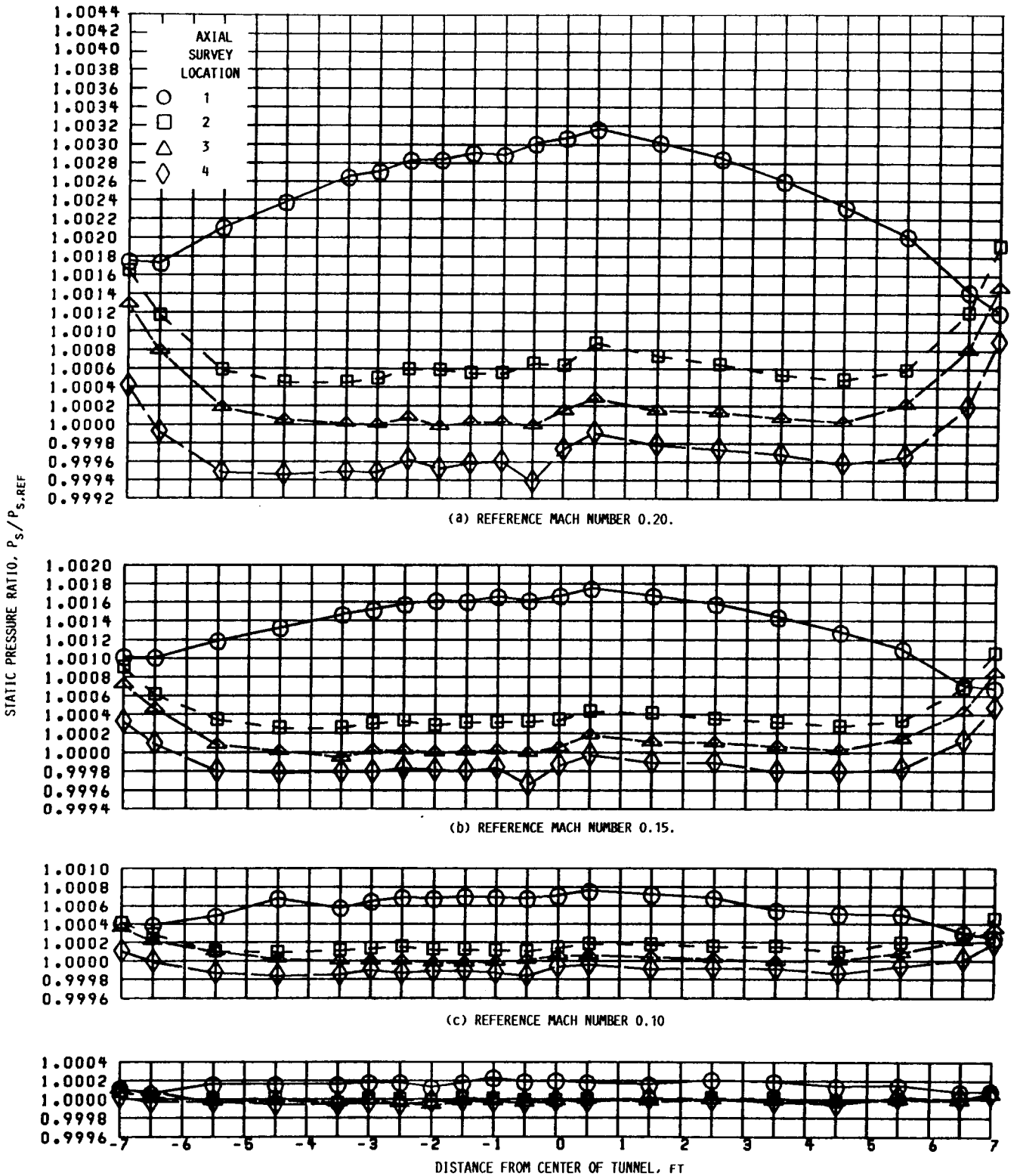

(a) REFERENCE MACH NUMBER 0.20.

(b) REFERENCE MACH NUMBER 0.15.

(c) REFERENCE MACH NUMBER 0.10

(d) REFERENCE MACH NUMBER 0.05.

FIGURE E-2. - STATIC PRESSURE AXIAL PROFILES AT VERTICAL SURVEY LOCATION 7 (AT CENTER OF TUNNEL).

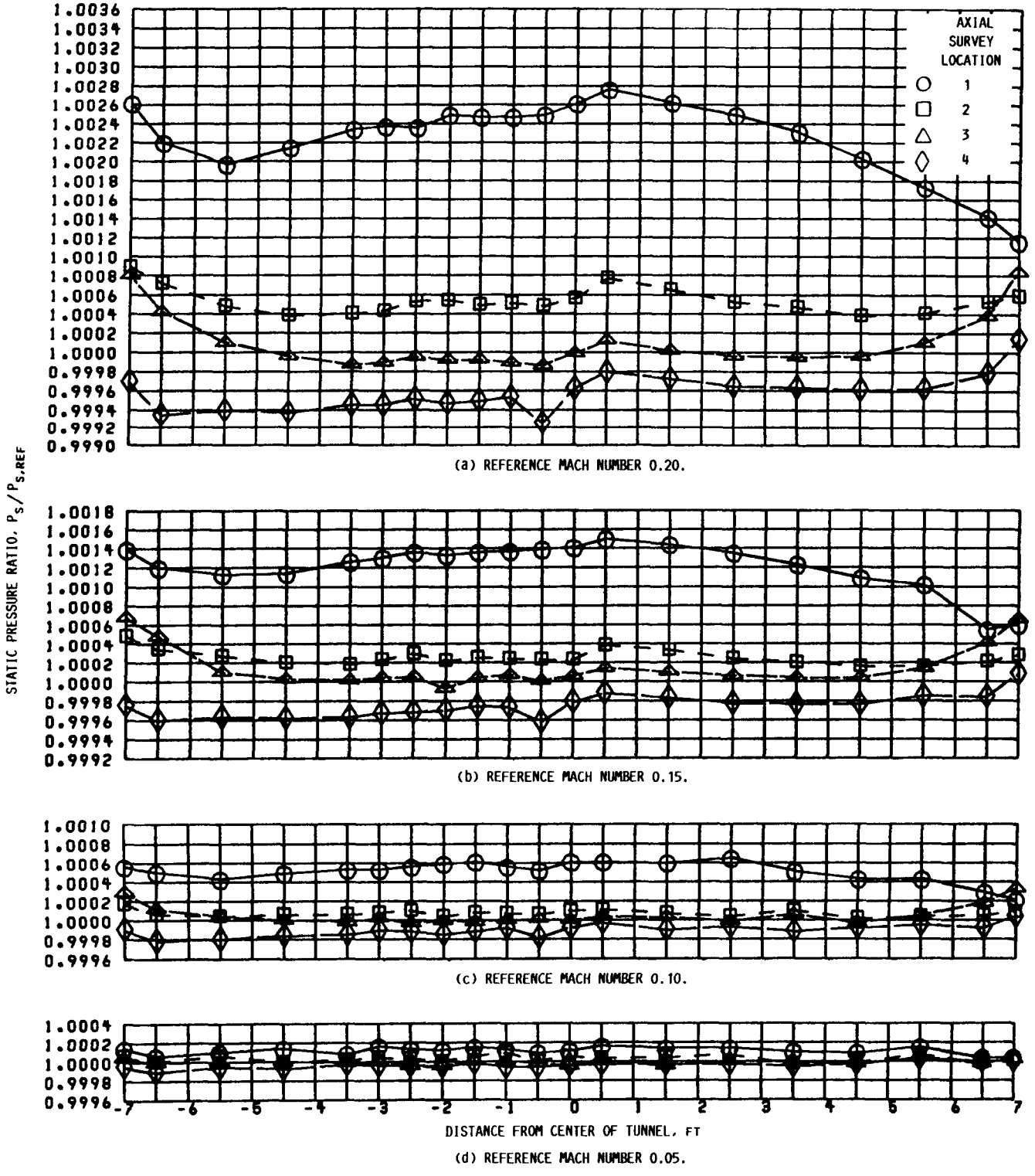

(a) REFERENCE MACH NUMBER 0.20.

(b) REFERENCE MACH NUMBER 0.15.

(c) REFERENCE MACH NUMBER 0.10.

(d) REFERENCE MACH NUMBER 0.05.

FIGURE E-3. - STATIC PRESSURE AXIAL PROFILES AT VERTICAL SURVEY LOCATION 11 (2.5 FT ABOVE CENTER OF TUNNEL).

APPENDIX F - TEST SECTION MACH NUMBER AXIAL PROFILES

Figures F-1 through F-3 provide quantitative results on the axial Mach number profiles in the test section for reference Mach numbers 0.20, 0.15, 0.10, and 0.05 at vertical survey locations 3, 7, and 11 (table I) for axial survey locations 1 through 4 (fig. 9). The Mach number ratio results are accurate to within ±0.004 psi (±1.0 percent at reference Mach number 0.20, ±1.5 percent at reference Mach number 0.15, ±4.0 percent at reference Mach number 0.10, and ±16.0 percent at reference Mach number 0.05). Some of the results within the test section boundary layer have been truncated for greater resolution of the results outside the boundary layer. Results shown near the center of the test section, at distances from 0 to 2 ft, are questionable because of possible hardware problems encountered with the flow survey rake.

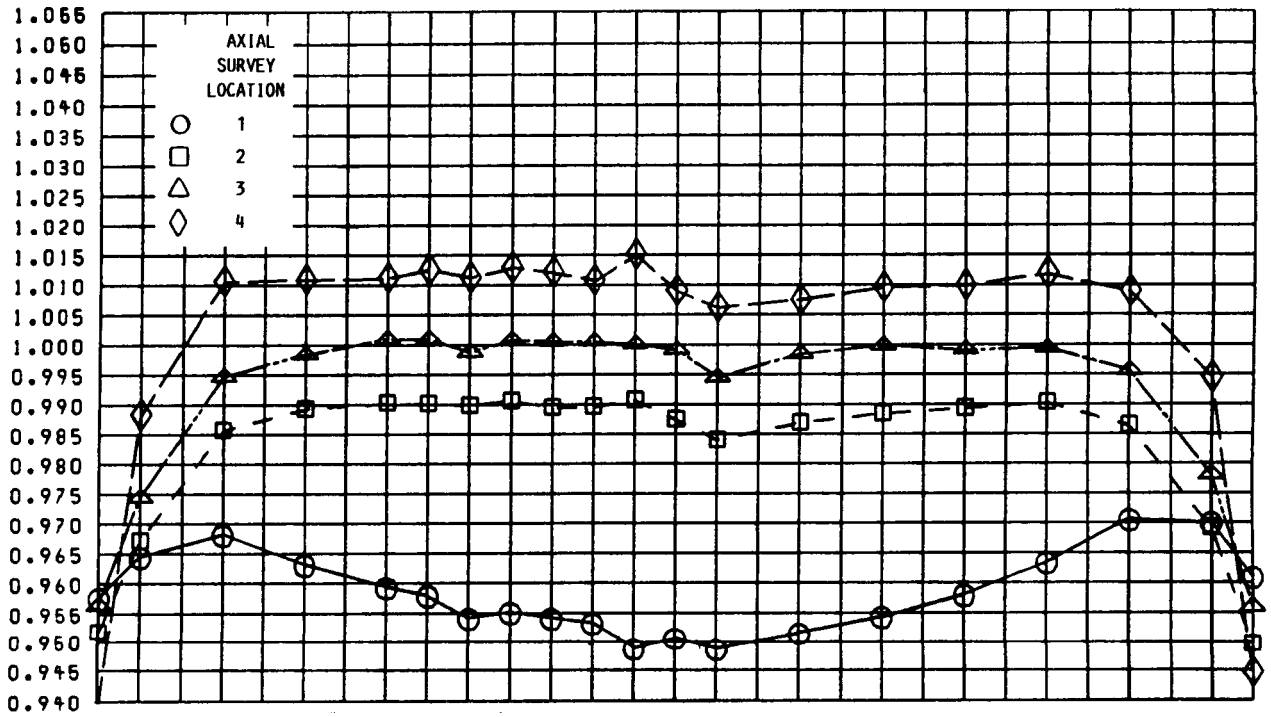

(a) REFERENCE MACH NUMBER 0.20.

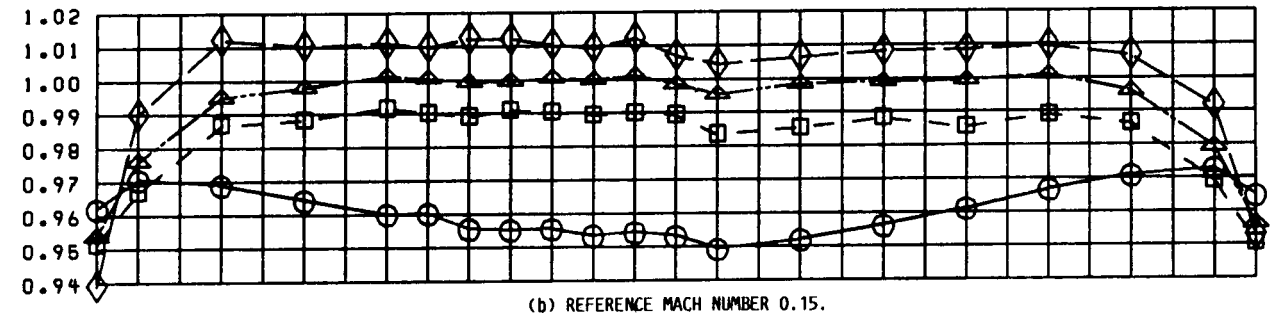

(b) REFERENCE MACH NUMBER 0.15.

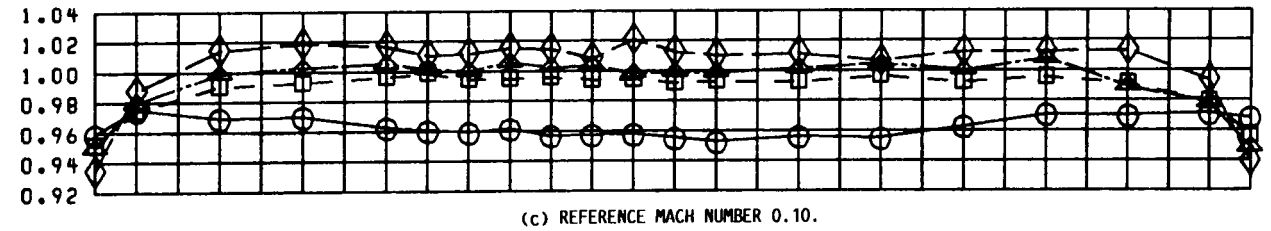

(c) REFERENCE MACH NUMBER 0.10.

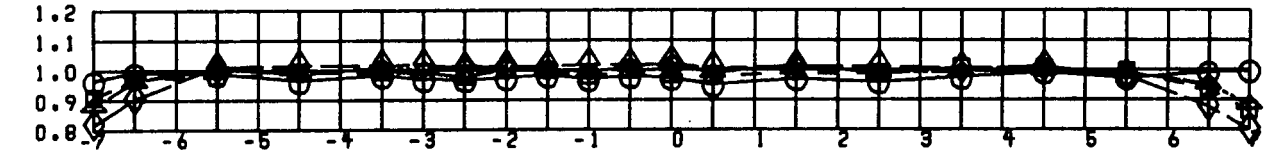

DISTANCE FROM TUNNEL CENTERLINE, FT

(d) REFERENCE MACH NUMBER 0.05.

MACH NUMBER RATIO, M/M_{REF}

FIGURE F-1. - MACH NUMBER AXIAL PROFILES AT VERTICAL SURVEY LOCATION 3 (2.5 FT BELOW CENTER OF TUNNEL).

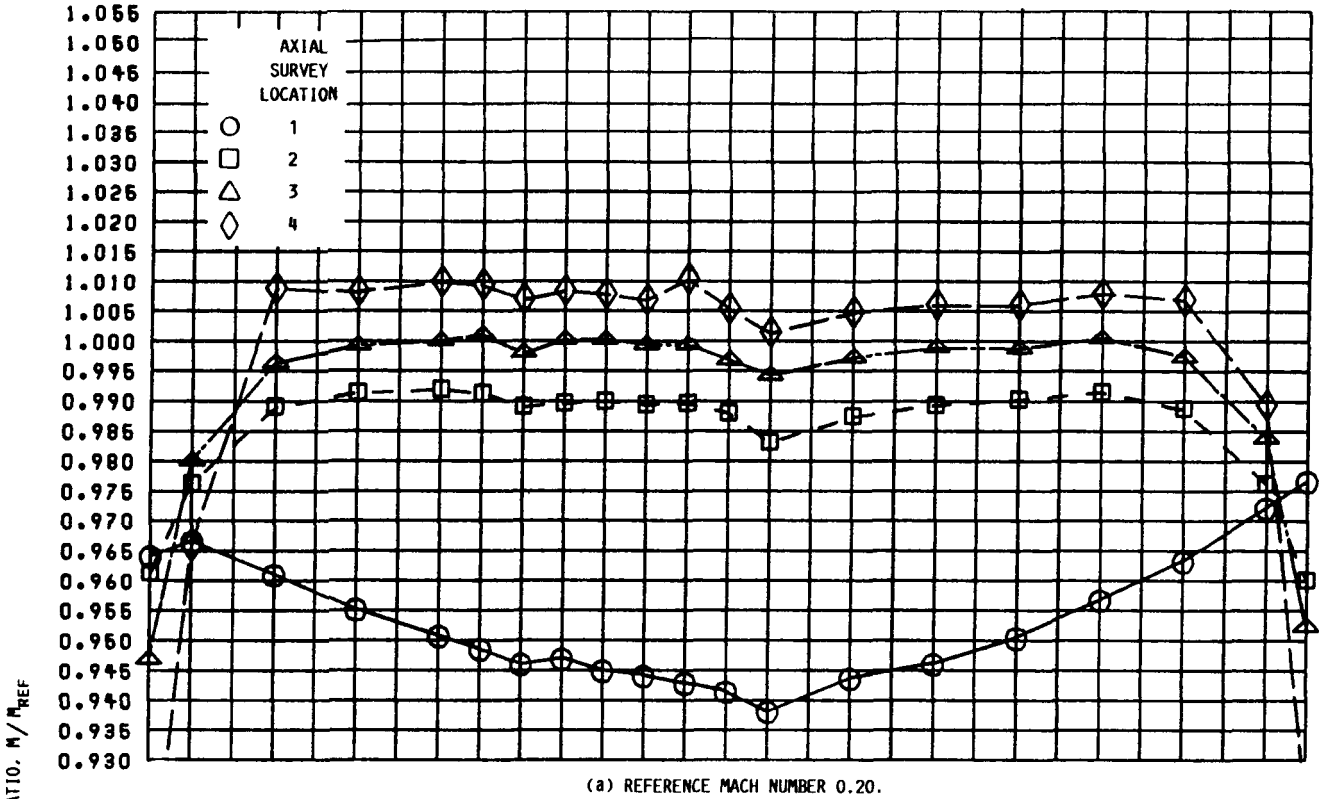

(a) REFERENCE MACH NUMBER 0.20.

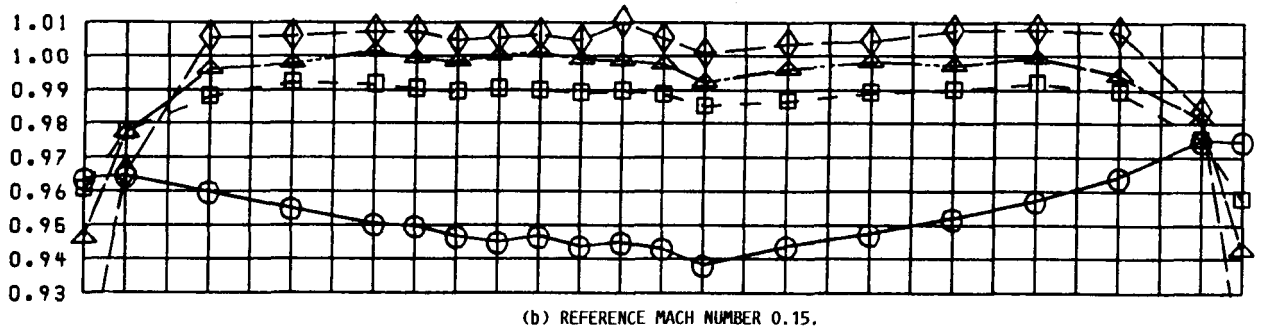

(b) REFERENCE MACH NUMBER 0.15.

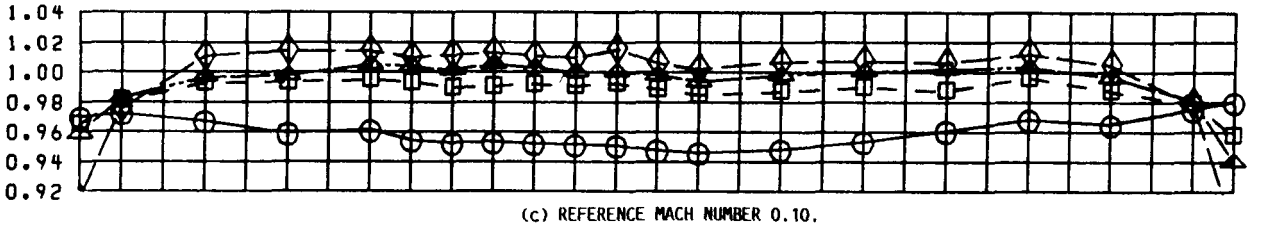

(c) REFERENCE MACH NUMBER 0.10.

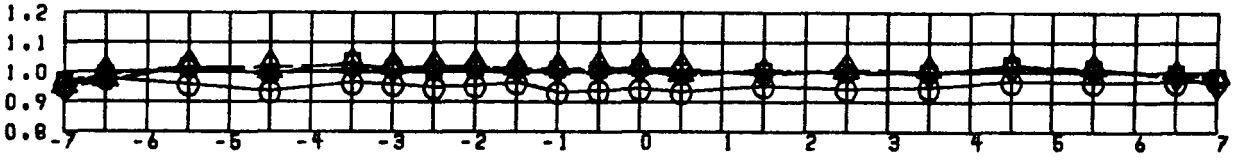

(d) REFERENCE MACH NUMBER 0.05.

FIGURE F-2. - MACH NUMBER AXIAL PROFILES AT VERTICAL SURVEY LOCATION 7 (AT CENTER OF TUNNEL).

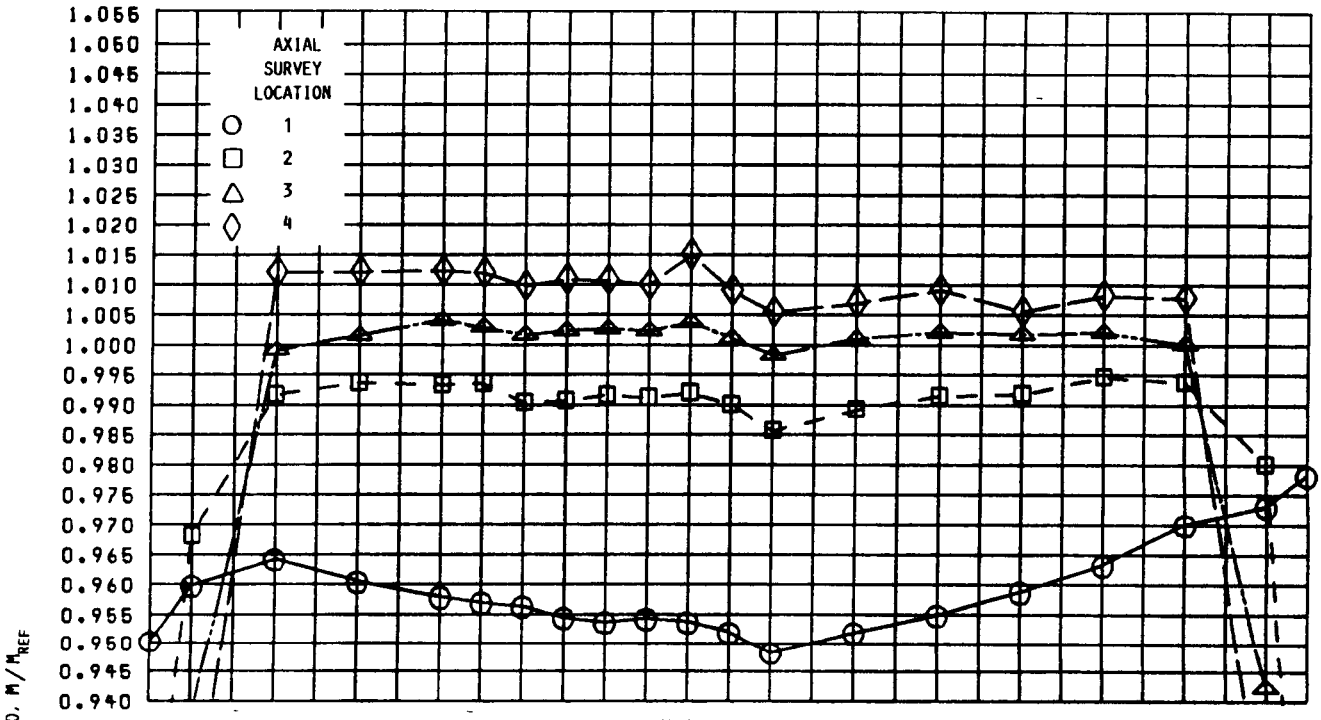

(a) REFERENCE MACH NUMBER 0.20.

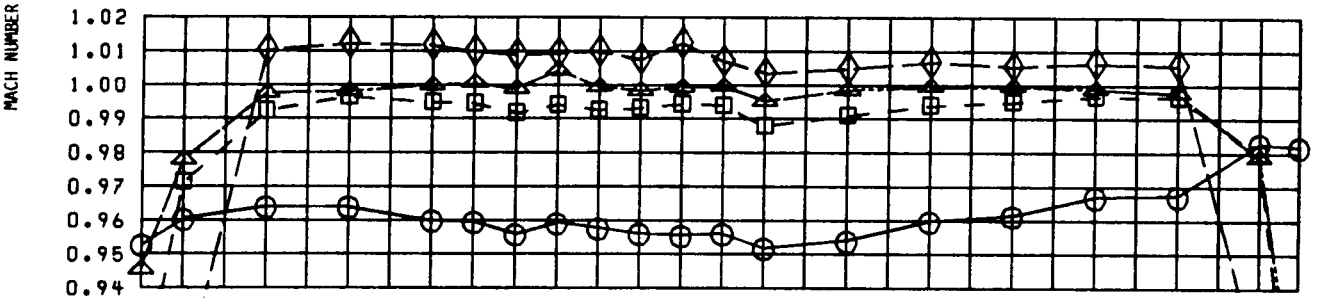

(b) REFERENCE MACH NUMBER 0.15.

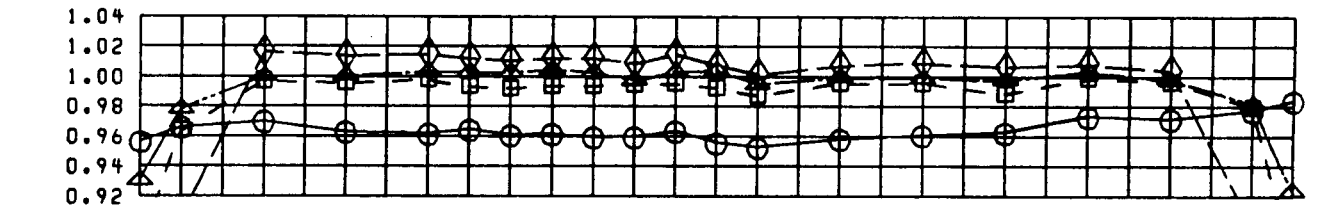

(c) REFERENCE MACH NUMBER 0.10.

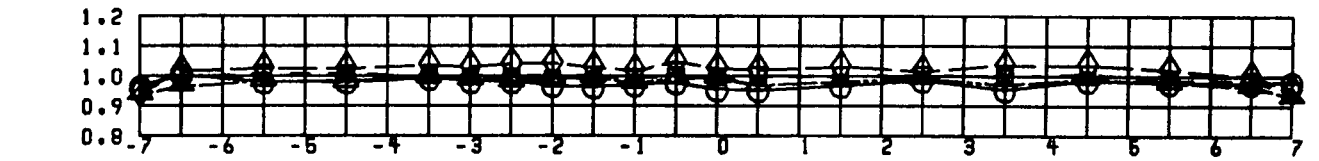

(d) REFERENCE MACH NUMBER 0.05.

MACH NUMBER RATIO, M/M_{REF}

FIGURE F-3. - MACH NUMBER AXIAL PROFILES AT VERTICAL SURVEY LOCATION 11 (2.5 FT ABOVE CENTER OF TUNNEL).

APPENDIX G - WIND TUNNEL RAKE INSTRUMENTATION PRESSURE CALIBRATION EQUATIONS

The tunnel freestream total pressure is a function of the tunnel reference total pressure, the normalized reference Q, and the derived equation constants. While using the upstream wind tunnel rake to obtain the tunnel reference operating conditions, the freestream total pressure is

$$P_{t,0} = (A_1 + K_1 A_2) P_{t,1}$$

where

K_1 normalized reference Q, $(P_{t,1} - P_{s,1})/P_{t,1}$
A_1 1.00000960
A_2 -0.00031153

The tunnel freestream static pressure is a function of the tunnel reference static pressure, the normalized reference Q, and the derived equation constants. While using the upstream wind tunnel rake to obtain the tunnel reference operating conditions, the freestream static pressure is

$$P_{s,0} = (B_1 + K_1 B_2) P_{s,1}$$

where

K_1 normalized reference Q, $(P_{t,1} - P_{s,1})/P_{t,1}$
B_1 1.00001660
B_2 -0.05561240

By using the downstream wind tunnel rake to obtain the tunnel reference operating conditions, the tunnel freestream total pressure from the reference total pressure is

$$P_{t,0} = (C_1 + K_2 C_2) P_{t,2}$$

where

K_2 normalized reference Q, $(P_{t,2} - P_{s,2})/P_{t,2}$
C_1 1.00001350
C_2 -0.00403159

By using the downstream wind tunnel rake to obtain the tunnel reference operating conditions, the tunnel freestream static pressure from the reference static pressure is

$$P_{s,0} = (D_1 + K_2 D_2) P_{s,2}$$

where

K_2 normalized reference Q, $(P_{t,2} - P_{s,2})/P_{t,2}$
D_1 0.99998397
D_2 0.01670421

REFERENCES

1. Yuska, J.; Diedrich, J.H.; and Clough, N.: Lewis 9- by 15-Foot V/STOL Wind Tunnel. NASA TM X-2305, 1971.

TABLE I. - TYPICAL BOUNDARY LAYER SURVEY RAKE DIMENSIONS

(a) Forward

Probe number	Distance from tunnel surface, in.
1	0.71
2	1.86
3	2.79
4	3.61
5	4.34
6	5.00
7	5.62

(b) Model test plane

Probe number	Distance from tunnel surface, in.	Probe number	Distance from tunnel surface, in.	Probe number	Distance from tunnel surface, in.
1	0.325	9	4.325	17	8.325
2	0.875	10	4.875	18	8.875
3	1.325	11	5.325	19	9.325
4	1.875	12	5.875	20	9.875
5	2.325	13	6.325	21	10.325
6	2.875	14	6.875	22	10.875
7	3.325	15	7.325	23	11.325
8	3.875	16	7.875	24	11.875

(c) Aft

Probe number	Distance from tunnel surface, in.	Probe number	Distance from tunnel surface, in.
1	0.12	9	9.04
2	0.52	10	11.06
3	1.17	11	12.01
4	2.04	12	13.23
5	3.02	13	15.62
6	4.22	14	18.22
7	5.62	15	21.01
8	7.22	16	24.02

TABLE II. - TEST SECTION
VERTICAL SURVEY
LOCATIONS

Vertical survey location	Distance from center of test section, ft
11	2.5
10	[a]1.5
9	[a]1.0
8	[a]0.5
7	0.0
6	[a,b]0.5
5	[a,b]1.0
4	[a,b]1.5
3	[b]2.5
2	[a,b]3.5

[a]Vertical survey locations at axial survey location 3 only.
[b]Distances below center of tunnel.

TABLE III. - PRESSURE AND MACH NUMBER RATIO PROFILE VARIATIONS AT REFERENCE MACH NUMBER 0.20

[Values without parentheses represent variations from axial survey locations 1 to 4, and values in parentheses represent variations from axial survey locations 2 to 4.]

(a) Cross-sectional

Axial survey location	$\frac{P_{t,max} - P_{t,min}}{P_{t,ref}} \cdot 100$, percent	$\frac{P_{s,max} - P_{s,min}}{P_{s,ref}} \cdot 100$, percent	$\frac{M_{max} - M_{min}}{M_{ref}} \cdot 100$, percent
1	0.021	0.126	2.59
2	.020	.021	0.56
3	.019	.018	.69
4	.023	.030	.60

(b) Axial

Vertical survey location	$\frac{P_{t,max} - P_{t,min}}{P_{t,ref}} \cdot 100$, percent	$\frac{P_{s,max} - P_{s,min}}{P_{s,ref}} \cdot 100$, percent	$\frac{M_{max} - M_{min}}{M_{ref}} \cdot 100$, percent
3	0.007	0.309 (0.123)	5.78 (2.26)
7	.006	.333 (.097)	6.27 (1.79)
11	.009	.297 (.100)	5.69 (1.91)

TABLE IV. - WIND TUNNEL RAKE TO MODEL CENTERLINE PRESSURE RATIO VARIATIONS AT REFERENCE MACH NUMBER 0.20

Wind tunnel rake location	$\frac{P_t - P_{t,cl}}{P_t} \cdot 100$, percent	$\frac{P_s - P_{s,cl}}{P_s} \cdot 100$, percent	$\frac{M - M_{cl}}{M} \cdot 100$, percent
[a]1	0.002	0.153	-2.65
[b]2	.009	-.041	0.90

[a]Upstream wind tunnel rake.
[b]Downstream wind tunnel rake.

TABLE V. - TEST SECTION BOUNDARY LAYER THICKNESS AT REFERENCE MACH NUMBER 0.20

Boundary layer survey location	Survey rake number	Boundary layer thickness, in.
Forward	1	2.7
	2	3.3
	3	3.3
	4	3.5
	5	2.8
	6	3.4
	7	3.2
Model test plane	--	5.3
Aft	8	9.2
	9	9.4
	10	13.3
	11	10.0
	12	7.3
	13	7.3
	14	10.0
	15	13.8

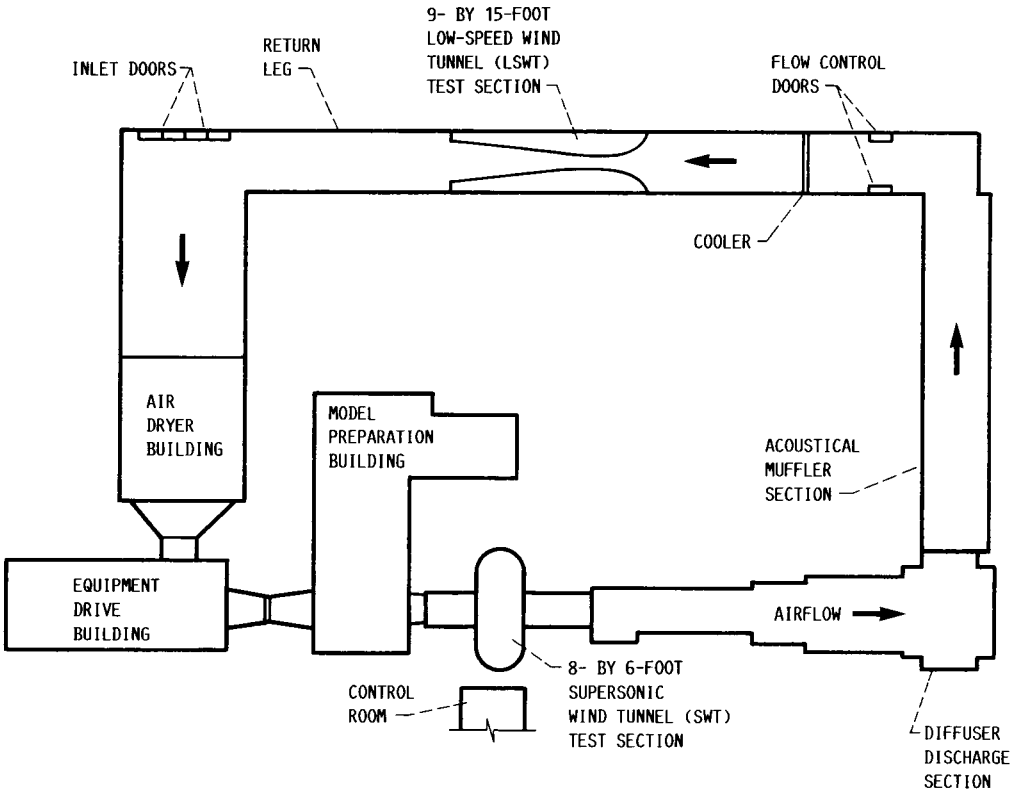

(a) OVERALL PLAN VIEW.

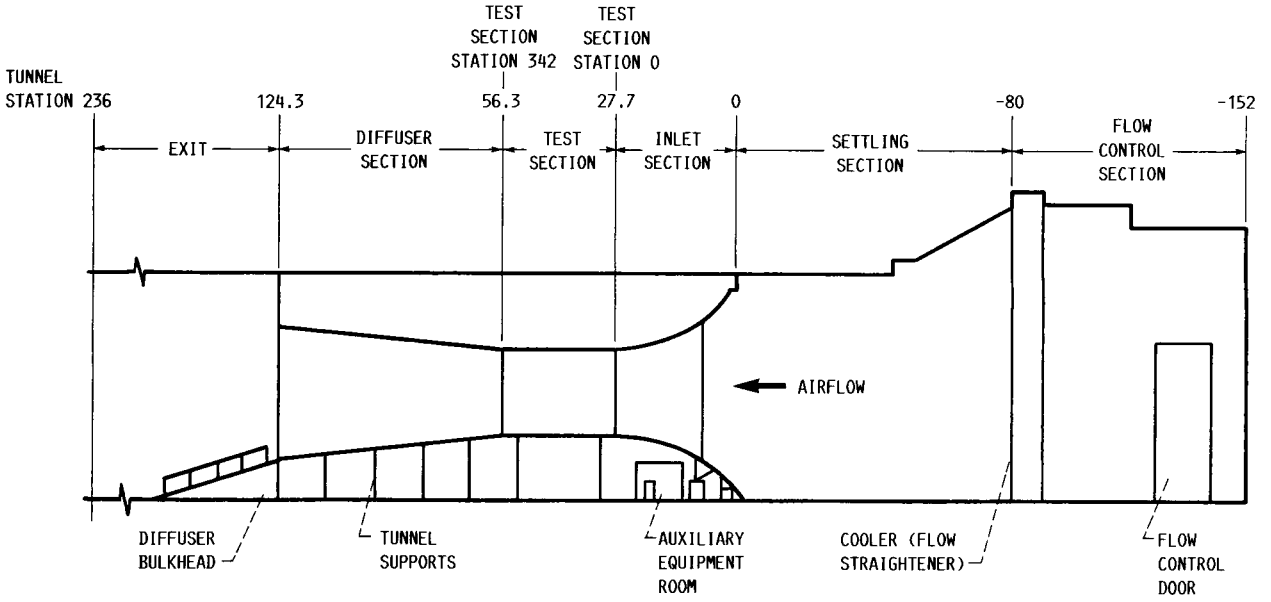

(b) SCHEMATIC ELEVATION VIEW OF 9- BY 15-FOOT SECTION.

FIGURE 1. - GEOMETRY OF NASA LEWIS RESEARCH CENTER 9- BY 15-FOOT LOW-SPEED WIND TUNNEL.

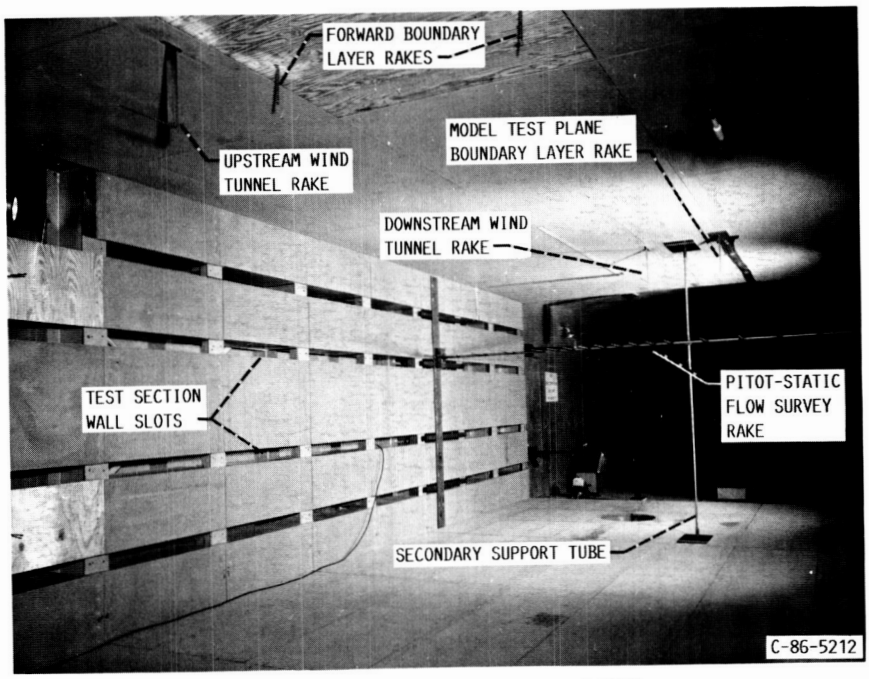

(a) TEST SECTION ENTRANCE, DOWNSTREAM VIEW.

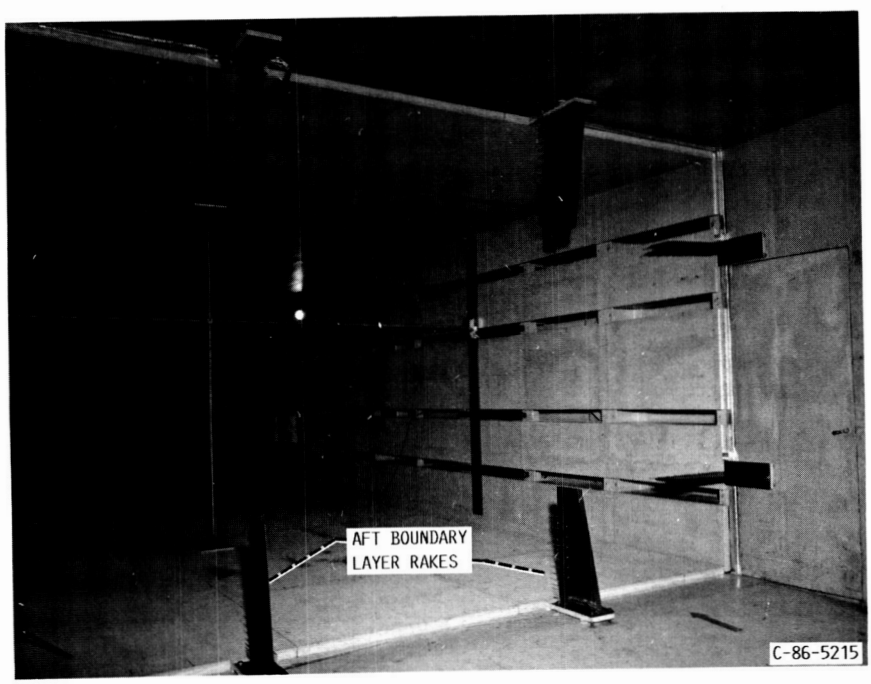

(b) TEST SECTION EXIT, UPSTREAM VIEW.

FIGURE 2. - INSTRUMENTATION USED IN TEST SECTION FLOWFIELD INVESTIGATION.

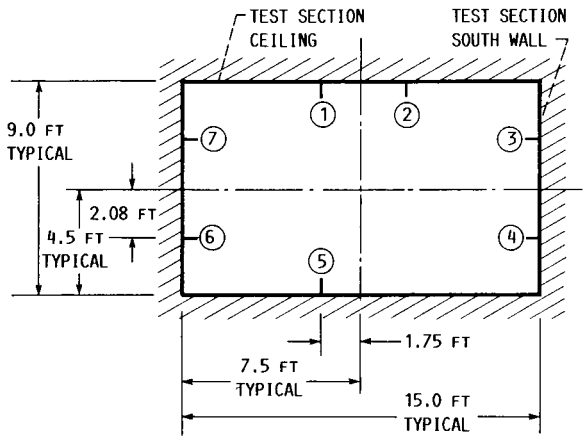

(a) FORWARD BOUNDARY LAYER, TEST SECTION STATION 28 (NEAR TEST SECTION ENTRANCE), DOWNSTREAM VIEW.

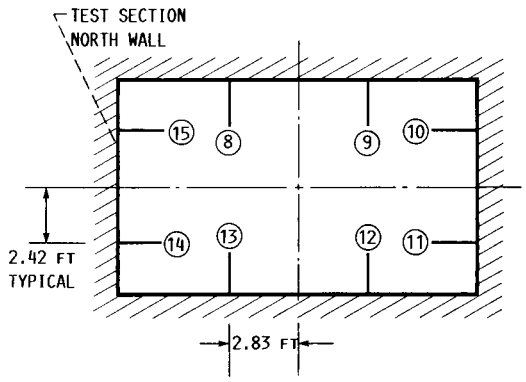

(b) AFT BOUNDARY LAYER, TEST SECTION STATION 336 (NEAR TEST SECTION EXIT), DOWNSTREAM VIEW.

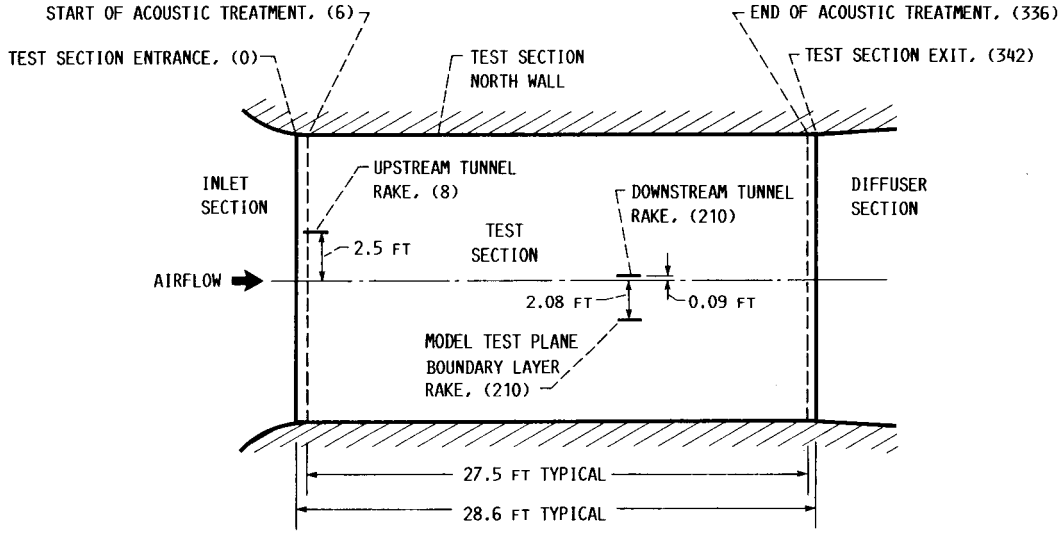

(c) WIND TUNNEL (TEST SECTION STATIONS 8 AND 215) AND MODEL TEST PLANE BOUNDARY LAYER (TEST SECTION STATION 210), VIEW FROM ABOVE TEST SECTION CEILING.

FIGURE 3. - WIND TUNNEL AND BOUNDARY LAYER SURVEY RAKE LOCATIONS IN TEST SECTION.

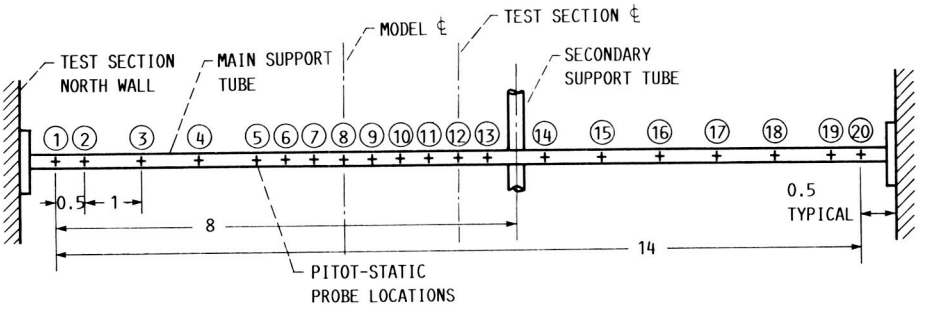

(a) SCHEMATIC OF FLOW SURVEY RAKE (DIMENSIONS IN FT).

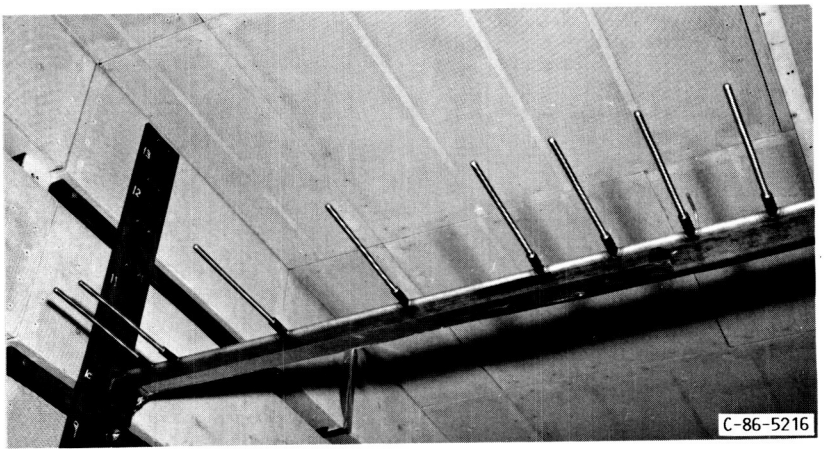

(b) FLOW SURVEY RAKE MOUNTED IN TEST SECTION, VIEW OF TEST SECTION NORTH WALL AND CEILING.

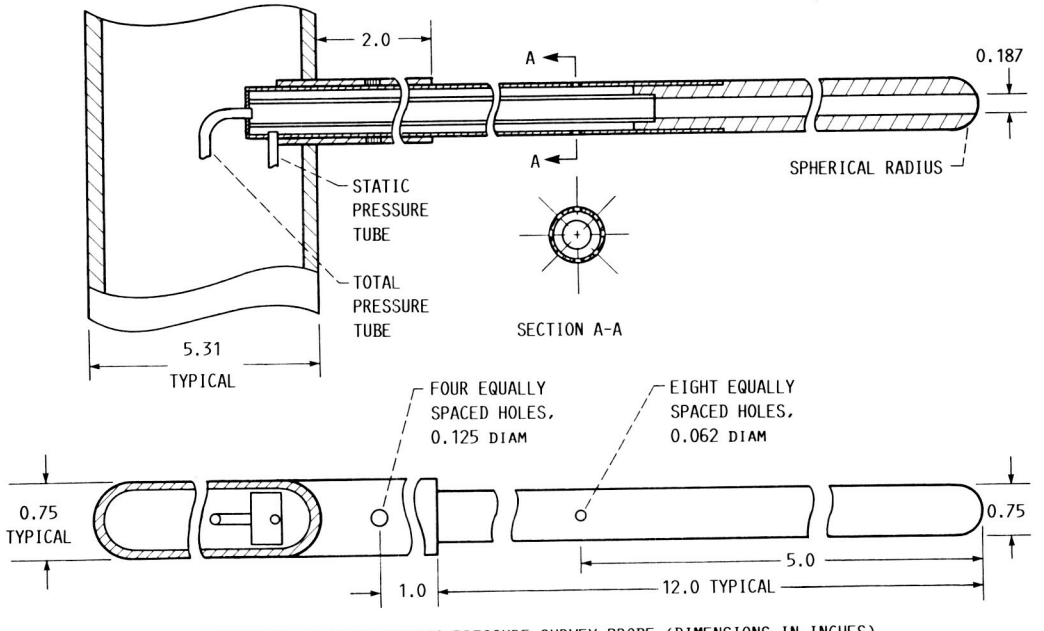

(c) SCHEMATIC OF PITOT-STATIC PRESSURE SURVEY PROBE (DIMENSIONS IN INCHES).

FIGURE 4. - PITOT-STATIC FLOW SURVEY RAKE USED IN FLOWFIELD INVESTIGATION.

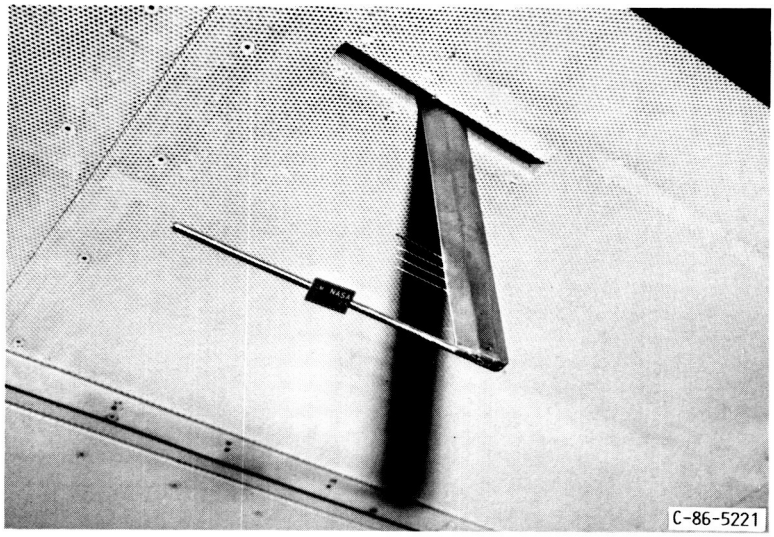

(a) DOWNSTREAM WIND TUNNEL RAKE, TEST SECTION STATION 210 (NEAR MODEL TEST PLANE).

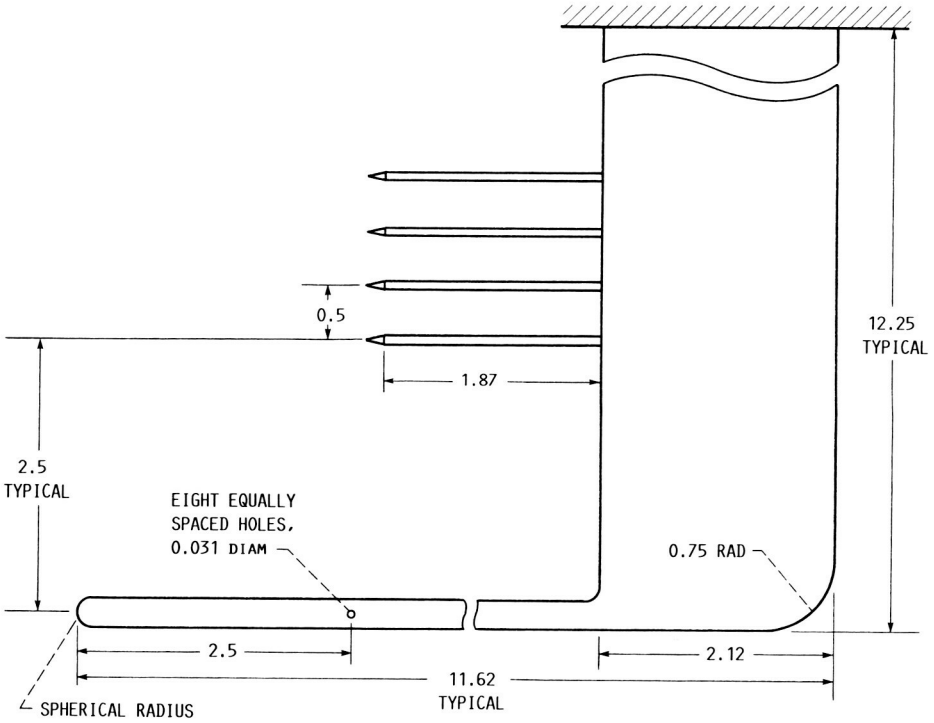

(b) SCHEMATIC OF WIND TUNNEL RAKE (DIMENSIONS IN INCHES).

FIGURE 5. - WIND TUNNEL RAKE INSTRUMENTATION IN TEST SECTION.

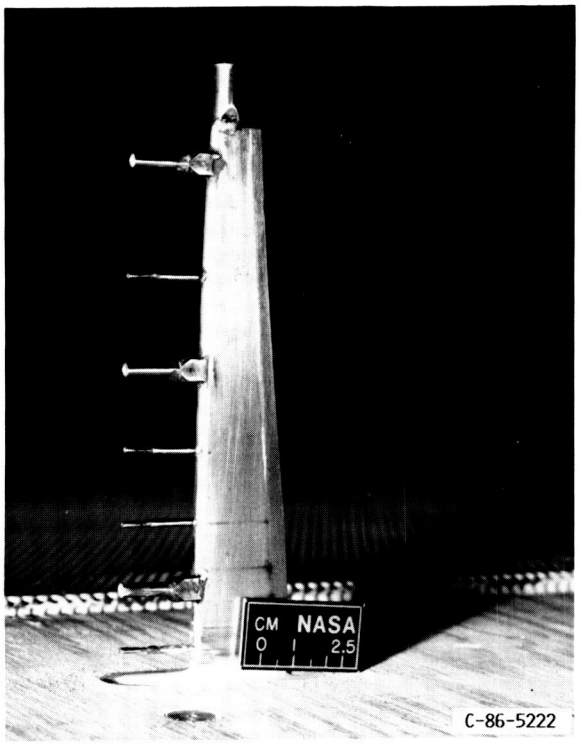

(a) FORWARD BOUNDARY LAYER SURVEY RAKE 5, ON TEST SECTION FLOOR.

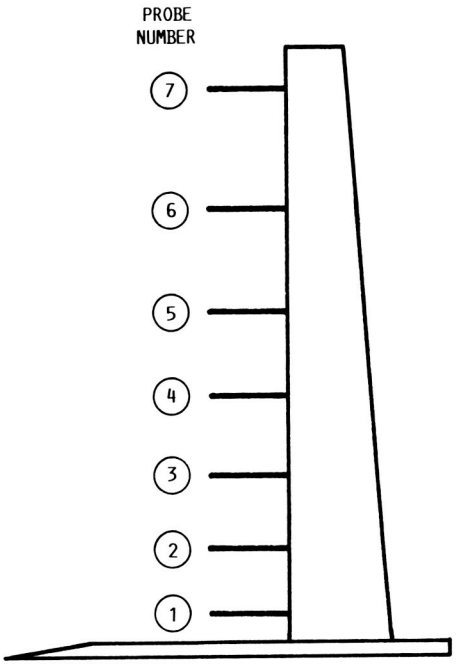

(b) SCHEMATIC OF TOTAL PRESSURE PROBE LOCATIONS ON RAKE.

FIGURE 6. - TYPICAL FORWARD BOUNDARY LAYER SURVEY RAKE AT TEST SECTION STATION 28 (NEAR TEST SECTION ENTRANCE).

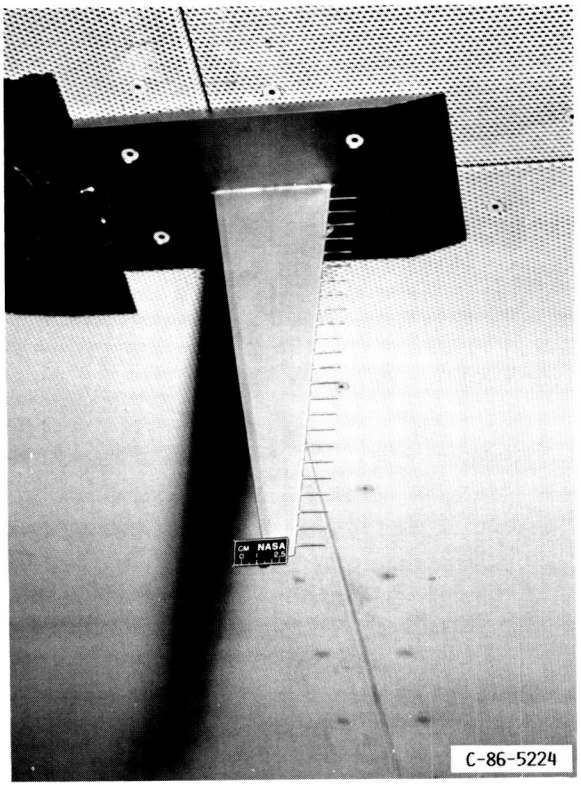

(a) MODEL TEST PLANE BOUNDARY LAYER SURVEY RAKE, ON TEST SECTION CEILING.

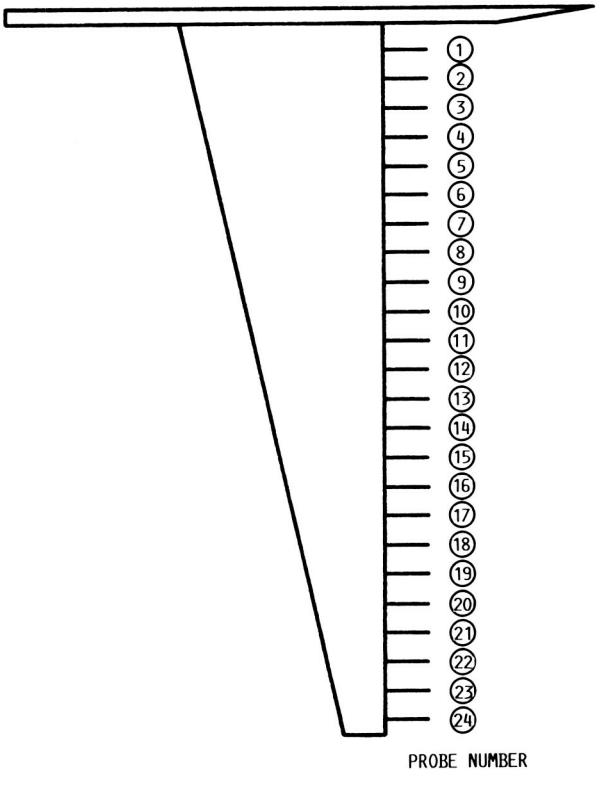

(b) SCHEMATIC OF TOTAL PRESSURE PROBE LOCATIONS ON RAKE.

FIGURE 7. - MODEL TEST PLANE BOUNDARY LAYER SURVEY RAKE AT TEST SECTION STATION 210.

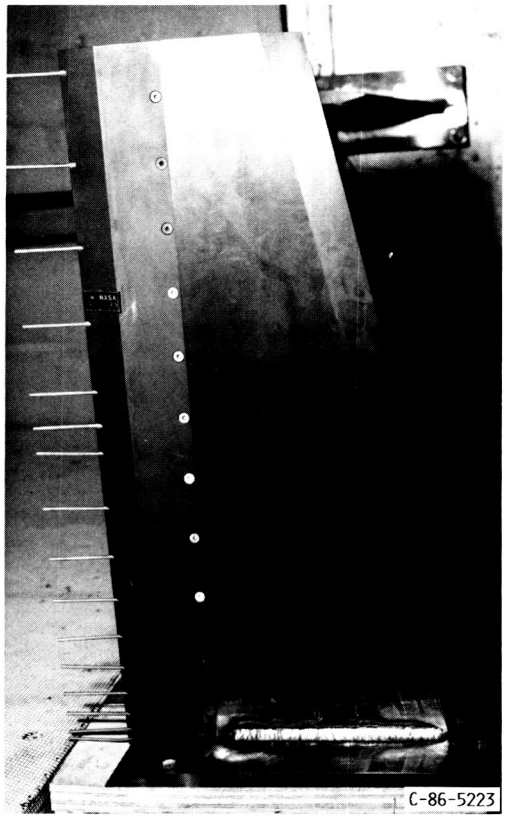

(a) AFT BOUNDARY LAYER SURVEY RAKE 13, ON TEST SECTION FLOOR.

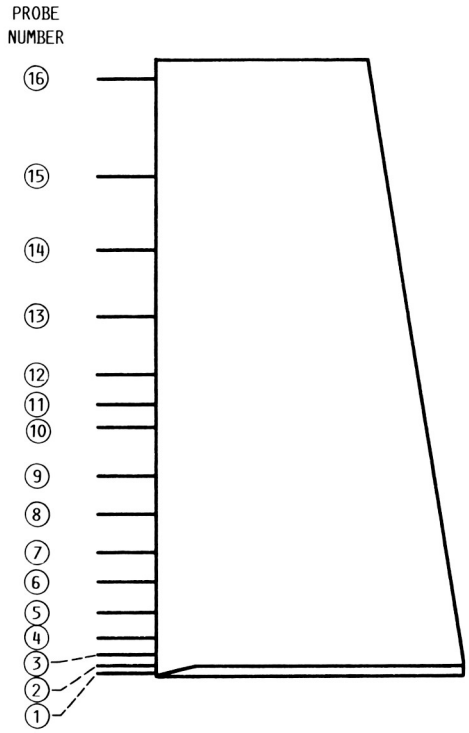

(b) SCHEMATIC OF TOTAL PRESSURE PROBE LOCATIONS ON RAKE.

FIGURE 8. - TYPICAL AFT BOUNDARY LAYER SURVEY RAKE AT TEST SECTION STATION 336 (NEAR TEST SECTION EXIT).

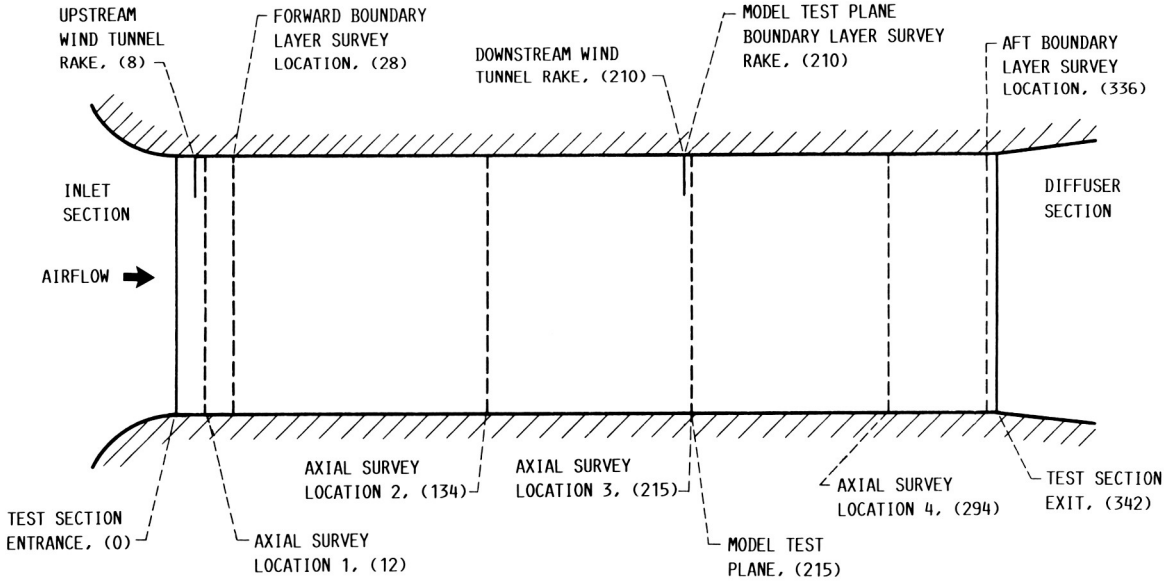

FIGURE 9. - LOCATION OF WIND TUNNEL AND BOUNDARY LAYER SURVEY RAKE INSTRUMENTATION AND AXIAL FLOWFIELD SURVEYS IN TEST SECTION (TEST SECTION STATION NUMBERS IN PARENTHESIS).

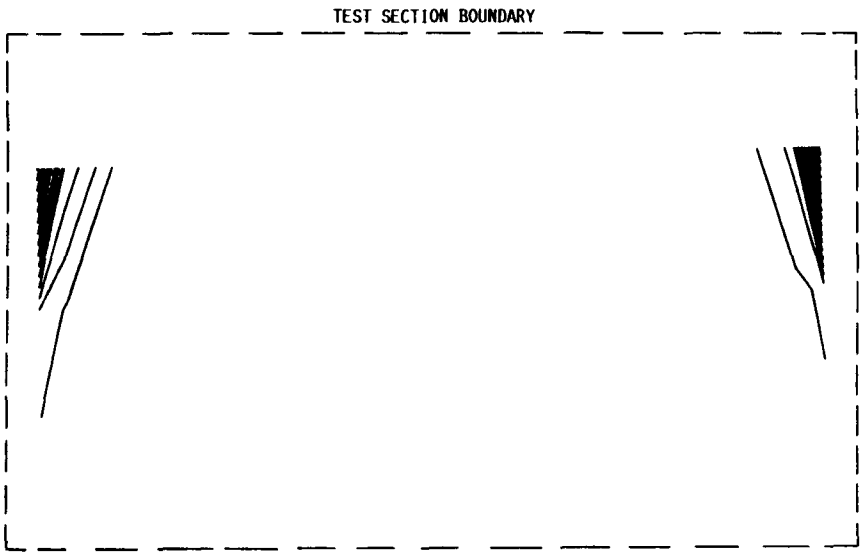

(a) AXIAL SURVEY LOCATION 2 (TEST SECTION STATION 134) AT REFERENCE MACH NUMBER 0.20.

(b) AXIAL SURVEY LOCATION 2 (TEST SECTION STATION 134) AT REFERENCE MACH NUMBER 0.15.

(c) AXIAL SURVEY LOCATION 2 (TEST SECTION STATION 134) AT REFERENCE MACH NUMBER 0.10.

FIGURE 10. - TOTAL PRESSURE CROSS-SECTIONAL PROFILES, DOWNSTREAM VIEW. DASHED OUTLINE REPRESENTS TEST SECTION CROSS-SECTIONAL BOUNDARY. CONTOUR LEVELS REPRESENT PRESSURE DIFFERENCES OF ±0.004 PSI.

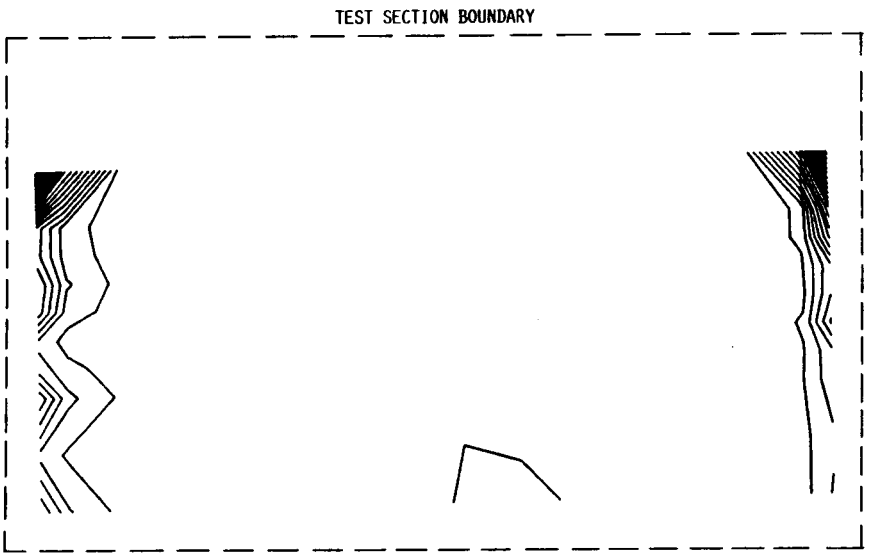

(d) AXIAL SURVEY LOCATION 3 (TEST SECTION STATION 215) AT REFERENCE MACH NUMBER 0.20.

(e) AXIAL SURVEY LOCATION 3 (TEST SECTION STATION 215) AT REFERENCE MACH NUMBER 0.15.

(f) AXIAL SURVEY LOCATION 3 (TEST SECTION STATION 215) AT REFERENCE MACH NUMBER 0.10.

FIGURE 10. - CONTINUED.

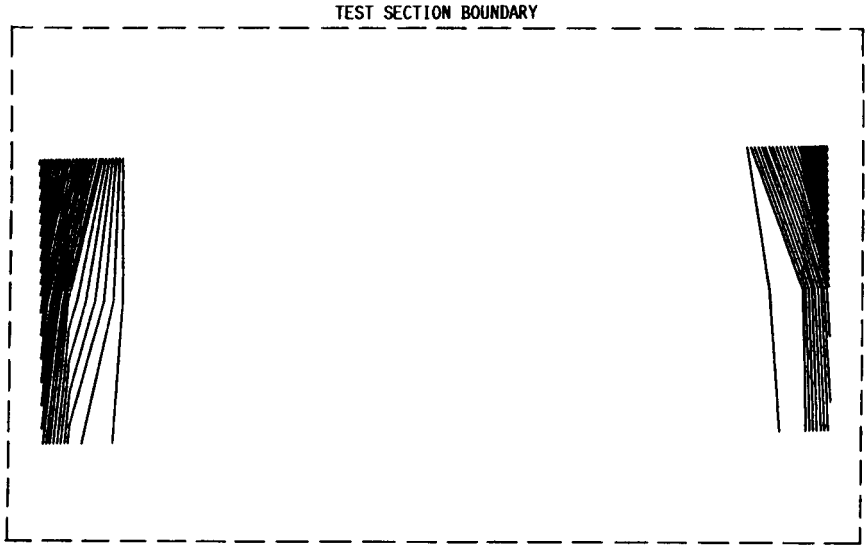

(g) AXIAL SURVEY LOCATION 4 (TEST SECTION STATION 294) AT REFERENCE MACH NUMBER 0.20.

(h) AXIAL SURVEY LOCATION 4 (TEST SECTION STATION 294) AT REFERENCE MACH NUMBER 0.15.

(i) AXIAL SURVEY LOCATION 4 (TEST SECTION STATION 294) AT REFERENCE MACH NUMBER 0.10.

FIGURE 10. - CONCLUDED.

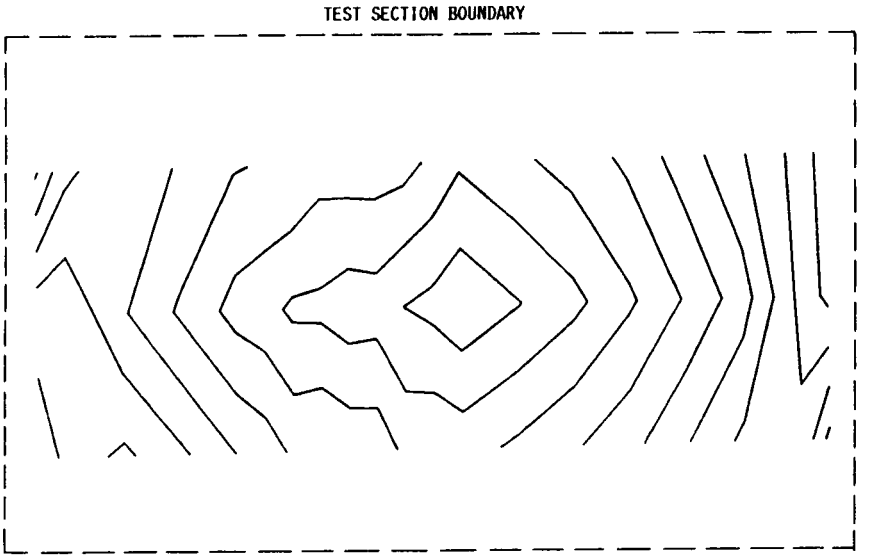

(a) AXIAL SURVEY LOCATION 1 (TEST SECTION STATION 12) AT REFERENCE MACH NUMBER 0.20.

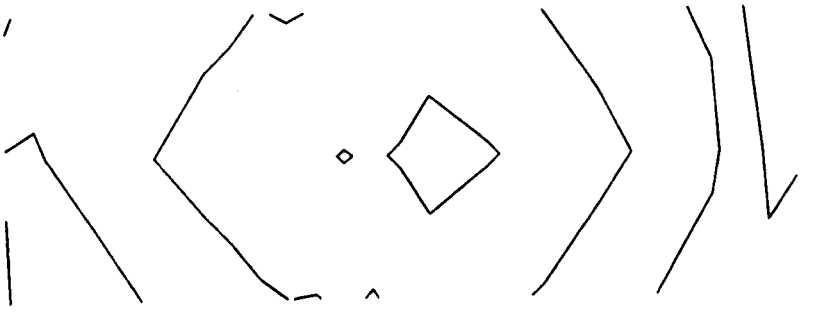

(b) AXIAL SURVEY LOCATION 1 (TEST SECTION STATION 12) AT REFERENCE MACH NUMBER 0.15.

(c) AXIAL SURVEY LOCATION 1 (TEST SECTION STATION 12) AT REFERENCE MACH NUMBER 0.10.

FIGURE 11. - STATIC PRESSURE CROSS-SECTIONAL PROFILES, DOWNSTREAM VIEW. DASHED OUTLINE REPRESENTS TEST SECTION CROSS-SECTIONAL BOUNDARY. CONTOUR LEVELS REPRESENT PRESSURE DIFFERENCES OF ±0.004 PSI.

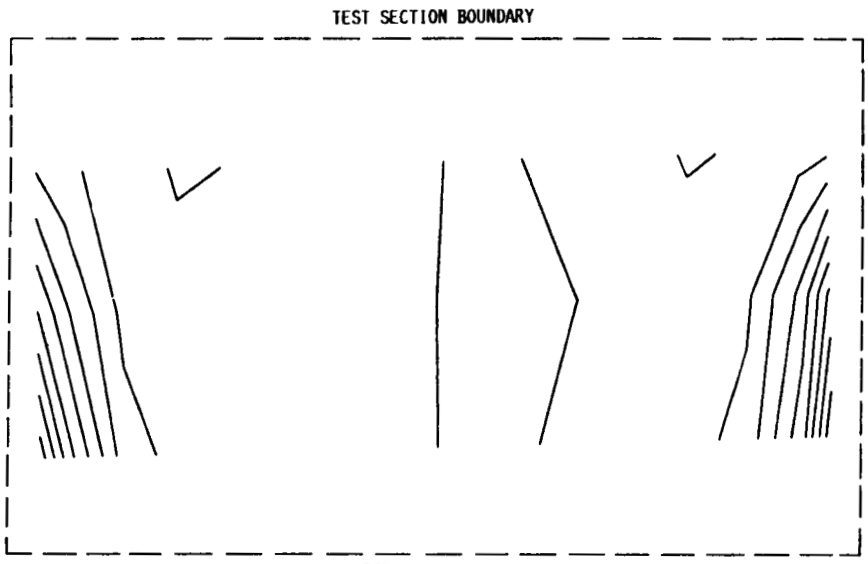

(d) AXIAL SURVEY LOCATION 2 (TEST SECTION STATION 134) AT REFERENCE MACH NUMBER 0.20.

(e) AXIAL SURVEY LOCATION 2 (TEST SECTION STATION 134) AT REFERENCE MACH NUMBER 0.15.

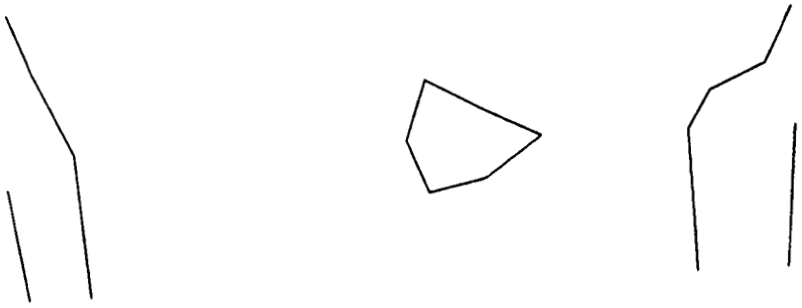

(f) AXIAL SURVEY LOCATION 2 (TEST SECTION STATION 134) AT REFERENCE MACH NUMBER 0.10.

FIGURE 11. - CONTINUED.

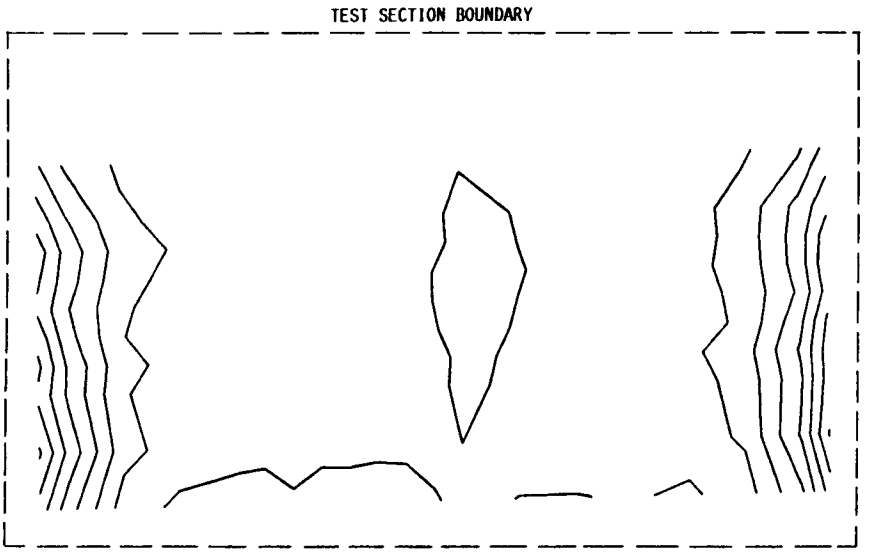

(g) AXIAL SURVEY LOCATION 3 (TEST SECTION STATION 215) AT REFERENCE MACH NUMBER 0.20.

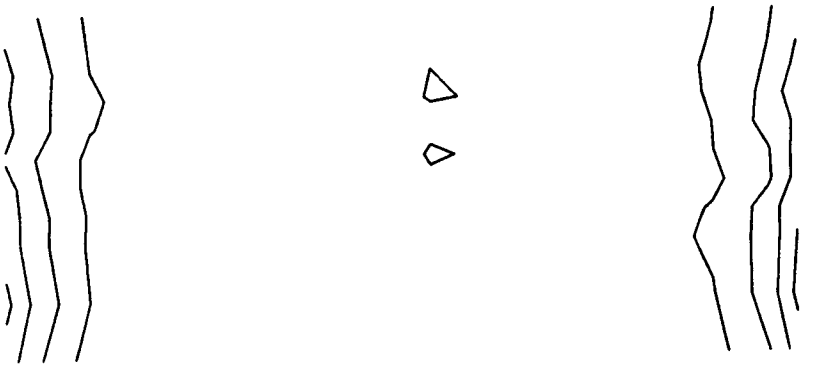

(h) AXIAL SURVEY LOCATION 3 (TEST SECTION STATION 215) AT REFERENCE MACH NUMBER 0.15.

(i) AXIAL SURVEY LOCATION 3 (TEST SECTION STATION 215) AT REFERENCE MACH NUMBER 0.10.

FIGURE 11. - CONTINUED.

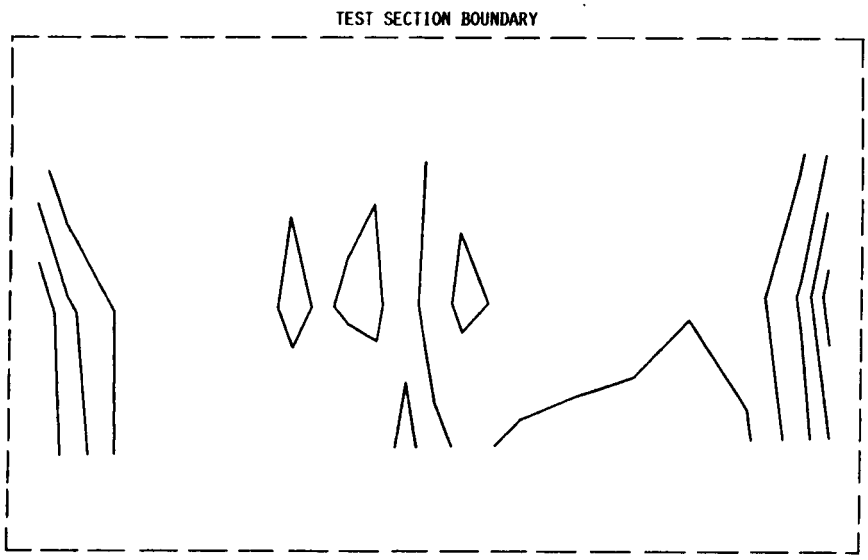

(j) AXIAL SURVEY LOCATION 4 (TEST SECTION STATION 294) AT REFERENCE MACH NUMBER 0.20.

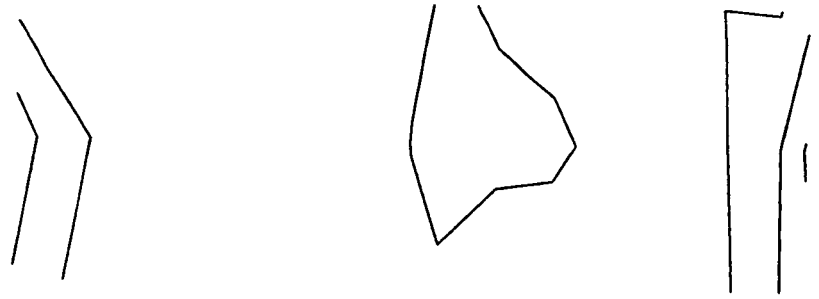

(k) AXIAL SURVEY LOCATION 4 (TEST SECTION STATION 294) AT REFERENCE MACH NUMBER 0.15.

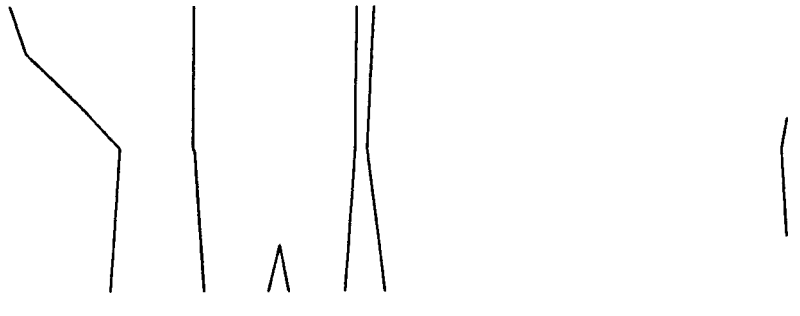

(l) AXIAL SURVEY LOCATION 4 (TEST SECTION STATION 294) AT REFERENCE MACH NUMBER 0.10.

FIGURE 11. - CONCLUDED.

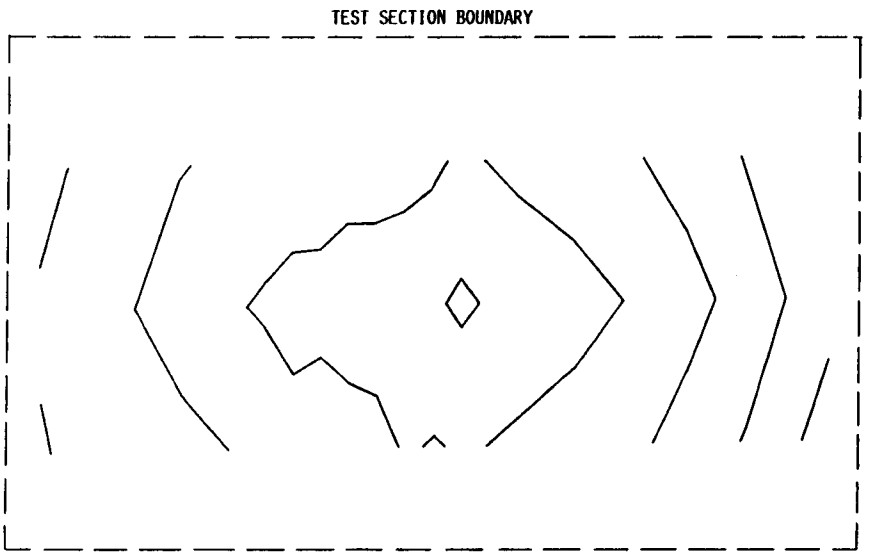

(a) AXIAL SURVEY LOCATION 1 (TEST SECTION STATION 12) AT REFERENCE MACH NUMBER 0.20.

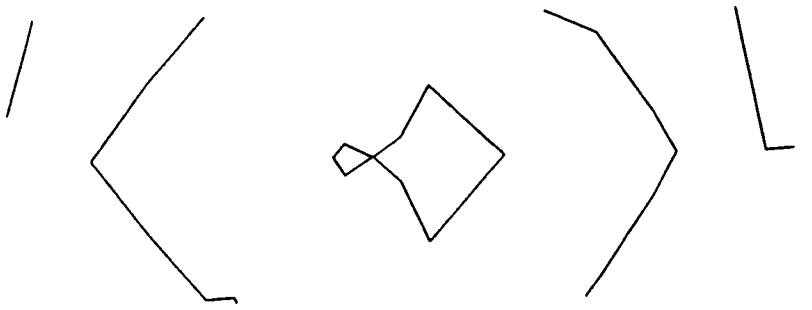

(b) AXIAL SURVEY LOCATION 1 (TEST SECTION STATION 12) AT REFERENCE MACH NUMBER 0.15.

(c) AXIAL SURVEY LOCATION 1 (TEST SECTION STATION 12) AT REFERENCE MACH NUMBER 0.10.

FIGURE 12. - MACH NUMBER CROSS-SECTIONAL PROFILES, DOWNSTREAM VIEW. DASHED OUTLINE REPRESENTS TEST SECTION CROSS-SECTIONAL BOUNDARY. CONTOUR LEVELS REPRESENT PRESSURE DIFFERENCES OF ±0.004 PSI.

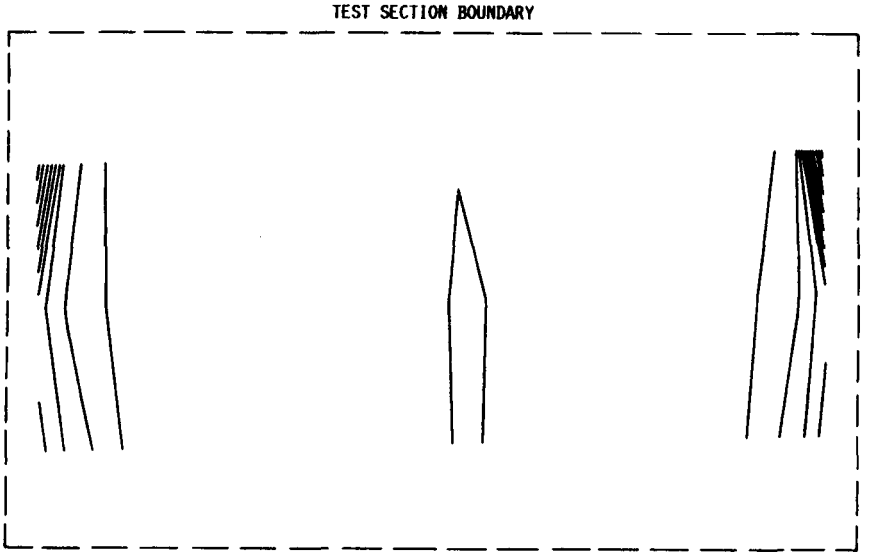

(d) AXIAL SURVEY LOCATION 2 (TEST SECTION STATION 134) AT REFERENCE MACH NUMBER 0.20.

(e) AXIAL SURVEY LOCATION 2 (TEST SECTION STATION 134) AT REFERENCE MACH NUMBER 0.15.

(f) AXIAL SURVEY LOCATION 2 (TEST SECTION STATION 134) AT REFERENCE MACH NUMBER 0.10.

FIGURE 12. - CONTINUED.

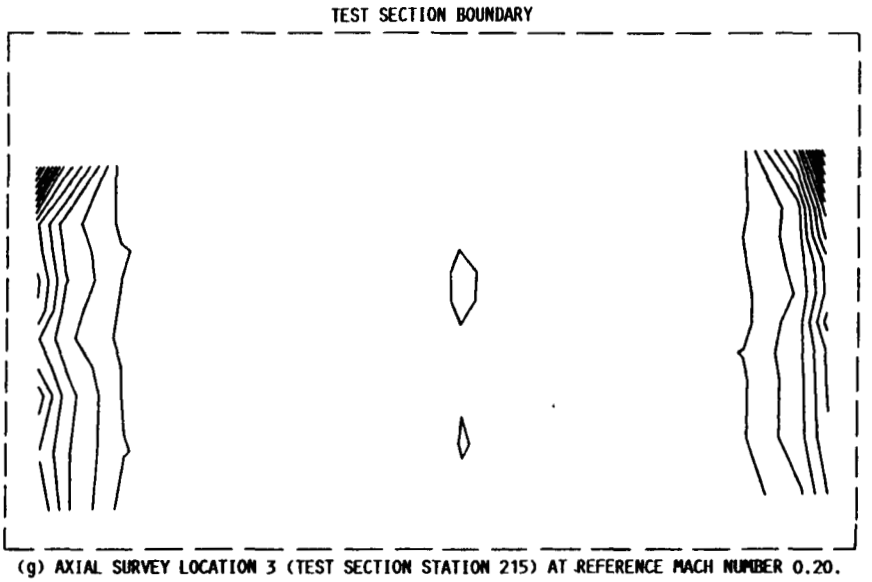

(g) AXIAL SURVEY LOCATION 3 (TEST SECTION STATION 215) AT REFERENCE MACH NUMBER 0.20.

(h) AXIAL SURVEY LOCATION 3 (TEST SECTION STATION 215) AT REFERENCE MACH NUMBER 0.15.

(i) AXIAL SURVEY LOCATION 3 (TEST SECTION STATION 215) AT REFERENCE MACH NUMBER 0.10.

FIGURE 12. - CONTINUED.

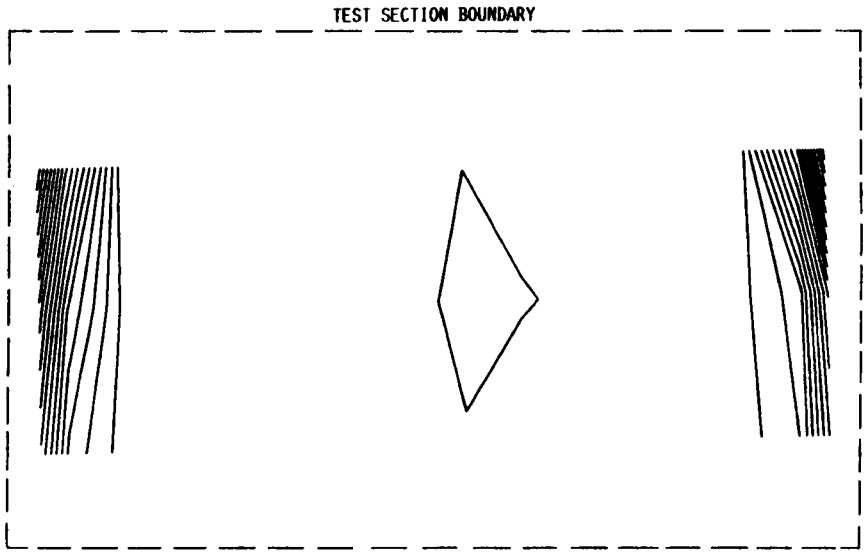

(j) AXIAL SURVEY LOCATION 4 (TEST SECTION STATION 294) AT REFERENCE MACH NUMBER 0.20.

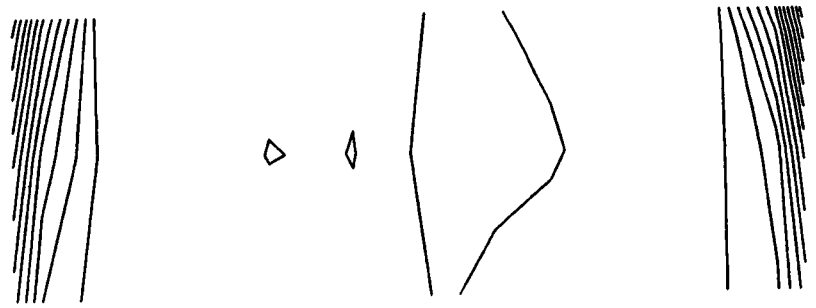

(k) AXIAL SURVEY LOCATION 4 (TEST SECTION STATION 294) AT REFERENCE MACH NUMBER 0.15.

(l) AXIAL SURVEY LOCATION 4 (TEST SECTION STATION 294) AT REFERENCE MACH NUMBER 0.10.

FIGURE 12. - CONCLUDED.

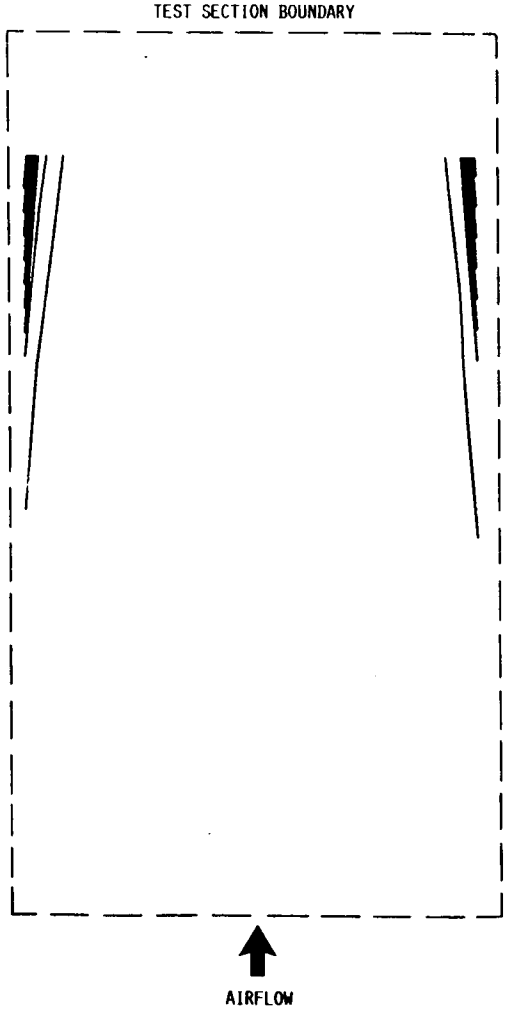

(a) VERTICAL SURVEY LOCATION 3 (2.5 FT BELOW CENTER OF TUNNEL) AT REFERENCE MACH NUMBER 0.20.

(b) VERTICAL SURVEY LOCATION 3 (2.5 FT BELOW CENTER OF TUNNEL) AT REFERENCE MACH NUMBER 0.15.

(c) VERTICAL SURVEY LOCATION 3 (2.5 FT BELOW CENTER OF TUNNEL) AT REFERENCE MACH NUMBER 0.10.

FIGURE 13. - TOTAL PRESSURE AXIAL PROFILES. DASHED OUTLINE REPRESENTS TEST SECTION BOUNDARY. CONTOUR LEVELS REPRESENT PRESSURE DIFFERENCES OF ±0.004 PSI.

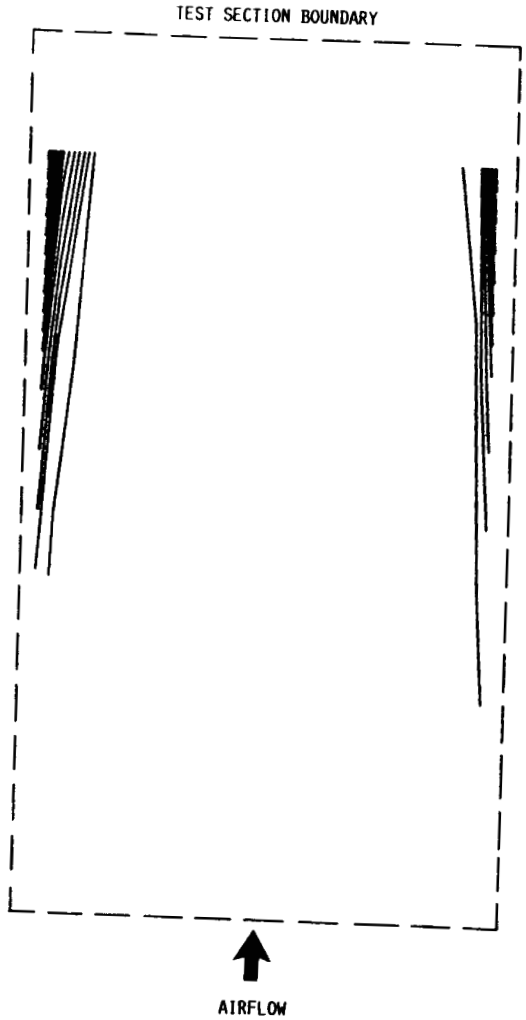

(d) VERTICAL SURVEY LOCATION 7 (AT CENTER OF TUNNEL) AT REFERENCE MACH NUMBER 0.20.

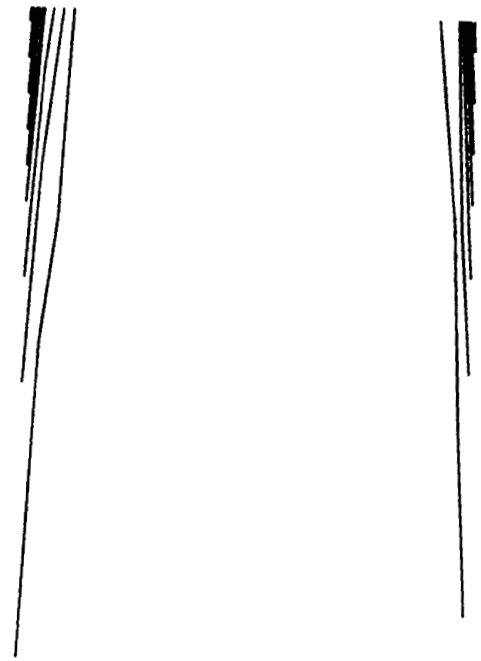

(e) VERTICAL SURVEY LOCATION 7 (AT CENTER OF TUNNEL) AT REFERENCE MACH NUMBER 0.15.

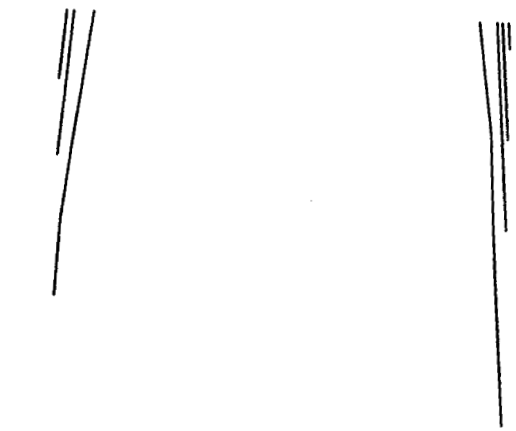

(f) VERTICAL SURVEY LOCATION 7 (AT CENTER OF TUNNEL) AT REFERENCE MACH NUMBER 0.10.

FIGURE 13. - CONTINUED.

ORIGINAL PAGE IS
OF POOR QUALITY

(g) VERTICAL SURVEY LOCATION 11 (2.5 FT ABOVE CENTER OF TUNNEL) AT REFERENCE MACH NUMBER 0.20.

(h) VERTICAL SURVEY LOCATION 11 (2.5 FT ABOVE CENTER OF TUNNEL) AT REFERENCE MACH NUMBER 0.15.

(i) VERTICAL SURVEY LOCATION 11 (2.5 FT ABOVE CENTER OF TUNNEL) AT REFERENCE MACH NUMBER 0.10.

FIGURE 13. - CONCLUDED.

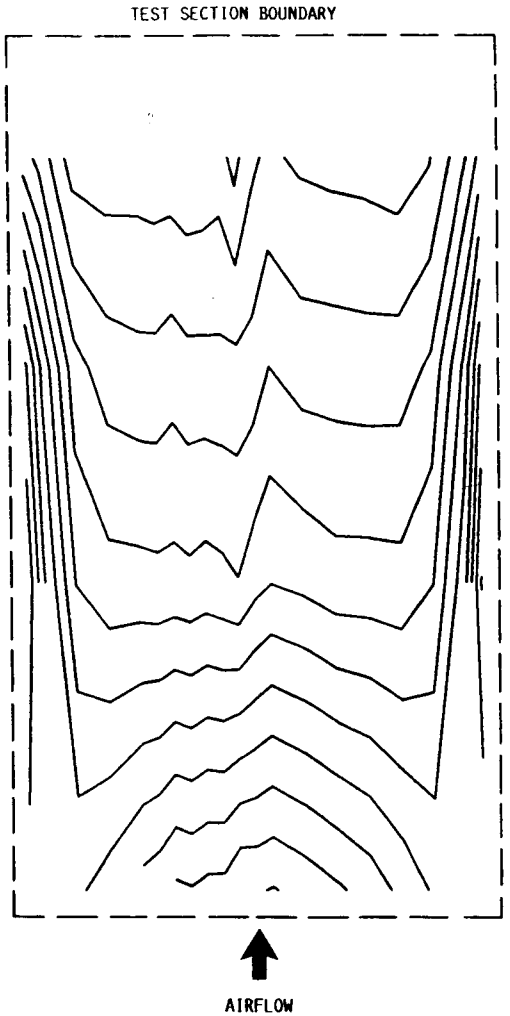

(a) VERTICAL SURVEY LOCATION 3 (2.5 FT BELOW CENTER OF TUNNEL) AT REFERENCE MACH NUMBER 0.20.

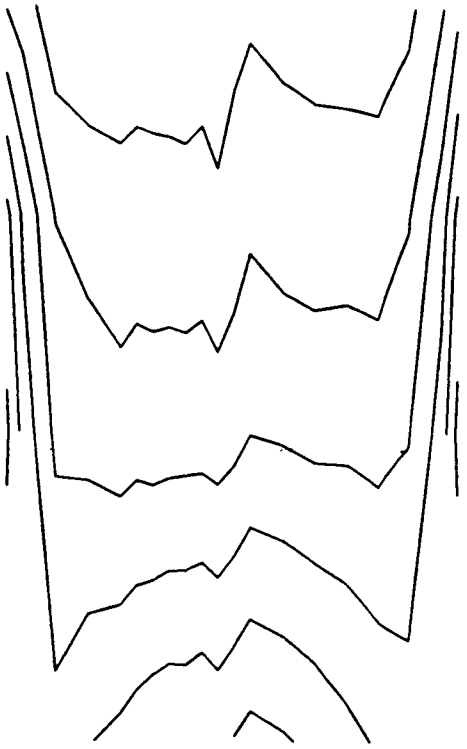

(b) VERTICAL SURVEY LOCATION 3 (2.5 FT BELOW CENTER OF TUNNEL) AT REFERENCE MACH NUMBER 0.15.

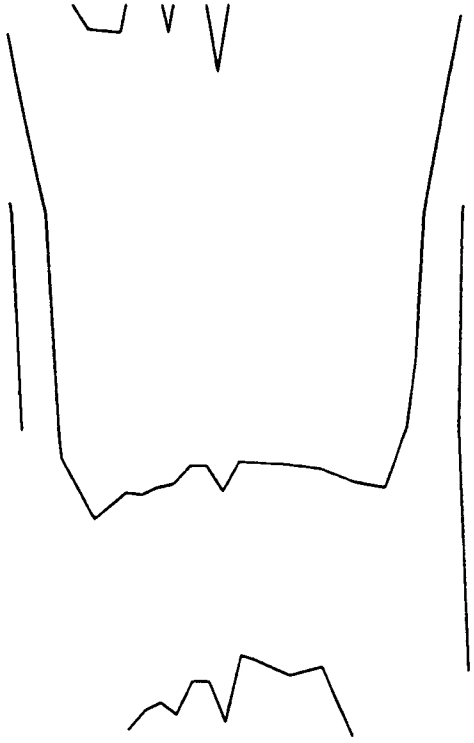

(c) VERTICAL SURVEY LOCATION 3 (2.5 FT BELOW CENTER OF TUNNEL) AT REFERENCE MACH NUMBER 0.10.

FIGURE 14. - STATIC PRESSURE AXIAL PROFILES. DASHED OUTLINE REPRESENTS TEST SECTION BOUNDARY. CONTOUR LEVELS REPRESENT PRESSURE DIFFERENCES OF ±0.004 PSI.

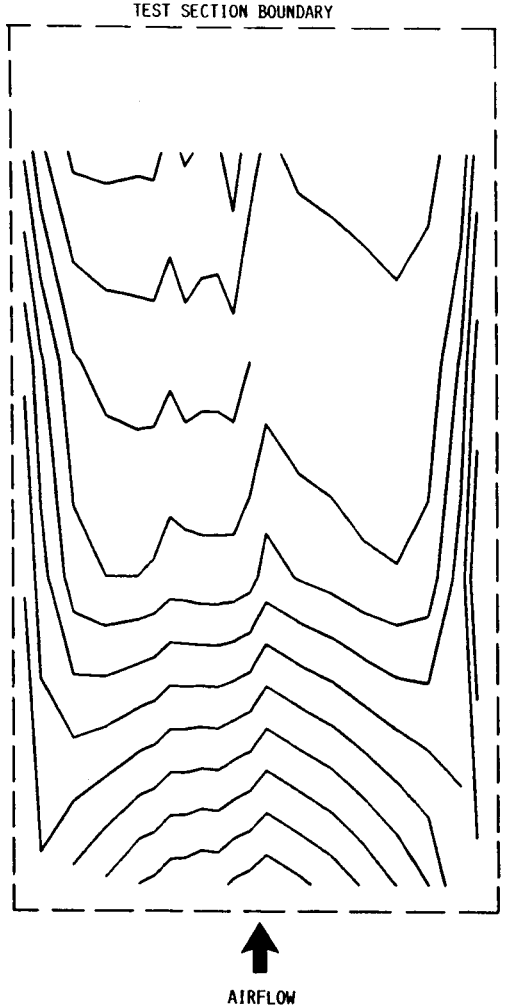

(d) VERTICAL SURVEY LOCATION 7 (AT CENTER OF TUNNEL) AT REFERENCE MACH NUMBER 0.20.

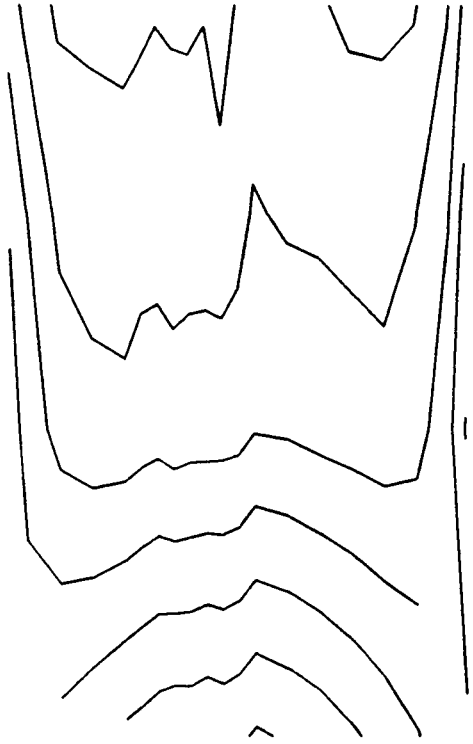

(e) VERTICAL SURVEY LOCATION 7 (AT CENTER OF TUNNEL) AT REFERENCE MACH NUMBER 0.15.

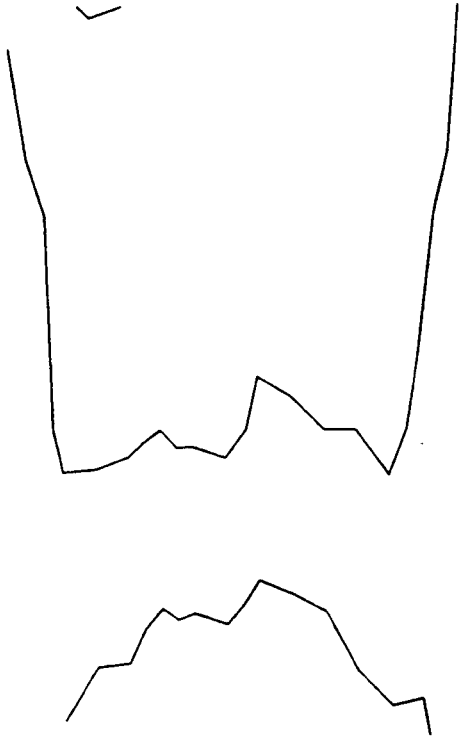

(f) VERTICAL SURVEY LOCATION 7 (AT CENTER OF TUNNEL) AT REFERENCE MACH NUMBER 0.10.

FIGURE 14. - CONTINUED.

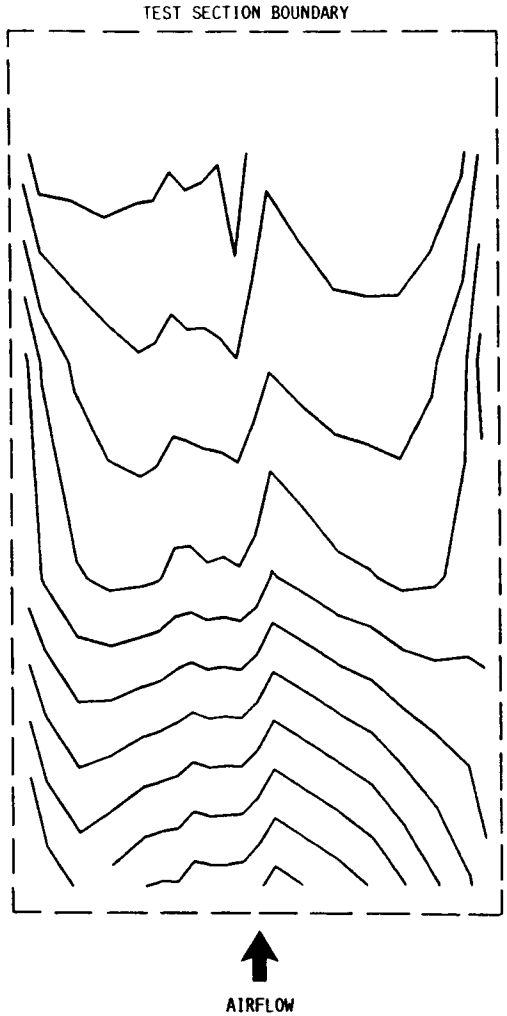

(g) VERTICAL SURVEY LOCATION 11 (2.5 FT ABOVE CENTER OF TUNNEL) AT REFERENCE MACH NUMBER 0.20.

(h) VERTICAL SURVEY LOCATION 11 (2.5 FT ABOVE CENTER OF TUNNEL) AT REFERENCE MACH NUMBER 0.15.

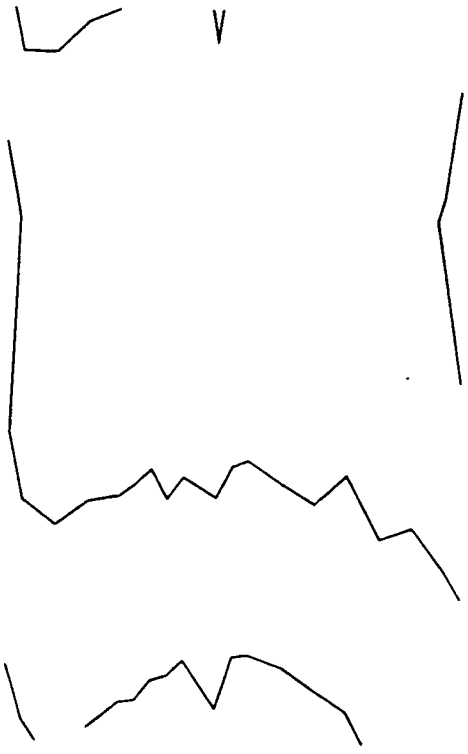

(i) VERTICAL SURVEY LOCATION 11 (2.5 FT ABOVE CENTER OF TUNNEL) AT REFERENCE MACH NUMBER 0.10.

FIGURE 14. - CONCLUDED.

(a) VERTICAL SURVEY LOCATION 3 (2.5 FT BELOW CENTER OF TUNNEL) AT REFERENCE MACH NUMBER 0.20.

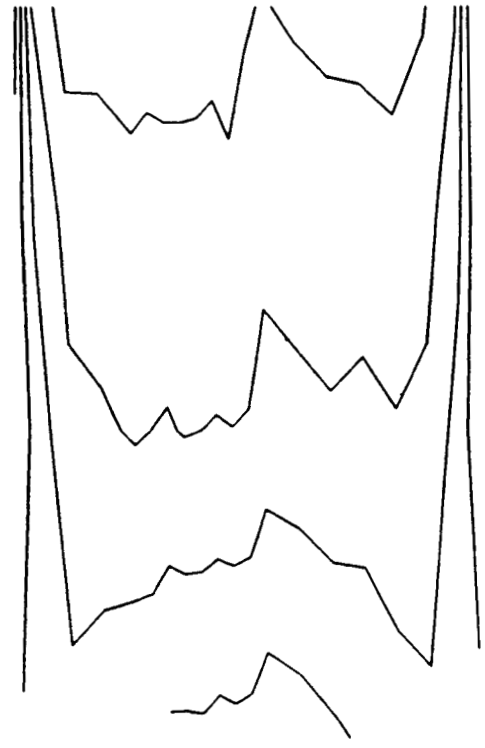

(b) VERTICAL SURVEY LOCATION 3 (2.5 FT BELOW CENTER OF TUNNEL) AT REFERENCE MACH NUMBER 0.15.

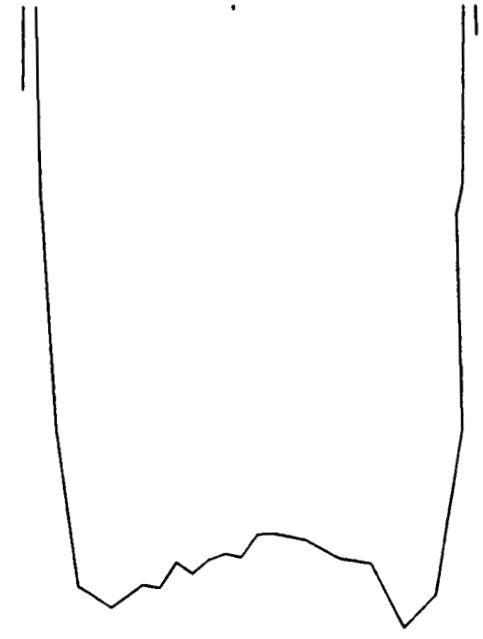

(c) VERTICAL SURVEY LOCATION 3 (2.5 FT BELOW CENTER OF TUNNEL) AT REFERENCE MACH NUMBER 0.10.

FIGURE 15. - MACH NUMBER AXIAL PROFILES. DASHED OUTLINE REPRESENTS TEST SECTION BOUNDARY. CONTOUR LEVELS REPRESENT PRESSURE DIFFERENCES OF ±0.004 PSI.

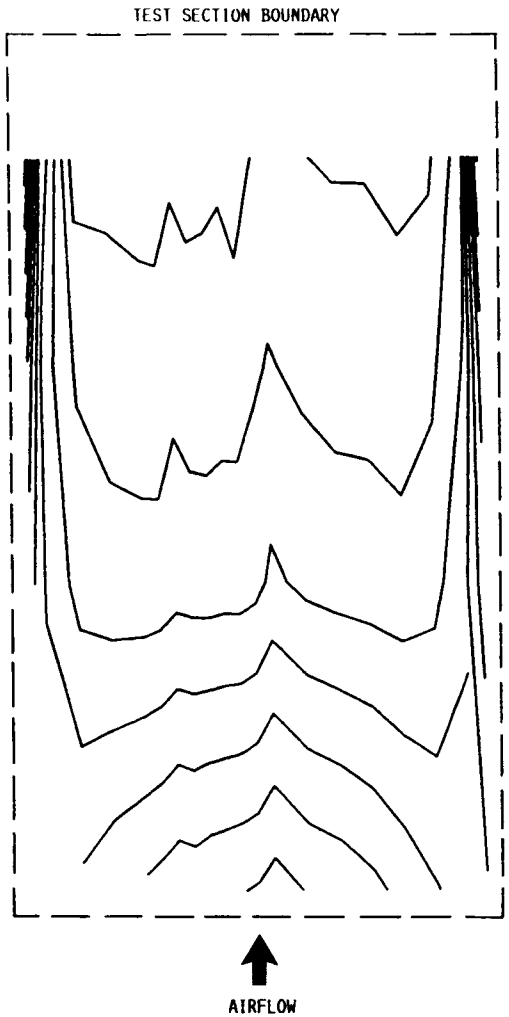

(d) VERTICAL SURVEY LOCATION 7 (AT CENTER OF TUNNEL) AT REFERENCE MACH NUMBER 0.20.

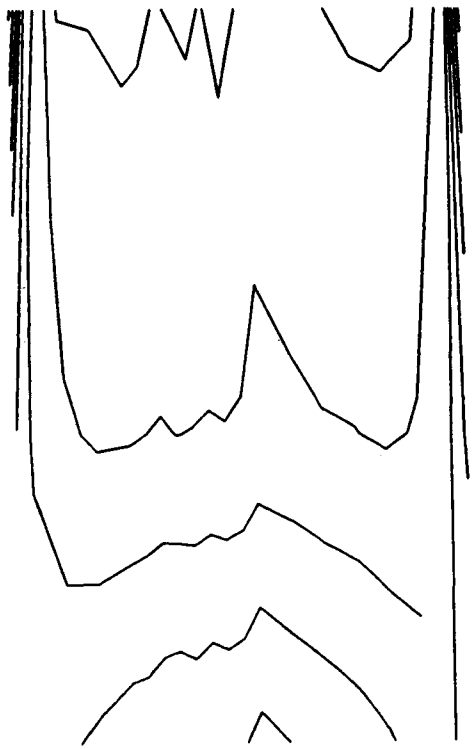

(e) VERTICAL SURVEY LOCATION 7 (AT CENTER OF TUNNEL) AT REFERENCE MACH NUMBER 0.15.

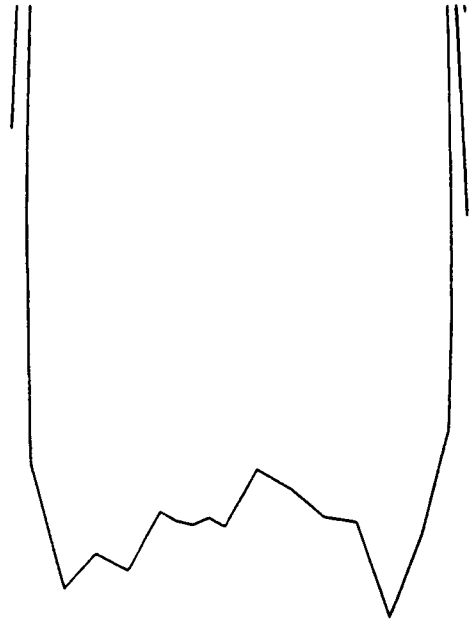

(f) VERTICAL SURVEY LOCATION 7 (AT CENTER OF TUNNEL) AT REFERENCE MACH NUMBER 0.10.

FIGURE 15. - CONTINUED.

(g) VERTICAL SURVEY LOCATION 11 (2.5 FT ABOVE CENTER OF TUNNEL) AT REFERENCE MACH NUMBER 0.20.

(h) VERTICAL SURVEY LOCATION 11 (2.5 FT ABOVE CENTER OF TUNNEL) AT REFERENCE MACH NUMBER 0.15.

(i) VERTICAL SURVEY LOCATION 11 (2.5 FT ABOVE CENTER OF TUNNEL) AT REFERENCE MACH NUMBER 0.10.

FIGURE 15. - CONCLUDED.

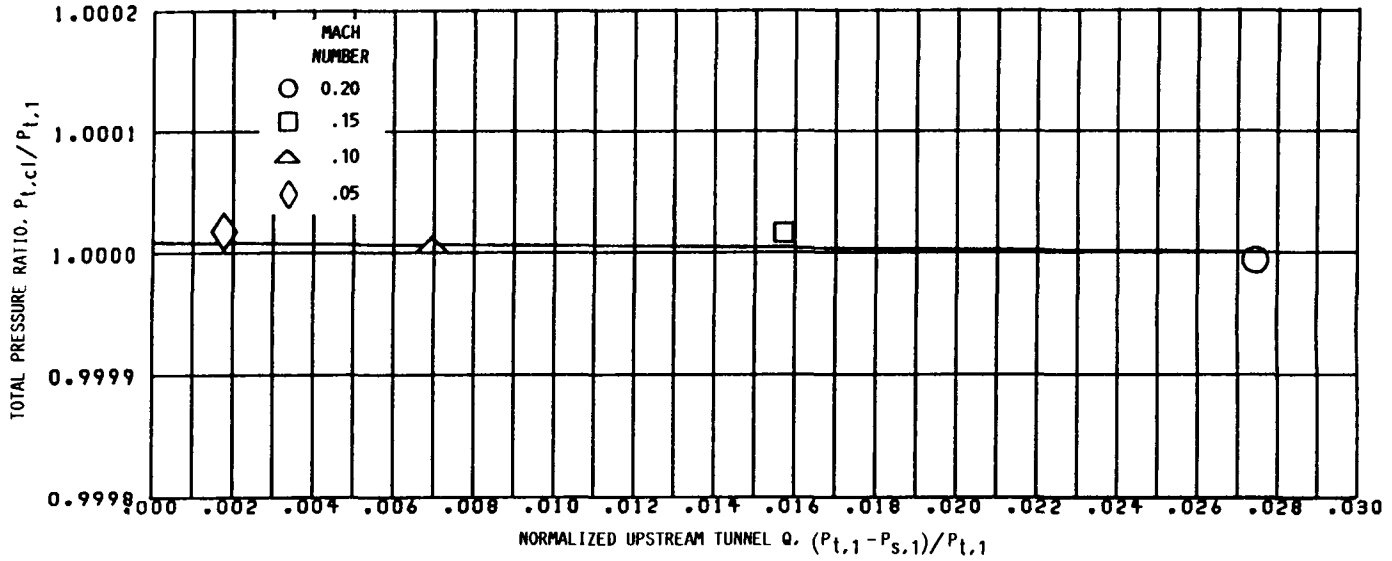

(a) UPSTREAM TUNNEL RAKE AT TEST SECTION STATION 8.

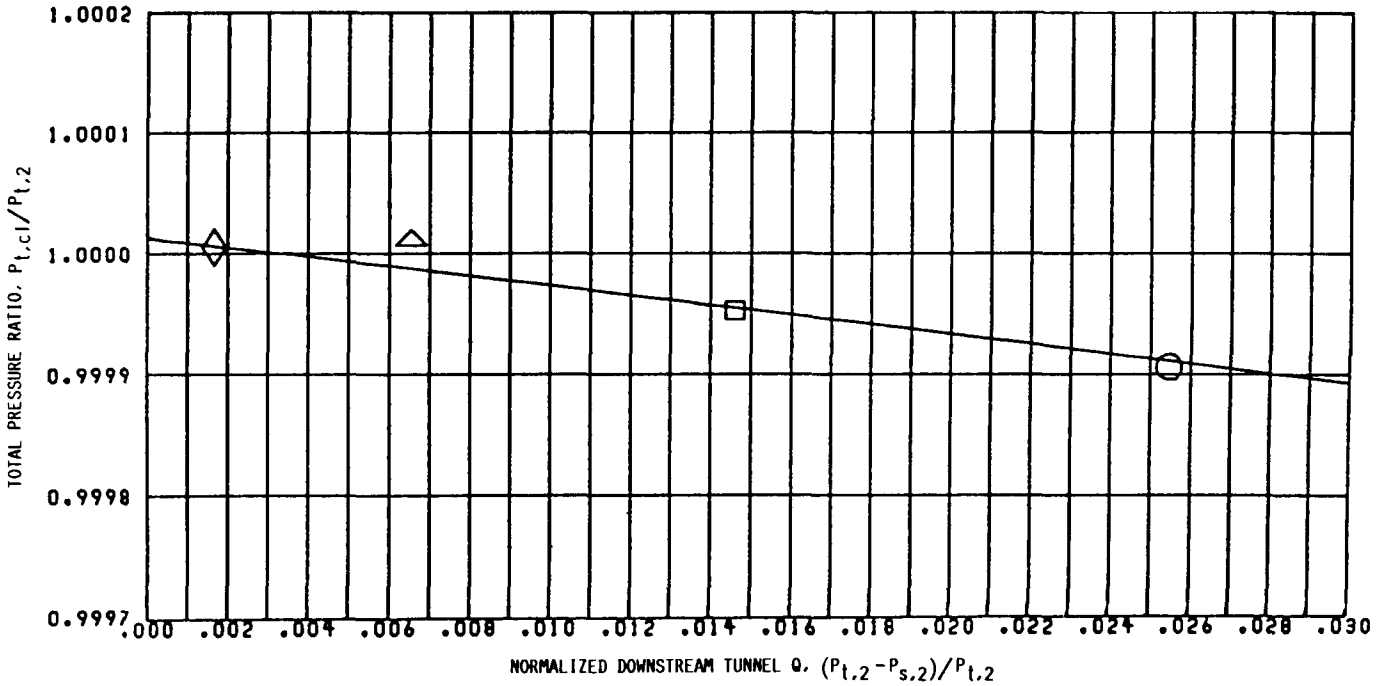

(b) DOWNSTREAM TUNNEL RAKE AT TEST SECTION STATION 210.

FIGURE 16. - WIND TUNNEL RAKE TOTAL PRESSURE CALIBRATION RESULTS.

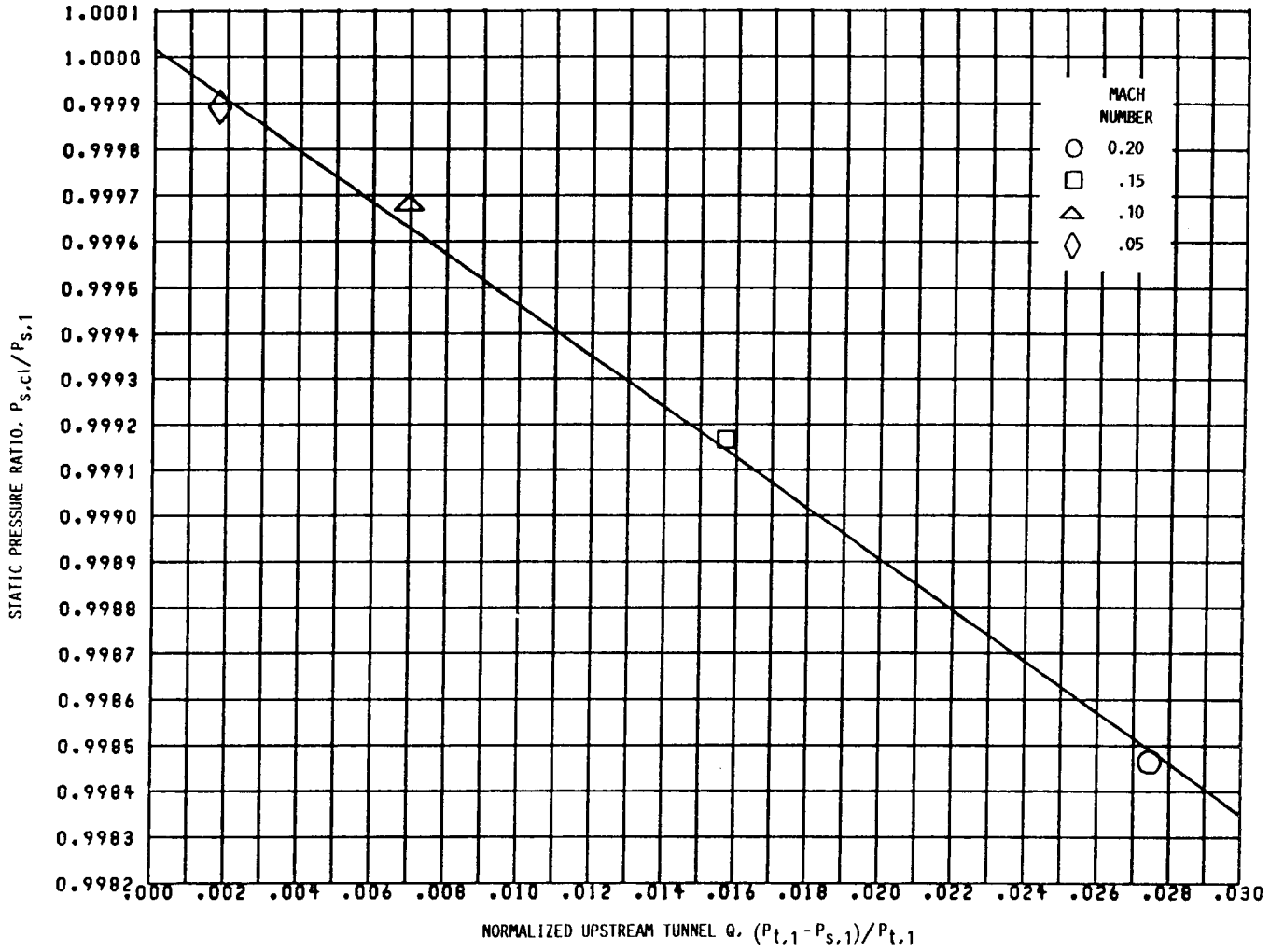

(a) UPSTREAM TUNNEL RAKE AT TEST SECTION STATION 8.

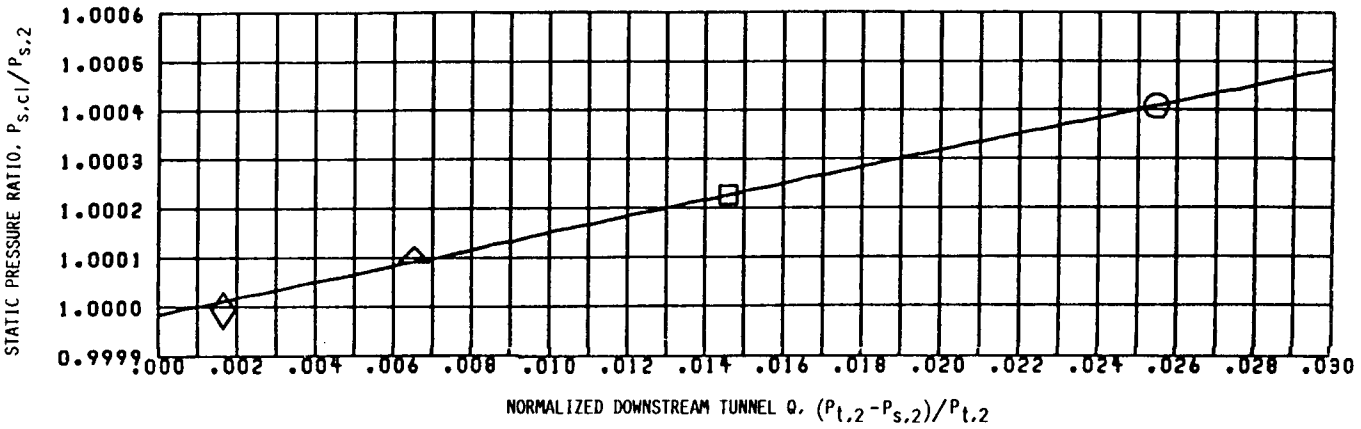

(b) DOWNSTREAM TUNNEL RAKE AT TEST SECTION STATION 210.

FIGURE 17. - WIND TUNNEL RAKE STATIC PRESSURE CALIBRATION RESULTS.

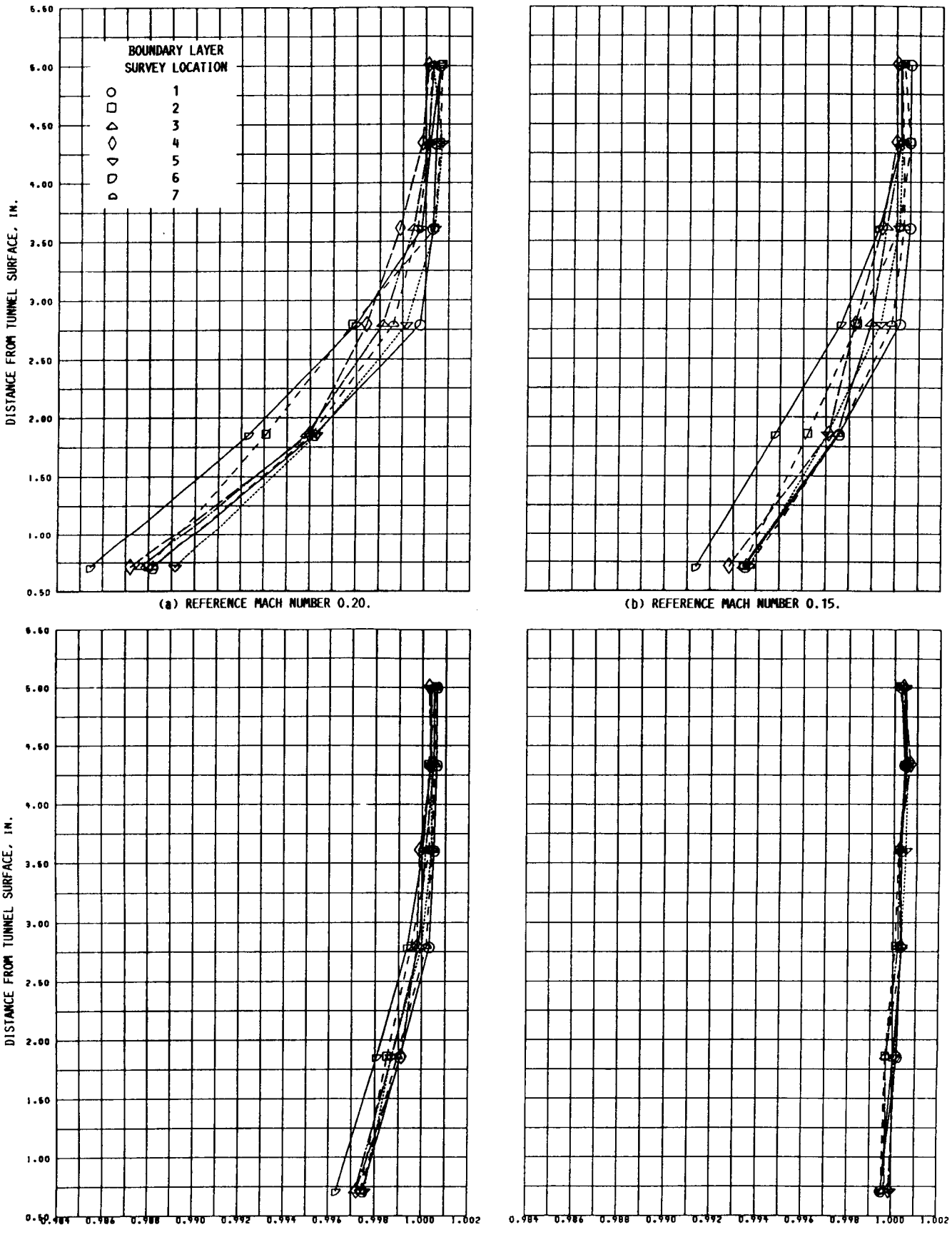

(a) REFERENCE MACH NUMBER 0.20.

(b) REFERENCE MACH NUMBER 0.15.

(c) REFERENCE MACH NUMBER 0.10.

(d) REFERENCE MACH NUMBER 0.05.

FIGURE 18. - FORWARD BOUNDARY LAYER SURVEY RESULTS AT TEST SECTION STATION 28 (NEAR THE TEST SECTION ENTRANCE).

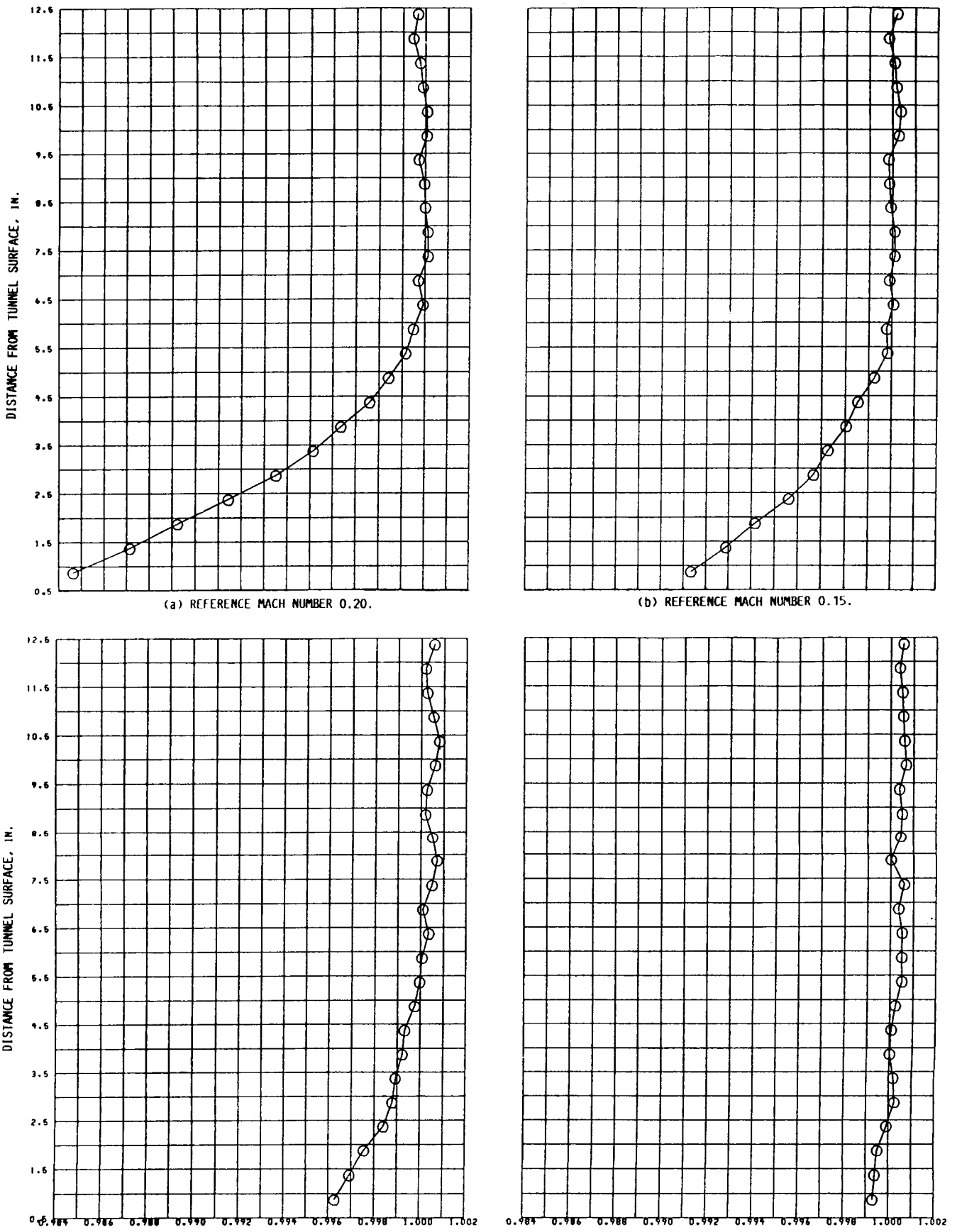

(a) REFERENCE MACH NUMBER 0.20.

(b) REFERENCE MACH NUMBER 0.15.

(c) REFERENCE MACH NUMBER 0.10.

(d) REFERENCE MACH NUMBER 0.05.

FIGURE 19. - MODEL TEST PLANE BOUNDARY LAYER SURVEY RESULTS AT TEST SECTION STATION 210.

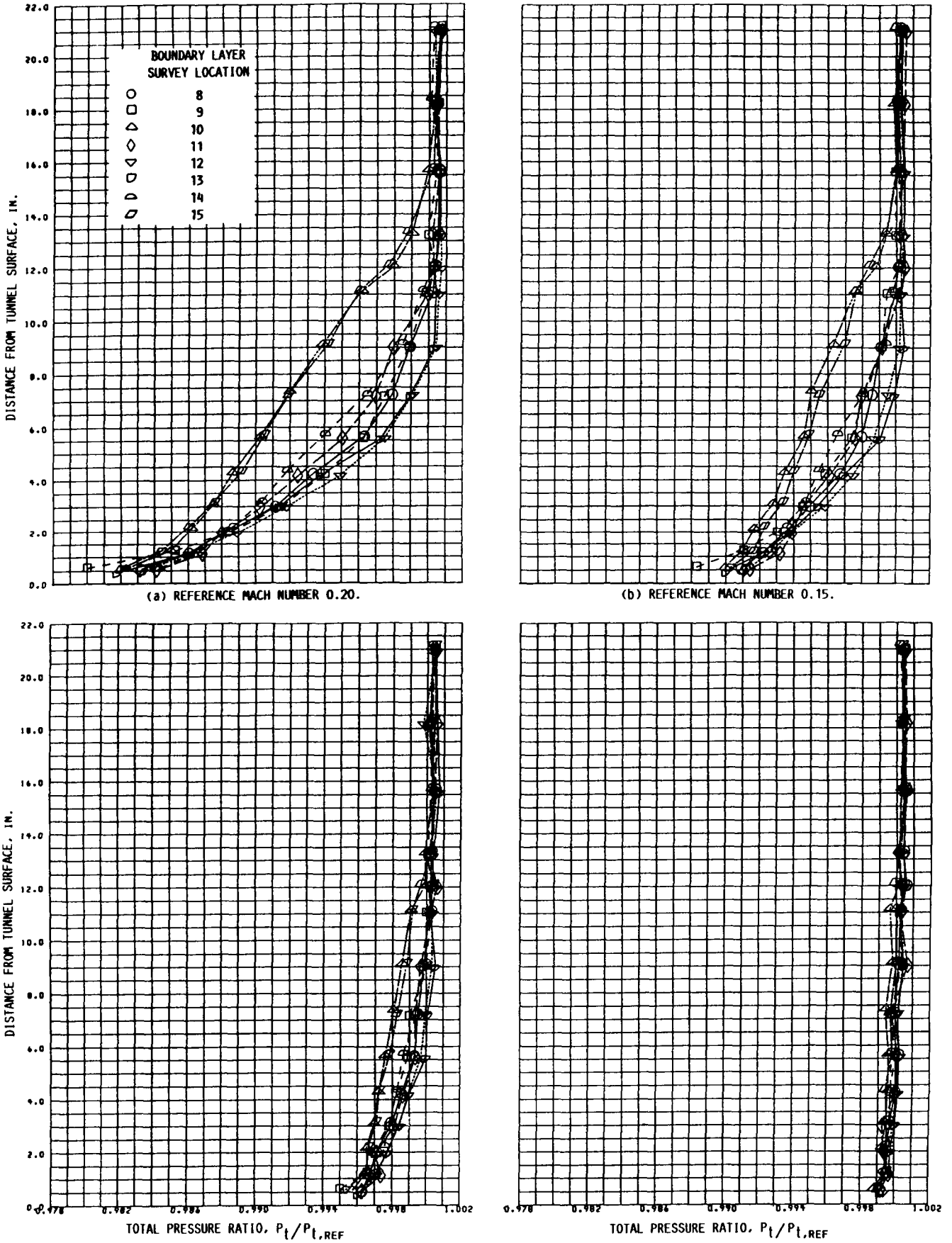

(a) REFERENCE MACH NUMBER 0.20.

(b) REFERENCE MACH NUMBER 0.15.

(c) REFERENCE MACH NUMBER 0.10.

(d) REFERENCE MACH NUMBER 0.05.

FIGURE 20. - AFT BOUNDARY LAYER SURVEY RESULTS AT TEST SECTION STATION 336 (NEAR THE TEST SECTION EXIT).

NASA
National Aeronautics and Space Administration

Report Documentation Page

1. Report No.	2. Government Accession No.	3. Recipient's Catalog No.
NASA TM-100883		

4. Title and Subtitle	5. Report Date
Flowfield Measurements in the NASA Lewis Research Center 9- by 15-Foot Low-Speed Wind Tunnel	March 1989
	6. Performing Organization Code

7. Author(s)	8. Performing Organization Report No.
Christopher E. Hughes	E-4116
	10. Work Unit No.
	535-03-01

9. Performing Organization Name and Address	11. Contract or Grant No.
National Aeronautics and Space Administration Lewis Research Center Cleveland, Ohio 44135-3191	
	13. Type of Report and Period Covered
	Technical Memorandum

12. Sponsoring Agency Name and Address	14. Sponsoring Agency Code
National Aeronautics and Space Administration Washington, D.C. 20546-0001	

15. Supplementary Notes

16. Abstract

An experimental investigation was conducted in the NASA Lewis 9- by 15-Foot Low-Speed Wind Tunnel to determine the flow characteristics in the test section during wind tunnel operation. In the investigation, a 20-probe horizontally-mounted pitot-static flow survey rake was used to obtain cross-sectional total and static pressure surveys at four axial locations in the test section. At each axial location, the cross-sectional flowfield surveys were made by repositioning the pitot-static flow survey rake vertically. In addition, a calibration of the new wind tunnel rake instrumentation, used to determine the wind tunnel operating conditions, was performed. Boundary laser surveys were made at three axial locations in the test section. The investigation was conducted at tunnel Mach numbers 0.20, 0.15, 0.10, and 0.05. The test section profile results from the investigation indicate that fairly uniform total pressure profiles (outside the test section boundary layer) and fairly uniform static pressure and Mach number profiles (away from the test section walls and downstream of the test section entrance) exist throughout in the wind tunnel test section. The static pressure and Mach number results near the test section walls were influenced by the flow around the test section wall slots and by the large contraction ratio in the tunnel inlet section near the test section entrance. The results of the wind tunnel rake instrumentation calibration indicate differences exist between the pressure measured by wind tunnel rakes and the pressures measured in the model test plane at the model centerline location. Therefore, pressure measurements obtained from either of the wind tunnel rakes to define the wind tunnel operating conditions must be corrected to determine accurate freestream conditions at the model centerline at all tunnel conditions. The test section boundary layer survey results indicate that the boundary layer thickness varies from approximately 2.8 to 3.5 in. near the test section entrance, to approximately 5.3 in. near the model test plane, and from approximately 7.3 to 13.5 in. near the test section exit.

17. Key Words (Suggested by Author(s))	18. Distribution Statement
Wind tunnel Flowfield measurement Subsonic Calibration	Unclassified – Unlimited Subject Category 09

19. Security Classif. (of this report)	20. Security Classif. (of this page)	21. No of pages	22. Price*
Unclassified	Unclassified	78	A05

NASA FORM 1626 OCT 86

*For sale by the National Technical Information Service, Springfield, Virginia 22161